FLOATING SULPHUR BIOFILMS: STRUCTURE, FUNCTION AND BIOTECHNOLOGY

A thesis in fulfilment of the requirements for the degree of

DOCTOR OF PHILOSOPHY
(BIOTECHNOLOGY)

of

RHODES UNIVERSITY

by

JENNIFER BALATEDI MOLWANTWA

November 2007

Abstract

Mine wastewaters generated during active production operations, and decanting streams following mine closure have major environmental impacts, and volumes requiring treatment are expected to increase substantially as the South African mining industry matures. Biological treatment of mine waters has been the subject of increasing interest, where sulphate reducing bacteria are employed for the reduction of sulphate to sulphide, precipitation of metals and the production of alkalinity. However, the sulphide if not removed from the system can be oxidised back to sulphate. As a result there have been limitations especially in the provision of technological options that are sustainable over the long-term, where the total sulphur (in its different forms) can be removed from the system. These, however, are the subject of a number of constraints including, importantly, the process capability to remove reduced sulphur from the treated stream, in one of its oxidation states, and thus linearise the biological sulphur cycle. This remains a major bottleneck in the development of biological wastewater treatment technology.

Floating sulphur biofilms are observed as surface layers in numerous aquatic sulphide-rich environments, and it has been suggested that they play a role in the biological cycling of sulphur. The use of sulphur biofilms for the removal of elemental sulphur was identified in this study as a possible means for addressing the technological bottleneck, especially in passive wastewater treatment systems. There is, however, little documented information in the literature on the structure of floating sulphur biofilms, the microbial species responsible for their occurrence or bio-process applications of the system.

A linear flow channel reactor was developed to simulate natural conditions and enabled the study of floating sulphur biofilm under controlled laboratory conditions. It was observed that these biofilms developed through three distinct stages termed Thin, Sticky and Brittle films. A microprobe study showed the presence of a steep Redox gradient established across (260 to 380 µm) depth of the floating sulphur biofilm of ~ 0 to -200 mV (top to bottom), which correlated with pH and sulphide gradients across the system. Structural investigations embedded in an exopolymeric matrix containing clearly defined channels and pores. Sulphur crystals were found to develop within the biofilm and above a certain size these disengaged and then settled in the liquid phase below the biofilm. These features, together with the ability of the biofilm to remain suspended at the air/water interface thus provide the surface requirement, and indicate that these structures may be understood as “true” biofilms.

In order to study an apparent functional differentiation within the floating sulphur biofilm system, a method was developed to expand its various components over a 13 cm length of agarose tube and across which an oxygen/sulphide gradient was established. This was done by inserting a sulphide plug in the bottom of the tube, overlaying this with the biofilm mixed and suspended in agarose and leaving the tube to open air. After allowing for growth, the different components of the microbial population occurring at various levels across the oxygen/sulphide gradient were sampled. The microbial population was found to resort in distinct functional layers. Aerobes including *Acidithiobacillus* and *Azoarcus*, *Acidithiobacillus*, *Thiothrix*, *Thiovirga* and *Sulfurimonas* were found in the upper oxidised layer. Aerobe and

facultative anaerobes such as *Chryseobacterium*, *Bacteroides* and *Planococcus* were found in the middle and heterotrophic anaerobes such as *Brevundimonas* and uncultured anaerobes were found in the bottom anoxic layer. This enabled the development of a first descriptive structural/functional model accounting for the performance of floating sulphur biofilms.

The potential of the floating sulphur biofilm for use as a bioprocess unit operation for sulphide removal in lignocellulose-based low-flow passive systems for acid mine drainage wastewater treatment was investigated. The linear flow channel reactor was scaled up and it was shown that the optimum sulphide removal of 74 % and sulphur recovery of 60 % could be achieved at 20 ^{o}C. In a further scale up of the linear channel reactor, the floating sulphur biofilm reactor was developed and operated. Sulphide removal and sulphur recovery of 65 and 56 % respectively was measured in the process.

An understanding of the nature and function of floating sulphur biofilms and the further development of their potential application in sulphide removal in aquatic systems may provide a useful contribution to the treatment of acid mine drainage and other sulphidic wastewaters.

Table of Contents

List of Figures

List of Tables

List of Abbreviations

AMD	Acid mine drainage
Amp	Ampicillin
AO	Acridine orange
APHA	American public health association
APS	Alkalinity producing systems
BLAST	Basic local alignment search tool
bp	Base pairs
BSE	Back scattered electron
CE	Constant environment
CLSM	Confocal laser scanning microscope
COD	Chemical oxygen demand
DGGE	Denaturing gradient gel electrophoresis
DNA	Deoxyribonucleic acid
dNTPs	Deoxynucleoside triphosphates
DO	Dissolved oxygen
DPBR	Degrading packed bed reactor
EBRU	Environmental Biotechnology Research Unit
EDX-SEM	Energy dispersive X-Ray – scanning electron microscopy
Eh	Redox potential
EM	Electron Microscopy
EMU	Electron Microscopy Unit
EPS	Exopolymeric substance
FISH	Fluorescence *in situ* hybridization
FSB	Floating sulphur biofilm
FSBR	Floating sulphur biofilm reactor
G+C	Guanine + Cytosine content
HPLC	High pressure liquid chromatography
LB	Luria Bertani
LFCR	Linear flow channel reactor
M	Molarity
MPB	Methane-producing bacteria

N	Normality
NCBI-BLAST	National Centre for Biotechnology Information Basic Local Alignment Tool
BLAST	Basic local alignment search tool
PCR	Polymerase chain reaction
PHD	Pulles Howard and de Lange
RNA	Ribonucleic acid
rRNA	Ribosomal RNA
SEM	Scanning electron microscopy
SOBR	Sulphide oxidation biofilm reactor
SOB	Sulphide oxidizing bacteria
SPARRO	Slurry precipitation and recycle reverse osmosis
SRB	Sulphate reducing bacteria
STR	Stirred tank reactor
TDS	Total dissolved solids
UV	Ultra violet
WRC	Water Research Commission
XANES	X-Ray absorption near edge spectroscopy
XRF	X-Ray fluorescence

Acknowledgements

I would like to thank the Almighty for seeing me through so much that I have finally arrived at this stage. May this be a testimony of Your grace and greatness.

I am indebted to the following people who have been there throughout this thesis:

Professor Peter Rose who has been a supervisor, mentor, father and friend, thank you very much for the guidance, support, enthusiasm, inspiration, vision and financial support. Ke a leboga Prof.

Michelle Isaacs (nee Bowker) you are greatly appreciated. Kathy Knight, you are so special, without you the hard times would have been harder. Dr Hart and support staff thank you for all the work on the reactor set up. To my colleagues and friends at EBRU it was great sharing the experience of learning with you. Dr Yvonne van Breugel, thank you for proof reading my work.

I owe much debt to the Water Research Commission for the generous funding and Rhodes University for the opportunity to study and making this dream come true.

To Shirley Pinchuk of the EM unit, Dr Prange from Bonn University, Prof Marsh from the Geology Department your assistance is appreciated.

To Dr Ralph Heath, Pulles Howard and de Lange, Zitholele Consulting and Golder Associates, thank you for your encouragement and understanding that I had to complete my studies.

My parents, *T.*Z and Malekgeto Molwantwa, I am humbled and blessed with parents like you. The support you gave me through the years I will always cherish for as long as I am alive. I dedicate this thesis to my son Thitelle, and the Masibi and Molwantwa families.

List of Publications

Molwantwa, J. B., Bowker, M., Gilfillan, J., Rein, *N*, Hart, O. O and Rose, P.D. (2007). Investigation of and development of the biotechnology of the floating sulphur biofilm in the beneficiation and treatment of wastewaster. WRC final report on Project: No. 1454. Water Research Commission, South Africa.

Whittington-Jones K.W., **Molwantwa J.B.,** and Rose, P.D**.** (2006). Enhanced hydrolysis of carbohydrates in primary sludge under biosulfidogenic conditions. *Water Research* **40** (8): 1577-1582.

Coetser, S. E., Heath, R., **Molwantwa, J. B.,** Rose P. D. and Pulles, W. **(**2005). Implementation of the degrading packed bed reactor technology and verification of the long-term performance of passive treatment plants at Vryheid Coronation Colliery. Water Research Commission report No. 1348/ 1/ 05.

Molwantwa, J. B., Whittington- Jones, K. W. and Rose, P. D. (2004). An investigation into the mechanism underlying enhanced hydrolysis of complex carbon in a biosulphidogenic recycling sludge bed reactor (RSBR). *Water SA* Vol. 30 No. 5

Molwantwa, J. B., Coetser, S. E., Heath, R and Rose, P. D. (2004). Development of the floating sulphur biofilm reactor for sulphide oxidation in biological water treatment systems. Water Institute of Southern Africa Mine Water Division, Award Winning Paper. *Water SA* Vol. 30 No. 5

Molwantwa, J. B., Coetser, S. E., Heath, R. and Pulles, W. (2003). The monitoring, evaluation and verification of a long-term performance of passive treatment plants at Vryheid Coronation Colliery pilot plant. Final Report to Water Research Commission on Project No.:K5/1348. Water Research Commission, South Africa.

Molwantwa J. B. (2002). The enhanced hydrolysis of sewage sludge under sulphidogenic conditions. MSc Thesis, Rhodes University, South Africa.

Molwantwa, J. B., Molipane, *N.* P. and Rose, P. D (2000). Biological sulphate reduction utilising algal extracellular products as a carbon source. Poster presentation at the WISA Conference, Sun City, 28 May – 01 June 2000.

Chapter One

THE MINE WATER PROBLEM

1.1 ACID MINE DRAINAGE

The salinisation of the public water system has been a subject of increasing concern in South Africa, and acid mine drainage (AMD) wastewaters have contributed substantially to this problem (Barnes and Romberg, 1986; Maree and Hill, 1989; Pulles *et al.*, 1995; Scott, 1995; Gazea *et al.*, 1996; Rose, *et al.*, 1998; Younger, 2001; Johnson *et al.*, 2002; Rose, 2002; Neba, 2006). Considerable research effort has been directed at process development for the remediation and treatment of these wastewaters (Maree *et al.*, 1988; Lens *et al.*, 2000; Whittington-Jones, 2000; Schoeman and Steyn, 2001; Rose, 2002; Neba, 2006). For this reason, biological systems have been the subject of particular interest given the need for sustainability over the long periods of time AMD flows are anticipated to require treatment (Rose *et al.*, 1998; Chang *et al.*, 2000; Johnson *et al.*, 2002; Younger, 2001; Johnson and Hallberg, 2005; Neba, 2006). Both active (Rose, 2002, Neba, 2006) and passive biological sulphate reduction treatment systems (Pulles *et al.*, 1995; Younger *et al.*, 1997; Younger, 1998; Zipper and Jage, 2001; Molwantwa *et al.*, 2003; Younger, 2004; Coetser *et al.*, 2005; Neba, 2006) have been developed for the removal of sulphate salinity (reducing sulphate to sulphide) and heavy metal contamination, for neutralization of the acidic stream.

Since the sulphate reduction is the central operation of these various biological AMD treatment processes (Johnson and Hallberg, 2003; Neba, 2006), the sulphide produced in this way needs to be removed from the system in order to prevent its reoxidation to sulphate. This would result in the linearization of sulphur (total removal and not re-cycling from one form to another) and therefore biodesalinisation in a treatment operation (Rose, 2002; Molwantwa *et al.*, 2007).

1.2. SULPHIDE REMOVAL

Sulphide is a toxic, corrosive and odorous compound and its removal from wastewater treatment effluent is therefore mandatory. Strategies that have been used include

precipitation as metal sulphide (Davidson *et al.*, 1989; Johnson, 1995; Boshoff *et al.*, 1996, van Hille and Duncan, 1996; Molipane, 1999; Dvorak *et al.*, 2004), oxidation to elemental sulphur (Buisman, *et al.*, 1989; Buisman *et al.*, 1996; Janssen *et al.*, 1999; Rein, 2002), solvent extraction (Hammond, 1986; Steudel, 1996; Lagas, 2000; Janssen *et al.*, 2000; Johnson, 2000) and electrochemical oxidation (Waterson *et al.*, 2006).

The development of reliable technology for the oxidation of sulphide to form elemental sulphur would increase the application potential of wastewater treatment technologies where waste carbon sources are used for biological sulphate reduction out of which sulphide is a by-product (Molipane, 1999; Whittington-Jones, 2000; Bowker, 2002; Madikane, 2002; Molwantwa, 2002; Rein, 2002; Son and Lee, 2004, Roman, 2005; Neba, 2006). A process that can produce elemental sulphur from sulphide under heterotrophic conditions would contribute significantly to the enhancement of an integrated biological AMD treatment process (where sulphate in AMD is reduced to sulphide, an the residual sulphide left after metal precipitation is removed from the effluent) to treat the large volumes of AMD that are predicted to occur in South Africa (Scott, 1995; Jansen *et al.*, 1999; Rein, 2002; Rose, 2002).

1.2.1 Sulphide Oxidation

The two most important oxidation reactions which sulphide may undergo are shown in Equations 1.1 and 1.2 (Janssen *et al.*, 1999). In these reactions, sulphide can be converted to sulphur and sulphate during oxidation processes which can be either chemically or biologically driven.

$$2HS^- + O_2 \rightarrow 2S^o + 2OH^- \quad (1.1)$$

$$2HS^- + 4O_2 \rightarrow 2SO_4^{2-} + 2H^+ \quad (1.2)$$

H_2S is a weak acid that dissociates into HS^- (pKa_1= 7.04) and S_2^- (pKa_2). The pKa_2 has been reported to be >12 (Weast, 1981; O'Flaherty *et al.*, 1999, Stuedel, 2000) and for practical purposes the formation of S_2^- may be disregarded. The term sulphide is commonly used for any of the reduced sulphur species that may be present.

Possible products of oxidation include thiosulphate ($S_2O_3^-$) and polythionates ($-SO_3^-$-S_n-SO_3^-) In addition to this, polysulphide (S_n^{2-}, n = 2 to 5) have been identified as important intermediates in the oxidation of sulphide (Yao and Millero, 1996; Steudel, 1996; Janssen *et al.*, 1999; Stuedel, 2000). An indication of the thermodynamic forces and ionic activities acting on a chemical system can be obtained from the Pourbaix diagram (Figure 1.1), which represents the equilibrium distribution of the domains of dominance of various chemical species at specific pH and Eh (Redox) values (Stumm and Morgan, 1995; Middelburg, 2000; Steudel, 2000).

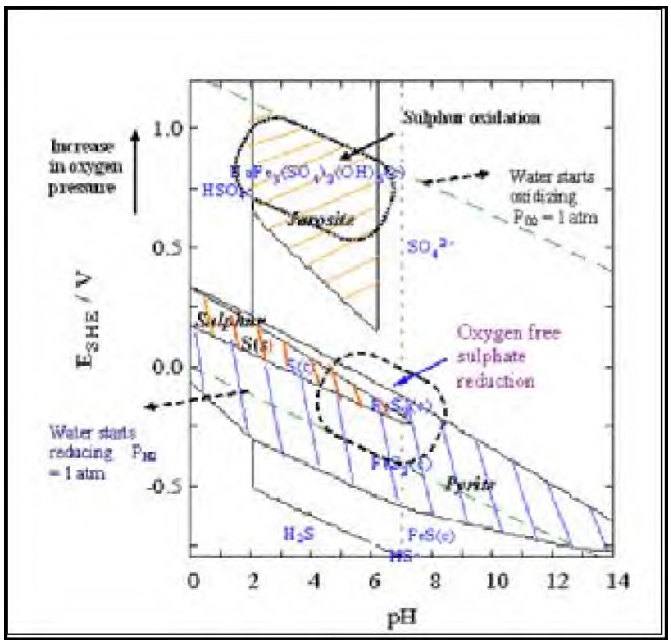

Figure 1.1 A Pourbaix diagram showing the different sulphur species at specific pH and **E**h values (Middelburg, 2000).

Compared to the other oxidized forms of sulphur, elemental sulphur is formed in a narrow band of Redox potential and pH conditions (Bruser *et al.*, 2000). Stumm and Morgan (1995) suggested that for a biological process, equilibrium thermodynamics have less of an influence on the major product of sulphide oxidation than kinetic considerations do. It is also possible that conditions in the bulk phase (those which are measured for chemical reaction process control purposes) are quite different from the intracellular conditions in living systems (Janssen *et al.*, 1999; Bruser *et al.*, 2000).

1.2.1.1 Chemical Sulphide Oxidation

The removal of sulphide from solutions has been tackled in a number of ways. Physico-chemical processes include chemical oxidation reactions (Sublette, 1992;

Reinhoudt and Moulijn, 2000), and chemical precipitation (Buisman *et al.*, 1989; Lens *et al.*, 2000) usually resulting in the production of metal sulphide sludges which must be disposed of. Oxidative reactions involve the contact of sulphide ions with oxygen under constrained pH and Redox potential conditions to produce S^{o} (elemental sulphur) and hydroxide ions (Equation 1.1). The elemental sulphur formed has an oxidation state of zero and consists mainly of cyclic S_8 molecules which aggregate into larger crystals which can be separated from solution either by flotation or separation techniques (Steudel, 1996; Janssen *et al.*, 1999; Steudel, 2000).

Industrial physico-chemical sulphide removal processes include the Stredford Process (Hammond, 1986; Lens *et al.*, 2000; Steudel, 2000), in which sulphide is converted to elemental sulphur in the presence of a vanadium catalyst, and the Clause process (Janssen *et al.*, 1999; Steudel, 2000) used in the petrochemical industry to strip sulphide into an amine or glycol solution at high pressure and then catalytically convert it to sulphur (Guoqiang *et al.*, 1994; Gilfillan, 2000; Rein, 2002). These abovementioned treatment options are considered in general to be inappropriate for the treatment of large volumes of sulphate-containing wastewaters because of the high cost involved.

1.2.1.2 Biological Sulphide Oxidation

Sulphide oxidizing bacteria (SOB) use sulphide as a source of electron donors and produce sulphur particles in the submicron range (Bruser *et al.*, 2000). The particles are composed of a core of elemental sulphur covered by a layer of naturally charged polymers, comparable to those of the La-Mer sulphur sol, which renders the particles hydrophilic (Steudel, 1996; Bruser *et al.*, 2000; Janssen *et al.*, 2000). Archaea and bacterial genera capable of sulphide oxidation and sulphur formation include *Thiomicrospira*, *Acidithiobacillus*, *Thiothrix*, *Acidophilum*, *Leptospirillum*, *Thiovulum*, *Chromatium* and *Chlorobium* (Lane *et al.*, 1992; Okabe *et al.*, 1996, 1999a and 1999b; Cytryn *et al.*, 2005).

These genera are widely spread across the archaea and eubacteria, illustrating that traditional physiological groupings based on metabolic criteria are often not representative of phylogenetic relationship and produce overlapping groupings for many unrelated bacterial species (Okabe *et al.*, 1999b).

The three groups of microorganisms involved in sulphide oxidation are:

- Photosynthetic sulphur bacteria;
- Colourless sulphur bacteria;
- Certain heterotrophic bacterial groups, although not as well documented as the colourless sulphide oxidising bacteria

1.2.1.3 Photosynthetic Sulphur Bacteria

Photosynthetic sulphur bacteria, including both green and purple sulphur bacteria forms, use sulphide as an electron donor for photosynthesis, with carbon dioxide (CO_2) as a carbon source in a reaction powered by light (Equation 1.3).

$$CO_2 + H_2S \rightarrow CH_2O + H_2O + 2S^{o} \qquad (1.3)$$

The sulphur produced from sulphide oxidation is either located intracellularly (e.g. *Chromatium* sp.) or as extracellular sulphur globules (e.g. *Chlorobium* sp.). Alternately, under certain conditions, sulphide is fully oxidised to sulphate. The photosynthetic sulphide oxidisers play an important role in anaerobic shallow waters, where they provide one of the few means to oxidise reduced sulphur compounds (Johnson, 2000). Growth of photosynthetic sulphur bacteria in stratified lakes (< 15 m) is dependent on light penetration, wavelength and the depth of the chemocline (wavelength plays an important role in the niche occupied by different photosynthetic bacteria). The position (depth) of the photosynthetic bacteria is dependent on the position of chemocline and light penetration. The genera commonly found in these environments are *Chromatium*, *Chlorobium*, *Rhodobacter* and *Thiospirillum* (Widdel, 1988).

The sulphide oxidising potential of photosynthetic sulphur bacteria such as *Chlorobium limicola* have been used in sulphide oxidising bioreactors (Cork *et al.*, 1986; Kim *et al.*, 1990) and reportedly can transform up to 90 % of inlet hydrogen sulphide to sulphur (Kim *et al.*, 1990; Johnson, 2000). Photosynthetic sulphur bacteria are not, however, the first choice in biotechnological sulphide removal processes

because of the light requirement which complicates reactor design and, more importantly, because sulphide oxidation is strictly coupled to growth (Kim *et al.*, 1990). Photosynthetic sulphide oxidising bacteria (SOB) use carbon dioxide as a terminal electron acceptor with one to two grams of sulphur being produced per gram of cells (Kuenen and Robertson, 1992; Johnson, 2000).

1.2.1.4 Colourless Sulphur Bacteria

The colourless sulphur bacteria are a diverse group of sulphide oxidisers which includes both archaea and eubacteria (Robertson and Kuenen, 1991; Johnson, 2000). Colourless sulphur bacteria inherit their name from the lack of photo-pigments, although in dense cultures, they could appear pink or brown due to the presence of large amounts of cytochrome (Robertson and Kuenen, 1991; Johnson, 2000). The wide range of forms include *Acidithiobacillus*, *Thiomicrospira*, *Thiospaera*, *Sulfolobus*, *Leptospirillum*, *Acidianus*, *Thermothrix*, *Thiovulum*, *Beggiatoa*, *Thiothrix*, *Thioploca*, *Thiodendron*, *Thiobacterium*, *Macromonas*, *Achromatium* and *Thiospira*. The members of these genera have differing pH and thermal requirements for growth and some are capable of denitrification while others are not (Jørgensen and Revsbech, 1985; Widdel, 1988; Robertson and Kuenen, 1991; Janssen *et al.*, 1997; Gardner, 1998; Nielson *et al.*, 2000; Ito *et al.*, 2004).

The *Thiobacilli* are the most well documented group of colourless SOB. They mainly obtain energy from the chemolithotrophic oxidation of inorganic sulphur compounds, which is used to support autotrophic carbon synthesis (Kelly, 1985; Lens *et al.*, 2000). *Thiobacilli* are Gram negative, rod-shaped eubacteria, with very high diversity amongst members of the genus (Widdel, 1988). The six obligate chemolithotrophic species are characterized by a variation in G+C content from 51 to 68 %, have pH optima from pH 2 to 7 and grow at optimal temperatures ranging from 20 to 30 ^{oC} (Kelly, 1985). The wide variation in the genus has made it a challenging task to elucidate the enzymatic pathway involved in sulphur metabolism (Kelly, 1985).

Colourless sulphur bacteria are either aerobic or anaerobic, the latter using alternative electron acceptors such as hydrogen and ferrous iron. *T. denitrificans* has been characterised as an anaerobe, although Sublette and Sylvester (1987) found that

aerobic cultures can reduce sulphide to very low levels. Under anaerobic conditions, nitrate is used by *T. denitrificans* as a terminal electron acceptor, while producing nitrogen (Equation 1. 4).

$$5H_2S + 8KNO_3 \rightarrow 4K_2SO_4 + {}_{H2SO4} + 4N_2 + 4H_2O \quad (1.4)$$

The colourless sulphur bacteria may be present wherever reduced sulphur compounds, usually sulphide or sulphur, are found, for example hydrothermal vents, hot springs and wastewater treatment plants (Dart and Stretton, 1980; Robertson and Kuenen, 1991; Weller *et al.*, 1991; Voordouw *et al.*, 1996; Berbee and Taylor, 1999). Basu *et al.* (1995) reported a symbiotic relationship between sulphate reducing bacteria and the micro-aerophilic sulphide oxidising *Beggiatoa sp.* in a micro-aerophilic sulphate reducing bioreactor. The healthy population of *Beggiatoa*, observed in sludge granules, converted sulphide produced by the sulphate reducing bacteria (SRB) to sulphate, or to intracellular sulphur, while the SRB population was involved in anaerobic sulphate reduction using organic acids as a carbon and energy source (Basu *et al.*, 1995). Filamentous SOB (*Thiothrix* and *Beggiatoa*) in activated sludge was also reported (Williams and Unz, 1985; Bruser *et al.*, 2000; Ito *et al.*, 2002).

Well known biological sulphide removal systems using SOB include the Shell-Paques process operated at the Budelco zinc refinery in the Netherlands (Scheerem *et al.*, 1993; Janssen *et al.*, 1998; Janssen *et al.*, 2000). This process involves collection of sulphide from the wastewater in a scrubber followed by feeding it to SOB able to convert the sulphide into elemental sulphur. The sulphur is collected by a tilted plate settler, resulting in a 99.5 % removal of H_2S from the gas stream (Janssen *et al.*, 1999). Two further plants have been operated in India and one in Germany. However, the high process costs of this type of approach make it unsuitable for high volume flow and passive treatment systems (PHD, 2002; Younger *et al.*, 1997; Rose, 2002; Coetser *et al.*, 2005).

Guoqiang *et al.* (1994) developed a desulphurisation process using *Acidithiobacillus ferrooxidans*, and an iron sulphate feed. The bacteria catalyse the conversion of ferrous sulphate to ferric sulphate. Ferric sulphate subsequently oxidizes hydrogen

sulphide to S^{o} and is thereby reduced to ferrous sulphate. This reduced solution was then recycled.

1.3 FLOATING SULPHUR BIOFILMS

A possible area for the development of the sulphur bacterial system in wastewater treatment has been the application of more recent observation and investigation involving floating sulphur biofilms (FSBs). The appearance of white films on sulphate reducing systems has been the subject of previous comment (Jørgensen and Revsbech, 1985; Janssen *et al.*, 1997; Rose *et al.*, 1996; Dunn, 1998) but little if any detailed study has been reported on their occurrence in natural environments.

Researchers at the Environmental Biotechnology Research Unit (EBRU), at Rhodes University, Grahamstown, South Africa, had observed the appearance of white floating films on the surface of highly sulphidic tannery wastewater ponds (Figure 1.2). Preliminary investigations into their nature and function were initiated (Rose *et al.*, 1996; Dunn, 1998). Early reports by Gilfillan (2000) confirmed that these were clearly differentiated structures which were mainly populated by a diverse mix of microbial morphological types including mainly bacteria.

Figure 1.2 Occurrence of FSBs observed on high-organic load sulphidic tannery wastewater ponds in Wellington, South Africa.

They were provisionally identified as sulphur biofilms. Bowker (2002) then showed that SOB were indeed present in these structures and made a preliminary report on how the populations may be arranged within them. Rein (2002) initiated studies on the application of these FSB in a bioprocess and noted the importance, and extreme

sensitivity of, the system to Redox potential across the narrow **E**h range. Although these studies provided indications that the abovementioned systems operate as "true" biofilms, even though they occur at the air/water interface instead of attached to a solid surface, many questions remain unanswered. An understanding of structural/functional relationships, in this system, and of their performance in sulphide oxidation and elemental sulphur production would greatly facilitate the development of this biotechnology.

1.4. THE STUDY OF BIOFILMS

Biofilms occur ubiquitously in aquatic environments and have been the subject of substantial attention in the last decade (Carpentier and Cerf, 1993; Costerton *et al.*, 1994; Vroom *et al.*, 1997; Davey and O' Toole, 2000; Wuertz, 2003; Okubo *et al.*, 2006). In the water treatment industry, biofilms are problematic due to adverse effects on water quality, pipeline corrosion, and disinfectant consumption (Ramesh *et al.*, 2006).

The study of these structures has been limited by the constraints of traditional microbial culture-dependent techniques, which do not allow exact localization of the organisms within the biofilm. Furthermore, these techniques often detect only a minor portion of the naturally occurring populations with spatial heterogeneity and aggregation increasing the uncertainty of enumeration (Okabe *et al.*, 1999a). The completely mixed stirred tank reactor (STR) has generally predominated in the basic studies of biofilms, and to some extent, has simplified the investigation of the microbial physiology and genetics of component organisms (Wuertz, 2003). However, pure culture planktonic growth is rarely how bacteria exist in nature, and commonly they occur in attached or aggregated forms in structured ecosystems (Davy and O' Toole, 2000, Johnson and Hallberg, 2005).

Carpentier and Cerf (1993) described biofilms simply as "a matrix, adhering to a surface". Costerton (1995) has provided a more comprehensive definition as "a structured community of bacterial cells enclosed in a self-produced polymeric matrix, adherent to an inert or living surface". Elder *et al.* (1995) described biofilms in cooperative terms as "a functional consortium of microorganisms organised within an

extensive exopolymeric substance (EPS) matrix". Dunne (2002) has commented that this description of biofilms is an oversimplification of a fairly complex process that does not take into account the type of microorganisms, composition of the surface, or the influence of environmental factors. However, what can be said is that there are three basic criteria underlying each of these definitions: microorganisms, glycocalyx or EPS matrix and surface (Costerton *et al.*, 1994; Elder *et al.*, 1995; Dunne, 2002).

It is important to note that a degree of functional organization and cooperation exists within the biofilm to allow interaction with the environment without compromising cell survival or exhausting available resources (Dunne, 2002). Zhang and Bishop (1994) have noted the spatially heterogeneous structure of these systems with complex groupings of cells organised along physical and nutrient gradients. Pores and channels occur within the biofilm allowing mass transfer into the internal structure from the outer surface and the bulk fluid surrounding the biofilm. While the initial colonizers of the surface will be mostly found within the biofilm closer to the attachment surface, the later colonizers and EPS production is mostly found at the bulk fluid/surface interface. Different species in the system could be either complementing or competing with each other for available nutrients, and later colonizers could utilise secondary metabolites produced by the initial colonisers and vice versa (Hermanowics, 2003; Wuertz, 2003).

The life of bacteria in a biofilm is different from that in the planktonic form in that bacterial biofilm communities develop internal heterogeneity (Zhang and Bishop, 1994; Wu and Janssen, 1996) and structural and functional relationships which are formed in response to environmental changes (Christensen *et al.*, 1999). The advantages of biofilm life forms include the higher availability of nutrients and the long-term positioning of microbial communities in relation to other communities (Nivens *et al.*, 1995; Watnick and Kolter, 2000).

Biofilms possess a general characteristic of being substantially more resistant than their planktonic counterparts to antimicrobial stressors such as antibiotics and host-defense responses (Gilbert *et al.*, 1997; Gilbert *et al.*, 2002; Parsek and Fuqua, 2004). This characteristic is enhanced by the reduced penetrability of the EPS matrix, commonly referred to as the slime layer or glycocalyx (Carpentier and Cerf, 1993).

This EPS matrix varies in composition depending upon the organisms present, and the type of environment, and is primarily produced by the microorganisms themselves (Davy and O' Toole, 2000; Dunne, 2002; Parsek and Fuqua, 2004). In most biofilms, the matrix is predominantly anionic and creates an efficient scavenging system for trapping and concentrating essential minerals and nutrients from the surrounding environment (Carpentier and Cerf, 1993; Dunne, 2002).

A white film adhering to the glass walls of a sulphide-rich reactor at the gas-liquid interface has been reported by Gadre (1989). These biofilms were thought to include SOB communities involved in the conversion of sulphide to elemental sulphur and their use as a means of final removal of sulphate in wastewater treatment was suggested (Janssen *et al.*, 2000). Rapid cycling of sulphur through both its oxidised and reduced forms within biofilms attached on membranes grown on domestic wastewaters has been documented by numerous authors (Kühl and Jørgensen, 1992; de Beer *et al.*, 1994; Goebel and Stackebrandt, 1994; Kolmert *et al.*, 1997; Okabe *et al.*, 1998; Yu and Bishop, 1998; Okabe *et al.*, 1999b). This cycling could play an important role in the overall reduction of the organic load in these systems. However, most work has focused on systems attached to solid substrates and the study of floating biofilms has not been described in any great detail as they occur at the interface between water and air.

Bacteria initiate biofilm development in response to specific environmental cues such as nutrient availability, and their formation may require coordination within, interactions of, and communication between multiple bacterial species (O' Toole *et al.*, 2000) indicating a symbiotic relation between the different species (Wuertz, 2003; Parsek and Fuqua, 2004). The key element in bacterial adaptability is their ability to position themselves in a niche where they can propagate (Dunne, 2002). Numerous methods of positioning have been described including flagella motility and different methods of surface translocation including twitching, darting and gliding (Davey and O' Toole, 2000). Some species are able to affect their position by synthesizing cellulose, thereby forming a fibrous pellicle that places cells near the air-water interface, and cellulose synthesis aids in attachment to surfaces such as plant cells (Ross *et al.*, 1991).

The positioning mechanism through aggregation or attachment enhances cell to cell interaction and the sedimentation rate of cells (Davey and O'Toole, 2000). Through attachment, bacteria can form communities and obtain the additional benefit of the phenotypic versatility of their neighbours (Hermanowicz, 2003). Where the different species can be symbiotically involved in attachment and EPS production, other species can easily aggregate around them. Additional species could produce by-products that provide nutrient sources for the members of the structure (Hermanowicz, 2003).

Wuertz (2003) noted that some films without an obvious attachment surface can form in extreme environments such as AMD where they are likely to contribute to sulphur cycling. Cyanobacterial mat biofilms have been studied in thermal hot springs (Ward *et al.*, 1998) and marine environments (Paerl and Pinckney, 1996).

The occurrence of the biofilms, although observed on the surface of sulphidic wastewater, has not been described in any detail. It is therefore imperative to investigate their structure, gain an understanding of their nature and physiological aspects, from which their function could be derived. This could lead to possibilities for manipulating these systems in wastewater treatment.

1.4.1 Biofilm Structure and Architecture

The characterisation of biofilm morphology is fundamental to an understanding of the interactions with the surrounding environment and the description of biofilm ecological structure is crucial for assessment of biofilm function (Hermanowicz, 2003). In this context, morphology refers to the geometric, physical form of the biofilm, whereas structure includes morphological features and also spatial distribution of different biofilm elements including various microbial populations, EPS and abiotic components (Hermanowicz, 2003; Wuertz, 2003). The dynamics of biofilm development, and the resulting structure, are dependent on the processes of attachment (deposition), growth, death and detachment (Wuertz, 2003). The rates of these processes and their importance may vary spatially and temporally (Hermanowicz, 2003).

1.4.2 Biofilm Diversity

Substantial phenotypic diversification occurs within biofilm communities (Parsek and Fuqua, 2004), which is a reflection of the micro-environments found within a biofilm. The biofilm phenotype is loosely defined as the patterns of protein and gene expression associated with biofilm growth in comparison to those associated with the planktonic growth (Parsek and Fuqua, 2004). Different gradients of oxygen and nutrients result in micro-niches and selective pressures, which produce variants with biofilm-specific phenotypes (Parsek and Fuqua, 2004). The resulting type of biofilm is determined by stage of development or maturity (Parsek and Fuqua, 2004). One of the variants, called the "Wrinkly" or "Sticky" variant is formed as small rough colonies on solid growth medium, and displayed as a hyper biofilm-forming phenotype on abiotic surfaces (de Beer and Schramm, 1999; Parsek and Fuqua, 2004). Examples of these have been reported in the literature for a number of species including *Salmonella enterica* (Parsek and Fuqua, 2004), and they exhibit heightened resistance to antibiotics and biocide bleach compared to biofilms formed by the wild-type parental strain (Parsek and Fuqua, 2004).

Different types of bacteria can leave a biofilm in a process that has been termed dispersion or dissolution, presumably achieved by coordinating the breakdown of the surrounding EPS matrix by secreted or cell surface-associated enzymes, with the activation of motility functions. This activity is thought to represent a final step in biofilm development, in which cells revert back to their planktonic state (Sauer *et al.*, 2002).

Taking into account the complexity of biofilm structure and function, their study has been heavily dependent on the development of appropriate techniques and as a result this has become something of an interdisciplinary field of enquiry.

1.5 TECHNIQUES USED IN THE STUDY OF BIOFILMS

1.5.1 Microscopy and Culture Techniques

Classical microscopic analyses relied on standard light microscopy using Gram and other staining methods for identifying microorganisms based on morphology. This

has severe limitations. The use of isolates in selective media and determining physiological parameters or chemotaxonomic markers has offered more progress (Wagner *et al.*, 1994). However, it has become apparent that only a limited number of microorganisms can be isolated from complex microbial populations, such as biofilms, by standard methods including enrichment and plating techniques (Wagner *et al.*, 1994; Lawrence *et al.*, 1994; Davey and O'Toole, 2000). Results from classical microscopy and culture techniques have thus offered a biased and incomplete view of the microorganisms present in such systems.

The application of confocal laser scanning microscopy (CLSM) to biofilm research has made a substantial impact on existing perceptions of biofilm structure and function. Prior to CLSM, electron microscopy (EM) was the method used to examine biofilms under high resolution. However, sample preparation for EM results in dehydration of samples, biofilm collapses, and a deceptively simplistic view of biofilm structures (Stewart *et al.*, 1995). CLSM has allowed the visualization of the three dimensional structure of fully hydrated biofilms, and has been used to monitor dynamic biofilm development in flow cells (Lewandowski, 1995). CLSM studies have shown that *in vitro* biofilms formed by single species exhibit similar overall structural features to those produced in nature by mixed species consortia (Stewart *et al.*, 1995). This includes a level of heterogeneity where aggregates are interspersed throughout an EPS matrix of various density, creating open zones where water channels are formed (Danese *et al.*, 2000).

The identification and quantification of members of a particular microbial community and a clearer understanding of the functional relationship between members is required to fully appreciate and possibly manage the complex processes that these communities perform. Examination of biofilm communities is complicated by the difficulty of identifying constituent biofilm members *in situ*, in quantifying physical, chemical and spatial aspects of biofilms and in linking processes and activity with specific biofilm bacteria (Okabe *et al.*, 1998). Molecular diagnostic tools such as phylogenetic analysis have contributed substantially to this task (Amann *et al.*, 1995; Head *et al.*, 1998; Santegoeds *et al.*, 1998; Davey and O' Toole, 2000).

1.5.2 Molecular Biology

Techniques based on the analysis of bacterial DNA and RNA may complement the conventional microbiological approach and now are routinely used to determine the presence and distribution of individual bacterial species in complex communities such as bacterial biofilms (Amann *et al.*, 1992; Ramsing, 1998; Raskin *et al.*, 1996; Santegoeds *et al.*, 1998; Chauke, 2000; Gilfillan, 2000; Bowker, 2002). Earlier molecular methods relied on the direct extraction, purification and sequencing of 5S ribosomal RNA (rRNA) from environmental samples. However, the limited length of the 5S rRNA molecule which is 120 base pairs (bp) long, did not allow for high resolution analysis (Head *et al.*, 1998). The use of 16S and 23S rRNA consisting of ~1 500 and ~3 000 bp respectively, contains sufficient information for a reliable phylogenic analysis of more complex communities (Amann *et al.*, 1995; Head *et al.*, 1998; Hugenholtz *et al.*, 1998).

Techniques used include polymerase chain reaction (PCR), degrading gradient gel electrophoresis (DGGE), hybridization and sequencing.

1.5.2.1 Polymerase Chain Reaction

Polymerase chain reaction relies on the use of oligonucleotide primers and DNA polymerase to amplify a targeted DNA sequence using temperature-controlled cycles which result in strand separation, primer annealing and primer extension, followed by viewing on an agarose gel (Head *et al.*, 1998; Amann *et al.*, 1995; Santegoeds *et al.*, 1998; Bowker, 2002). However, when used to selectively amplify a target in mixed DNA samples PCR can be biased as it is not quantitative. There is a possibility of preferential amplification of certain templates, rendering the representative assessment of natural abundance of the product genes inaccurate (Amann *et al.*, 1995; Santegoeds *et al.*, 1998). Selectivity in PCR amplification of rRNA genes is also a source of bias that can affect the results of molecular biological measures of diversity, where small differences in the sequence of universally conserved regions may result in selective amplification of some sequences particularly if primer annealing is at high stringency (Head *et al.*, 1998). The other concern could be that less abundant

sequences and high percentage G+C templates could be discriminated against (Head *et al.*, 1998).

1.5.2.2 Denaturing Gradient Gel Electrophoresis

Denaturing gradient gel electrophoresis technique is frequently applied to microbial ecology for comparison of the complex structure of microbial communities and to study their dynamics (Heuer *et al.*, 1999b). This technique employs separation of DNA fragments based on the length regardless of the different base-pair sequences. The partially denatured and melted DNA is separated according to the decreased electrophoretic mobility on a polyacrylamide gel (Muyzer *et al.*, 1993; Muyzer and Ramsing, 1995; Heuer *et al.*, 1999b).

1.5.2.3 Hybridization

Hybridization techniques use rRNA-targeted oligonucleotide probes to quantitatively determine the composition of complex microbial communities (Hugenholtz *et al.*, 1998). Ready to use species-specific probes are available for the identification of specific target organisms within mixed samples in their natural habitat (Amann *et al.*, 1995; Hugenholtz *et al.*, 1998). In cases where microorganisms are unknown, specific probes are designed using the cloned sequences obtained with the 16S rDNA approach.

Application of these probes in the dot blot (Raskin *et al.*, 1994; Lin and Stahl, 1995) or *in situ* techniques such as the *in situ* fluorescence hybridization (FISH) enables the detection and quantification of corresponding microorganisms present in a sample (Wagner *et al.*, 1993; Amann *et al.*, 1995; Daims *et al.*, 2001; Okabe *et al.*, 1999a).

Amann *et al.* (1995) investigated the micro-diversity in municipal activated sludge samples using rRNA-targeted probes. There was a concern that the method would provide misleading results since cultivation-independent comparative rRNA analysis relies on the PCR amplification of rRNA from nucleic acid extracts from environmental samples. This meant that at each step of the investigation, there would be several factors that could result in artificial sequence diversity in rRNA gene libraries. By using *in situ* probes and CLSM, the researchers were able to investigate

the potential for high micro-diversity in a natural microbial community without the selective bias of cultivation, extraction, or amplification (Amann *et al.*, 1995). Evidence for high micro-diversity was shown, indicating the presence of a relatively narrow phylogenic group in that environment.

1.5.3 Advances in Molecular Biology

Recent technological advances in the use of rRNA-based phylogenetic analysis provided a means of developing tools with which to investigate microbial communities (Amann *et al.*, 1992; O' Toole *et al.*, 2000). The tools including fluorescently labelled rRNA-targeted oligonucleotides, a variety of microsensors, real-time image analysis and CLSM, allow researchers to investigate biofilms *in situ* (Davey and O'Toole, 2000). One key advance has been the development of tools for cultivating communities such as chemostats, continuous flow slide cultures, microstats and colonization tracks (Davey and O'Toole, 2000).

Raskin *et al.* (1996) investigated the metabolically competitive methane-producing bacteria (MPB) and SRB in a biofilm reactor, and their relative response to sulphate availability. In this study the generally accepted notion that SRB and MPB were mutually exclusive in their natural habitats was questioned. It was found that the relation of the two communities was more complex than previously suggested and that SRB were selected for under high sulphate concentration whilst MPB were selected for in sulphate depleted environments.

The quantification of specific 16S rRNA compared to total 16S rRNA was used to monitor the two communities. In addition, sulphide and methane production were also assayed. It was found that, in the absence of sulphate, certain SRB types were present in high numbers (possibly due to the ability of certain SRB to function as fermenters or proton-reducing acetogens as previously reported by Hansen and Blackburn (1995). When sulphate was added, SRB levels increased and MPB and methane production levels decreased. These experiments illustrate how the rRNA-based approach can be combined with functional assays to monitor population dynamics in conjunction with metabolic changes in a biofilm community (Davey and O'Toole, 2000).

1.6 MICRO-ELECTRODES AND MICRO-SENSORS

The use of micro-electrodes has provided a breakthrough in the direct examination of the biofilm micro-zones *in situ*. These needle-shaped devices provide measurement in units of < 1µm and are made for the measurement of specific compounds such as oxygen, sulphide and Redox potential (de Beer and Muyzer, 1995; de Beer *et al.*, 1997; Santegoeds *et al.*, 1998; de Beer and Schramm, 1999; de Beer and Stoodley, 2006). Due to their small size, microsensor measurements cause minimal disturbance to the system and allows the examination of micro-environments and the measurement of micro-gradients (Santegoeds *et al.*, 1998; Lewandowski and Beyenal, 2003; de Beer and Stoodley, 2006). The measured gradients are a function of local transport processes (usually diffusion) and, if these transport processes are in control, the spatial distribution of microbial activity can be derived from the substrate profiles (Santegoeds *et al.*, 1998; de Beer *et al.*, 1997; de Beer and Stoodley, 2006).

Microsensors provide the opportunity to unravel closed cycles such as sulphate reduction coupled with sulphide oxidation within a biofilm (Kühl and Jørgensen, 1992). With microsensors, the measurement of *in situ* substrate consumption relative to product excretion can be measured in real time providing real time estimation of the process being investigated (Kühl and Jørgensen, 1992; de Beer *et al.*, 1997; Santegoeds *et al.*, 1998; de Beer and Stoodley, 2006).

The use of microsensors coupled with conventional molecular techniques has been employed to investigate the relation between species composition and the activity in a biofilm with gradually changing micro-environments (Santegoeds *et al.*, 1998; Okabe *et al.*, 1999a; Santegoeds *et al.*, 1999; Schramm *et al*, 2000). Microsensors with spatial resolution ~0.5 mm were used to measure oxygen and hydrogen sulphide profiles, and with this data, aerobic respiration and sulphate reducing activities were calculated (Okabe *et al.*, 1999b; Wuertz, 2003). The complexity of the microbial community in the biofilm and its behaviour over time was monitored with molecular techniques such as DGGE analysis of PCR amplified 16S rRNA fragments (Muyzer *et al.*, 1993 and 1995; Heuer *et al.*, 1999a; Santegoeds *et al.*, 1998; Okabe *et al.*, 1999b).

Studies combining the use of FISH with micro-electrode analysis for determining pH, oxygen and sulphide profiles have been reported to evaluate the distribution of different populations in relation to chemical profiles (Ramsing *et al.*, 1993; Schramm *et al.*, 1997; Okabe *et al.*, 1999a). The FISH technique was used in a study to localise organisms belonging to a microbial domain and various types of MPB in sludge granules (Harmsen *et al.*, 1996). It was shown that the outer layers of the granules were populated with a variety of bacterial colonies most likely involved in the hydrolysis of complex organic carbon, while the interior of the granule contained methanogenic micro-colonies (Harmsen *et al.*, 1996). These experiments provided convincing evidence of layered microbial architecture in sludge granules where the bacteria on the surface of the granule hydrolyze complex organic matter, providing the anaerobic bacteria in the interior of the biofilm with an energy source.

In a comprehensive study by Schramm *et al.* (1999), the use of microsensors (to measure oxygen, nitrite and sulphide concentration), in combination with CLSM (to determine a three-dimensional structure of the flocs), FISH and PCR specific primers for the dissimilatory sulphate reductase gene (to monitor the SRB population), was employed to investigate the occurrence of anaerobic processes such as denitrification and sulphate reduction in well-aerated activated sludge samples. It was discovered that anoxic micro-niches for SRB and denitrification activity could occur in well-aerated activated sludge, but this could be detrimental to the degradation of contaminants as a result of hydrogen sulphide production (Schramm *et al.*, 1999).

With the use of fluorescent probe hybridization, or staining cells with acridine orange (AO), researchers have been able to evaluate growth rates by determining cellular rRNA content (Davey and O'Toole, 2000). Therefore, using FISH combined with digital microscopy, cellular content of rRNA can be quantified and, thereby, the growth rate of cells can be estimated. Using this technique, Poulsen *et al.* (1993), discovered that in a young biofilm cells have a doubling time of 33 hours while in a mature biofilm the doubling time was increased to at least 70h. Rigler (1966) used AO staining to determine the RNA-DNA ratio. The need for isolation was eliminated as the AO-nucleic acid complex emits red-fluorescence when it is attached to a single stranded template and green-fluorescence if the nucleic acids are double stranded (Davey and O'Toole, 2000).

By combining FISH and specific enzyme activity probes to assign function to certain phylogenetic groups, Kloeke (1999) was able to determine that the Cytophaga-flavobacteria group was involved in the release of inorganic phosphate during wastewater treatment which contradicted the belief that these bacteria were not involved in phosphate removal (Bond *et al.*, 1995). In a study by Schramm *et al.* (1997), the use of CLSM, FISH and rRNA-targeted oligonucleotide probes provided a powerful tool to demonstrate micro-environments within a biofilm. It was possible to study the microbial interactions between ammonia and nitrite oxidizers, whose growth occurred in aggregates in close proximity to each other.

Although application of molecular techniques in microbial ecology has revolutionized the analysis of environmental samples and gave remarkable results, there are still limitations in their use. These include the reproducibility and therefore reliability of results obtained for biofilm samples. The selectivity of a particular species for PCR amplification is problematic when working with multi-species samples such as biofilms, where there could be inhibitors resulting in the preferential amplification of target DNA of some organisms rather than others (Liesack *et al.*, 1991; Reysenbach *et al.*, 1992). A specific limitation of the DGGE approach is that separation of PCR products obtained from a very complex mixture of microorganisms is problematic (Muyzer and Ramsing, 1995).

Speciation, identification and characterisation of the chemical states of elements in the environment (or unknown samples), is indispensable in determining the behaviour, bioavailability, and influence of elements on the quality of the environment (and the determination of composition of elements) (Takahashi *et al.*, 2004).

1.7 APPLICATION OF THE FLOATING SULPHUR BIOFILM REACTOR

As already noted, a substantial investment in sulphur systems biotechnology for the treatment of AMD (both active and passive systems) and industrial wastewaters has been made over a number of years (Rose, 2002). Biodesalination of these wastewaters requires that the sulphur-derived total dissolved solids (TDS), from a sulphate reduction treatment be finally removed from the treated stream (in its various forms) and, where this is recovered as elemental sulphur, a basis for a linearized waste treatment can be established.

Effective removal of total sulphur (in its various forms) remains a technological bottleneck in the widespread application of sulphur systems biotechnology (Younger *et al,* 2002; Coetser, 2004). The biological reduction of sulphate (in AMD) is well established in both passive and active AMD treatment systems. However the product sulphide (some of which is removed as metal sulphide precipitates) still need further removal (to prevent of its oxidation back to sulphate). Although the chemical removal of sulphide (Janssen *et al.*, 1999) and its biological oxidation in active systems is well established (Janssen *et al.*, 1998), the biological oxidation of sulphide in passive treatment systems is still limited (Coetser *et al.*, 2006). This is especially so in cases where the biological reduction of sulphate using lignocellulose-based carbon sources is concerned.

When the initial investigations into the biological oxidation of sulphide to elemental sulphur were undertaken at EBRU on low flow AMD systems targeted for passive treatment applications (preliminary study on microbial mechanisms underpinning sulphide oxidation in FSBs, WRC solicited programme, Project No. 1456) the sulphide generator (sulphate reduction system used to provide feed for sulphide oxidation) used sewage sludge as a carbon source (Gilfillan, 2000; Bowker, 2002; Rein, 2002). The subsequent challenge to EBRU was to investigate the oxidation of sulphide and potential process development in a lignocellulose-based sulphate reduction system (Innovation Fund and the WRC Project No. 1349) based on the successes of the passive biological sulphate reduction systems for AMD treatment using lignocellulose-based carbon sources (PHD, 2002).

While these application developments have been on-going, it has become apparent that little is known about the mechanisms involved in the formation of FSB systems. A shallow knowledge base underpins the possible application of this system, and competent mathematical modeling and up-scale engineering of the process will depend on developing a descriptive model accounting for the microbiological, chemical and biochemical determinants of the system.

1.8. AIMS

Based on this background the aims of the study were identified as follows:

1. Develop laboratory- and pilot-scale model systems which can be used to study the formation and productivity of FSBs under controlled laboratory conditions;
2. Describe the microbial ecology of FSBs;
3. Develop a descriptive model to account for the development and productivity of FSBs;
4. Evaluate appropriate reactor configurations incorporating the performance of the FSBs in the development of sulphide removal unit operations in mine drainage wastewater treatment.

Chapter Two

THE STRUCTURE OF FLOATING SULPHUR BIOFILMS

2.1 INTRODUCTION

Free floating biofilms have been described in the literature (Jørgensen *et al.*, 1998), and appear as pellicles (Marikawa *et al.*, 2006) composed of microorganisms with some surface to attach to, or aggregate on, such as diatoms and algal mats (Gaudes *et al.*, 2006).

Floating sulphur biofilms have been observed on the surface of tannery ponds and other sulphidic wastewater environments (Rose *et al.*, 1996; Dunn, 1998), however, no detail on their structure and physiological function has been described, and their role in these systems is not well defined. In literature, free floating biofilms have been reported to exist (Jørgensen *et al.*, 1998), and have been described as pellicles (Marikawa *et al.*, 2006) composed of microorganisms with some form of surface to attach to, or aggregate on, such as diatoms and algal mats (Gaudes *et al.*, 2006).

Observations made by EBRU researchers established an interest in the FSB and resulted in preliminary investigations into the possible role these structures could play in the treatment of sulphidic wastewater. Gilfillan (2000) reported possible structural differentiation of these biofilms while Bowker (2002) revealed the presence of a bacterial consortium and Rein (2002) investigated possible process design applications for wastewater treatment.

The objective of the study addressed in this chapter was to investigate the structure of the FSB and to determine whether the FSBs are indeed “true” biofilms. To achieve this objective, and since no methodology has previously been described for this purpose, the initial challenge involved the development and construction of a reactor environment in which the FSB could be cultivated under controlled laboratory conditions.

2.2 MATERIALS AND METHODS

2.2.1 Reactor Development

In order to study the FSB under controlled conditions, a 2-channel linear flow channel reactor (LFCR) was constructed and set up in a constant environment (CE) laboratory on which the FSB could be cultivated (Figure 2.1). This reactor comprised of two channels with a total surface area of 0.55 m^2 and a total volume of 0.022 m^3 (2.5 m x 0.11 m x 0.04 m). The shallow configuration of the reactor facilitated oxygen diffusion into the sulphidic water medium fed to the system.

Loading rates of between 1 309 and 2 618 $L/m^2/d^1$ were used for the FSB reactor feed and were selected empirically after a series of runs at different flow rates at which the biofilm was observed to form.

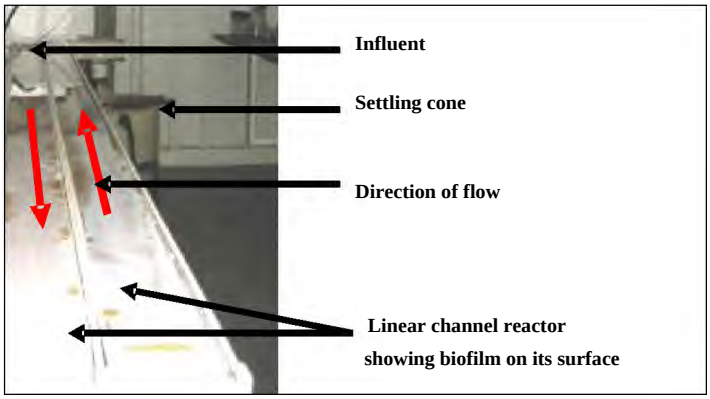

Figure 2.1 The linear flow channel reactor operating in a constant environment room showing the development of a Sticky floating sulphur biofilm on its surface.

Baffles were inserted to control the flow of the water directing it to above and below each baffle thus minimizing the mixing of the water as it flows through the reactor. The spacing of the baffles was 0.5 m apart in the channels and was arranged so that the water flowed alternatively over and under the baffles (Figure 2.2).

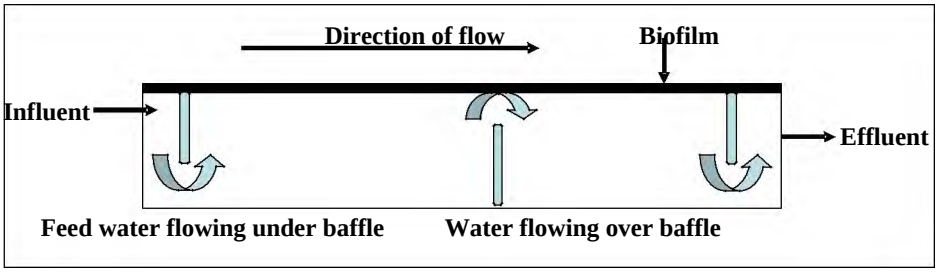

Figure 2.2 A longitudinal sectional illustration of the linear flow channel reactor showing the presence of baffles and the flow of water through the length of the channel.

The sulphide feed to the LFCR was drawn from a sulphide generating lignocellulose degrading packed bed reactor (DPBR) (Figure 2.3 and Figure 2.4) previously described by Coetser *et al. (*2005). The DBPR was packed with several layers of lignocellulosic carbon sources including hay, sewage sludge, bagasse and wood chips to form a sandwich (Figure 2.4). The bottom of the DPBR was packed with a layer of stone to act as a distribution manifold and it was fed with a 2 000 mg/L sulphate solution. The FSB developed on the surface of the LFCR.

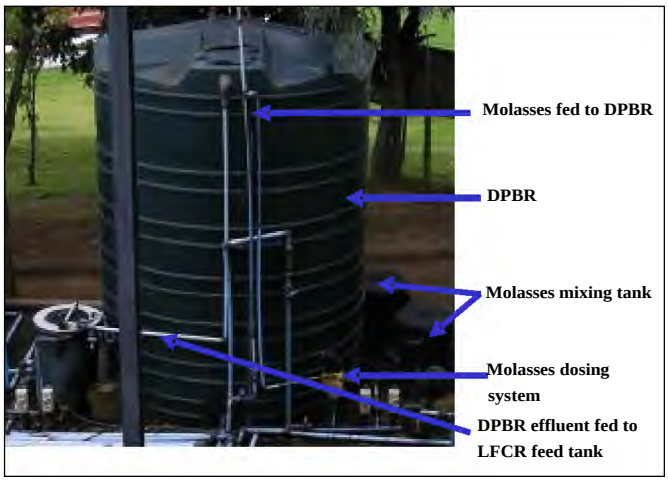

Figure 2.3 A lignocellulose degrading packed bed reactor used as a generator of sulphide containing feed for the linear flow channel reactor (Coetser *et al.*, 2005).

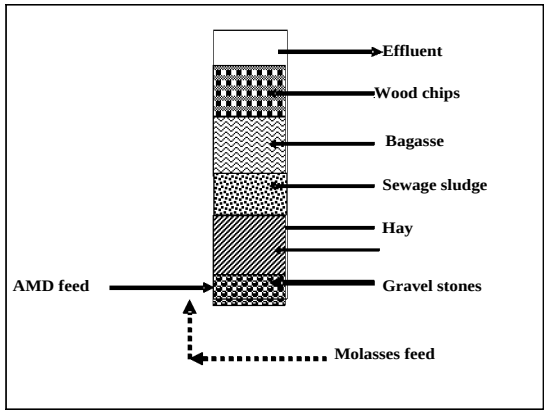

Figure 2.4 Longitudinal cross-sectional line diagram through the length of the degrading packed bed reactor showing various lignocellulosic carbon packing material (Coetser *et al.*, 2005).

Once operational, the FSB could be harvested every 8 to 24 hours, depending on its thickness. A number of harvesting methods were evaluated. Initially, the FSB was harvested by shutting the outlet valve, leading to a rise in the water level in the channel. The FSB was then floated off the surface into a settling cone (Figure 2.1), where it could be further drained of excess water and then dried. However, this resulted in a loss of material due to the break up of the FSB making it impossible to calculate a mass balance. Biofilm regeneration times were extended under this operating regime.

The second method entailed spraying a fine mist of water over the FSB surface which disturbed its surface tension and allowed the sulphur containing portion to fall to the bottom of the channel. A thin film remained on the surface of the water allowing rapid regeneration of a thick film. After numerous harvesting runs, the water in the channel was drained leaving the FSB sediment layer on the bottom of the channel. This was collected into settling cones where the residual water could be removed prior to drying.

2.2.2 Sampling

The samples of FSB were collected at each development stage by lifting off on a 0.2 µm nylon filter membrane. This was then prepared variously for examination by light microscopy, scanning electron microscopy (SEM), X-Ray fluorescence (XRF), X-Ray absorption near edge spectroscopy (XANES) and energy dispersive X-Ray (EDX) analyses.

The FSB sediment was collected and dried for three to five days at 80 ^{o}C in a drying oven, to obtain the dry weight. The dried FSB was used for sulphur determination and spectroscopic analysis.

2.2.3 Microscopy

Light and SEM analyses were carried out in the Electron Microscopy Unit (EMU), Rhodes University.

2.2.3.1 Light Microscopy

Floating sulphur biofilm samples collected at 4, 8, 12 and 18 hours for light microscopy analyses were heat fixed on microscope slides during Gram stain preparation and were used to visualize the cells present in the FSB at different development stages using an Olympus BX50 microscope.

2.2.3.2 Scanning Electron Microscopy

Due to the fragility of the thin FSB, a sandwich sampling technique was developed at EBRU (Gilfillan, 2000) to prepare material for SEM examination. This technique involved collecting the FSB on the surface of a 0.2 µm nylon filter and covering it with a similar filter. The sandwiched FSB and filters were stapled and then prepared for SEM. The method of Cross (2000) was followed for SEM sample preparation. Samples were compressed between "copper bookends" (Figure 2.5) for examination in a JEOL JSM B40 SEM.

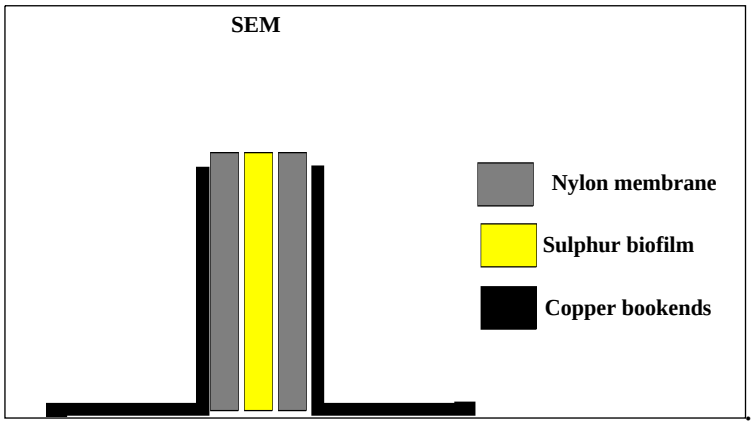

Figure 2.5 Schematic diagram of the "copper bookend" sample positioning system for sectioning samples for scanning electron microscope studies.

2.2.4 X-Ray Fluorescence Analysis

X-Ray fluorescence spectrometry analysis was undertaken using a Phillips PW 480 spectrometer. A rhodium tube provided the radioactive source and was operated at 40 kV and 70 mA. A fine collimator was used with the flow detector. The intensity of the kilo-counts per second (Kcps), which is determined by the sulphur element present in the sample, was measured against the 2 theta degrees ($2\theta^{o}$) related to the lithium fluoride crystal (LiF 220).

2.2.5 Determination of Biological Sulphur

A hexadecane-water partitioning test (Janssen *et al.*, 1999) was used to determine the wetting behaviour of biological sulphur and inorganic sulphur.

A 0.2 g of the sulphur standard (Sigma-Aldrich, SA) was mixed with 0.2 g of the dried FSB sample. The mixture was added to a test tube containing 1:1 mixture of water: hexadecane. The test tube was vortexed manually for 5 minutes and allowed to stand at room temperature until the layers had completely separated. The standard would remain in the upper hexadecane phase while sulphur of a biological origin would become partitioned in the lower water phase. The test is based on the hydrophobic nature of the surface of the inorganic orthorhombic S_8 crystals (Stuedel, 1996). The hydrophilic nature of the biological sulphur results from amphilic compounds covering the hydrophobic S_8 nucleus. These compounds are long-chain polythionates (SO_3-S_n-SO_3, n=5 – 20) (Steudel, 2000).

The separated products were removed from both the liquid and solvent phases and analysed qualitatively by reverse phase high pressure liquid chromatography (HPLC) (Mockel, 1984), on a 600 model Waters HPLC and a 2487 model dual λ absorbance detector fitted with a Nova-Pak® $_{C18}$ 3.9 x 150 mm column (Waters, South Africa). The samples were injected and run at 2 mL/min using a 5:95, water:methanol eluent (Hypersolv for HPLC, BDH from Merck, South Africa). A 20 ppm standard of elemental sulphur (Appendix B) in acetone was run for calibration and peak determination.

2.2.6 X-Ray Absorption Near-Edge Spectroscopy

Samples for XANES were analysed at Bonn University Institute of Biotechnology, by Prof Alexander Prange.

2.2.7 Energy Dispersive X-Ray Analysis

Sample preparation was similar to that described for SEM and was followed by the LEO energy EDX- SEM analysis. Imaging of the samples and analysis of phase composition was undertaken using a LEO® 1430VP SEM (Stellenbosch University). Samples were identified with back scattered electron (BSE) and/or secondary electron images, and phase compositions quantified by EDX analysis using an Oxford Instruments 133 KeV detector and Oxford INCA software. Beam conditions used during the quantitative analyses were 20 kV and approximately 1.5 nA, with a working distance of 13 mm and a specimen beam current of -3.92 nA. Despite the relatively low energy of the beam, X-Ray counts with the set-up used were typically ~ 5 000 cps. The counting time was 50 seconds live-time. Natural mineral standards were used for standardization and verification of the analyses. Pure Co, as well as Ti and Fe in ilmenite were used periodically to correct for detector drift. Beam conditions during semi-quantitative analyses, when used in the case of unpolished samples, were as described above and the specimen beam current was not controlled. The results were normalised to100 wt %.

2.3 RESULTS AND DISCUSSION

2.3.1 Floating Sulphur Biofilm Formation

During operation of the LFCR it was observed that the FSB appeared, formed and matured in three distinct stages (Figure 2.6). These were termed “Thin”, “Sticky” and “Brittle” biofilm based on observations of the FSB consistency.

The Thin FSB formed within two hours, where a thin and transparent layer on the surface of the water could be seen (Figure 2.6a) which was similar to that observed on the surface of tannery ponds in Wellington.

Figure 2.6 Photographs showing the developmental stages of the floating sulphur biofilm through the three distinct stages: a) Thin, b) Sticky and c) Brittle biofilm.

The Thin FSB thickened and within eight hours the transparent layer turned opaque. It was Sticky, and somewhat slimy and stuck to probes inserted into it. This was termed the "Sticky" FSB. In 12 to 18 hours, the Sticky FSB thickened to form a Brittle structure which breaks cleanly when disturbed. This was termed the "Brittle" FSB.

Cross-sectional measurement of the dry Brittle FSB averaged 50 to 60 µm, with the FSB structure collapsing once it was removed from the water surface presenting a problem for accurate measurement (Figure 2.7).

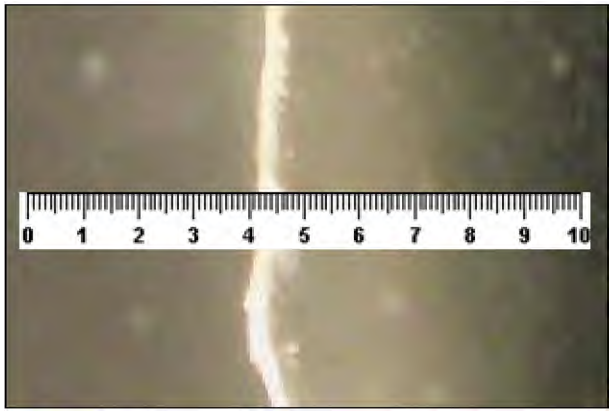

Figure 2.7 Cross section of the Brittle floating sulphur biofilm viewed under a dissecting microscope (X100 magnification) showing a structure that is 50 to 60 µm thick in its collapsed form following removal on a nylon filter.

After collection and drying of the sediment, the FSB formed a cream to yellow powder (Figure 2.8).

Figure 2.8 Dried floating sulphur biofilm sample from the harvested sediment accumulated at the bottom of the linear flow channel reactor.

2.3.2 Light Microscopy

Light microscopy examination of the FSB showed few distinct features for the different stages Thin to Brittle (Figures 2.9 to 2.12). The Thin FSB showed the presence of long-chained Gram positive streptococcal forms within large numbers of Gram negative cocci (Figure 2.9).

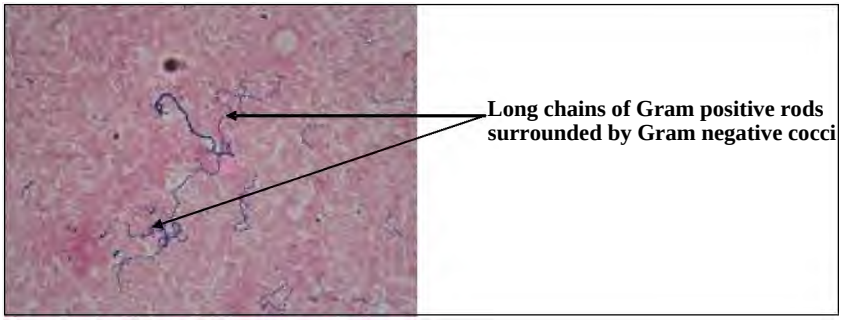

Figure 2.9 A representative Gram stain of the Thin floating sulphur biofilm showing long chains of Gram positive streptococcal forms surrounded by Gram negative cocci (1 000 x magnification).

As the FSB developed through the Thin-Sticky form, Gram positive streptococcal chains were less numerous than in the Thin FSB, while the Gram negative cocci predominated (Figure 2.10).

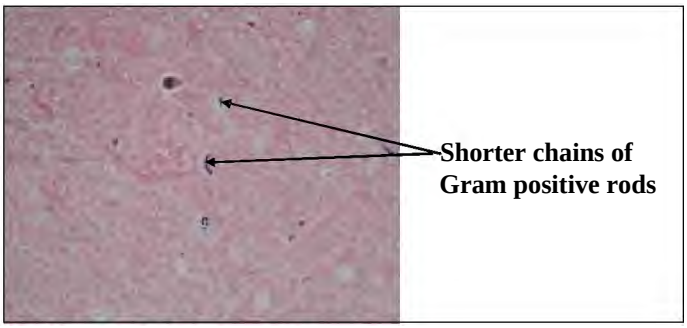

Figure 2.10 A representative Gram stain of the Thin to Sticky floating sulphur biofilm showing numerous Gram negative cocci and few Gram positive short rods and coccal forms under oil immersion (1 000 x magnification).

In the Sticky FSB, Gram negative inclusion bodies (circular shaped bodies) could be observed (Figure 2.11), while in the Brittle FSB large numbers of refractive granules appeared which were thought to be sulphur crystals (Figure 2.12).

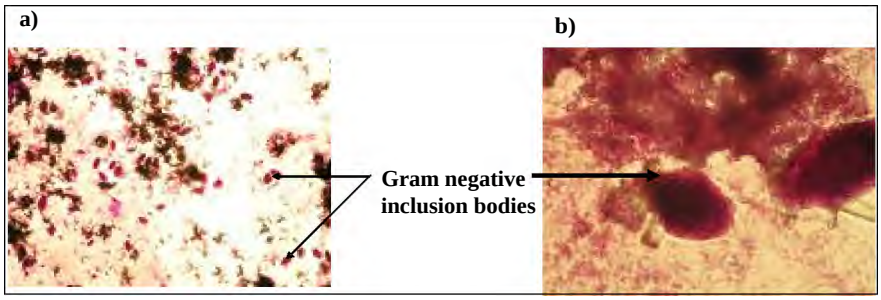

Figure 2.11 A representative Gram stain of the Thin to Sticky floating sulphur biofilm showing the presence of Gram negative inclusion bodies: a) 20X magnification; b) 80X magnification.

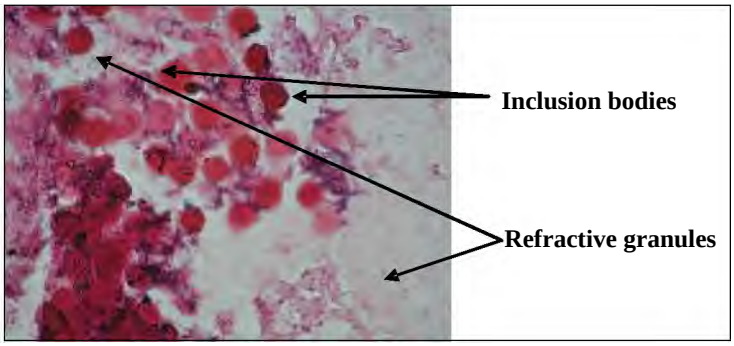

Figure 2.12 Representative Gram stain of Brittle floating sulphur biofilm showing Gram negative inclusion bodies surrounded by refractive granules (1 000 x magnification under oil immersion).

2.3.3 Scanning Electron Microscopy

Figure 2.13 shows an SEM micrograph of the copper bookend-nylon membrane sandwiched FSB.

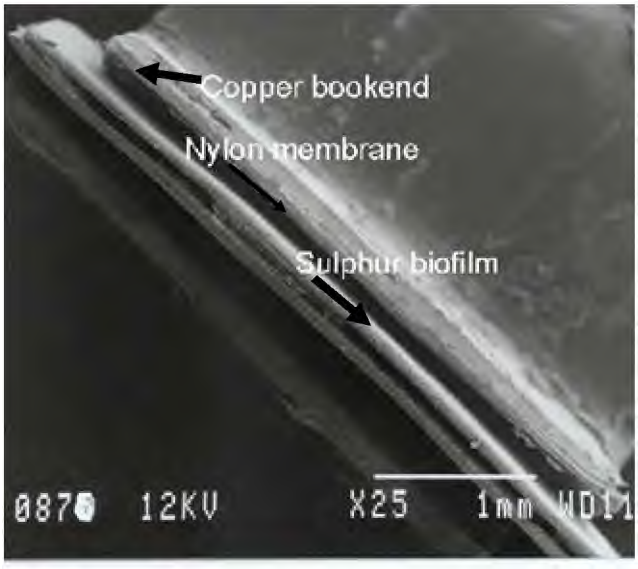

Figure 2.13 Scanning electron microscope micrograph of the "copper bookend" sample positioning system for viewing samples during scanning electron microscopic analyses. The nylon membrane is placed between the copper bookend and the biofilm.

SEM images of the Thin FSB show a mass of cocci and rods in the FSB (Figure 2.14).

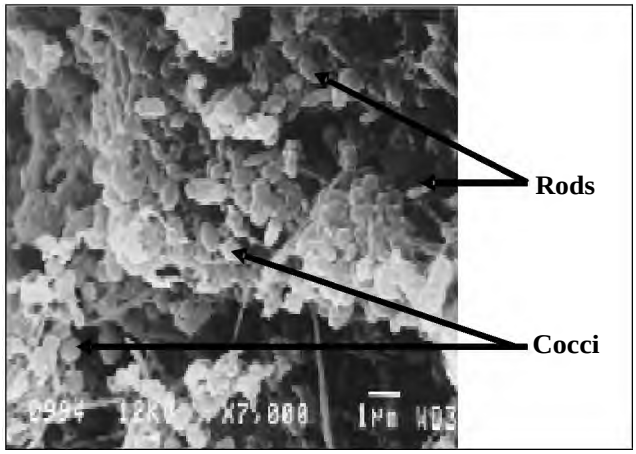

Figure 2.14 Scanning electron microscope micrograph of the Thin floating sulphur biofilm showing the presence of cocci and rods.

As the FSB progressed to the Sticky form, short rods predominated and the refractive bodies that were seen in Gram stain images (Figure 2.11 and Figure 2.12) were visible (Figure 2.15). The presence of channels and pores (Figure 2.15) in the EPS matrix (Figure 2.16a) are visible and suggest the structure of a true biofilm (Carpentier and Cerf, 1993; Costerton, 1995; Elder *et al.*, 1995; Dunne, 2002).

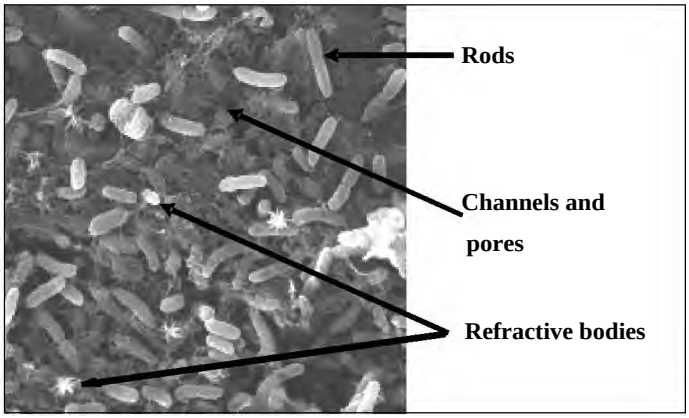

Figure 2.15 Scanning electron microscope micrograph of the Sticky floating sulphur biofilm showing numerous rods and refractive granules as well as channels and pores for mass transfer.

When ruptured, the earlier observed inclusion bodies (Figures 2.11 and 2.12) were observed to contain a mass of bacteria (Figure 2.16b).

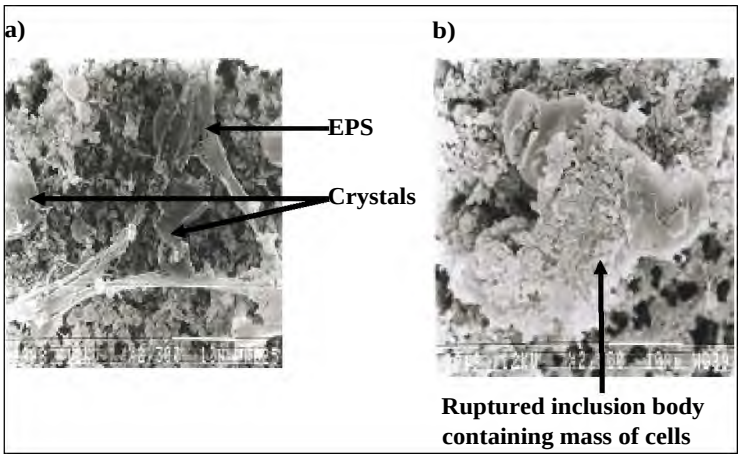

Figure 2.16 Scanning electron microscope micrographs of the Sticky floating sulphur biofilm showing: a) exopolymeric matrix binding bacteria and crystals together; b) ruptured inclusion body containing bacterial mass.

The SEM micrograph of the Brittle FSB shows numerous crystals of different sizes (2 to 20 μm), which appear to protrude from the FSB into the water phase (Figure 2.17). The smaller crystals were observed to lie within the bacterial EPS matrix (Figure 2.17 and Figure 2.18c), while the larger crystals were deposited outside the FSB (Figure 2.17 and Figure 2.18 b and c). The orthorhombic shape of the large crystals (Figure 2.18b and Figure 2.19) suggested that these were sulphur crystals of biological origin (Wantanabe, 1974; Rinaldi and Pawley, 1975; Hartman, 1984).

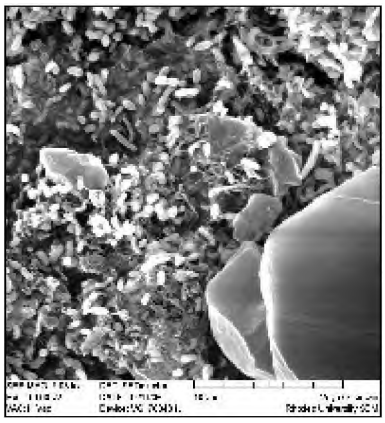

Figure 2.17 Scanning electron microscope micrograph of the Brittle floating sulphur biofilm showing smaller crystals firmly embedded within the exopolymeric matrix while the bigger crystals are protruding out of the floating sulphur biofilm.

Interesting observations in the Brittle FSB were the appearance of small vibrioid-shaped bacteria (Figure 2.18c -red arrow) and small globular forms (Figure 2.18c-blue arrow and Figure 2.19) too small to be bacterial cocci and, which are possibly sulphur globules. Vibrioids have been noted in the whitish veil that forms at the oxic-anoxic interface in sulphidic environments (Thar and Kühl, 2002). Ciliated protozoa (Figure 2.18e and f) were observed and ingestion of bacteria is indicated in the close-up view of a ruptured protozoan (Figure 2.19f) suggesting grazing of the FSB by these organisms.

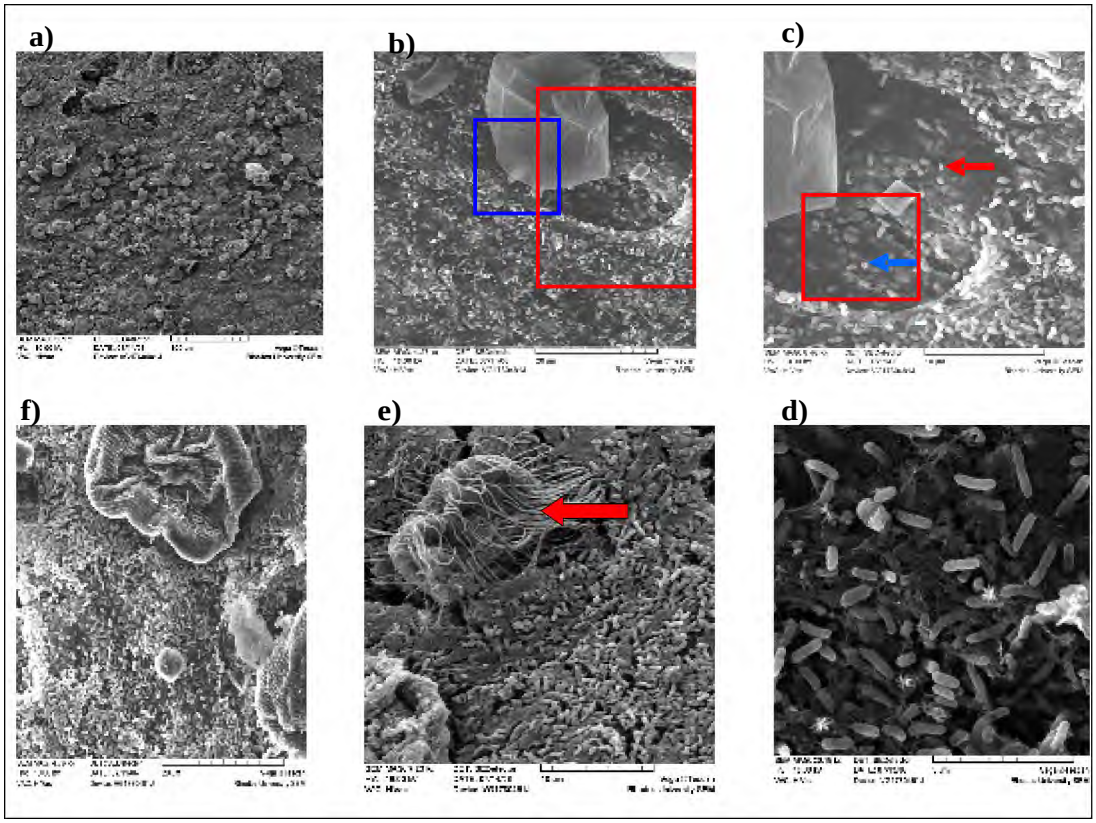

Figure 2.18 Scanning electron microscope micrographs of the Brittle floating sulphur biofilm showing: a) crystalline forms protruding from the biofilms; b) different sizes of crystals, including large orthorhombic crystals; c) bacteria and crystals held together in an exopolymeric matrix, a possible vibrioid bacterium (red arrow) and a possible biological sulphur globule (blue arrow); d) refractive structures (enlargement of red box in c); e) protozoa on the floating sulphur biofilm; f) ruptured protozoan with a mass of ingested bacteria revealed.

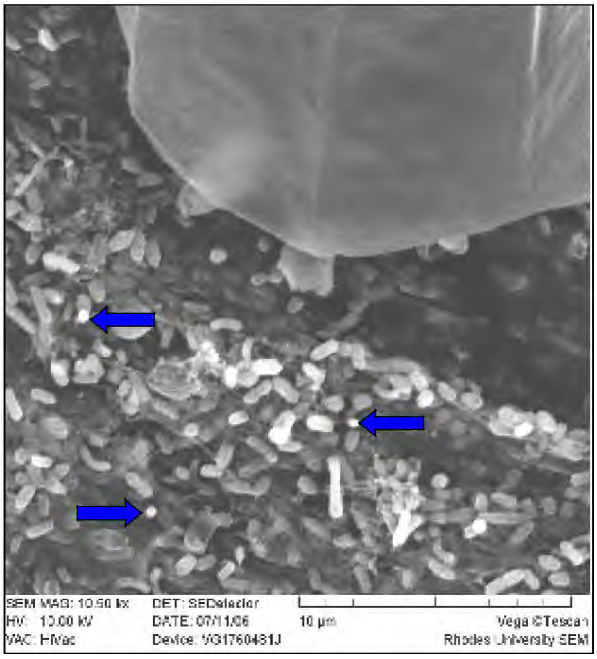

Figure 2.19 Enlargement of the blue box in the scanning electron microscope micrograph of Figure 2.18b of the Brittle floating sulphur biofilm showing a number of globules (blue arrows) visible in close proximity to the large crystal.

Channels and pores are clearly visible in the SEM image of the Brittle FSB (Figure 2.20). Also visible in this image are the large structures or inclusion bodies (10 µm diameter) which are thought to be protozoa.

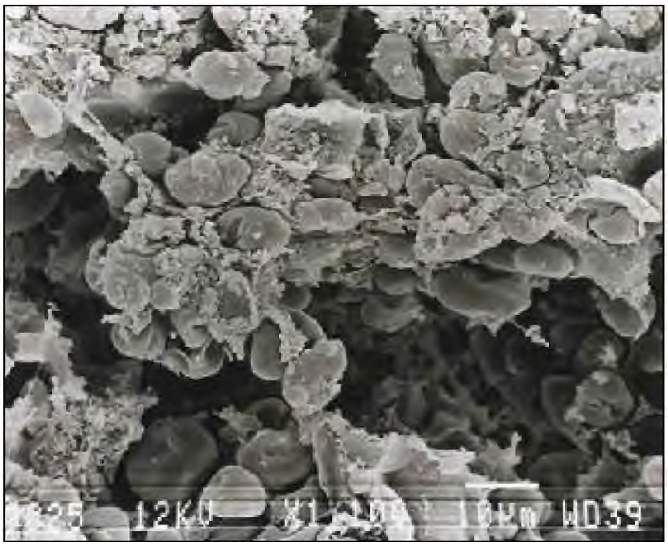

Figure 2.20 Scanning electron microscope micrograph of the Brittle floating sulphur biofilm showing a number of inclusion bodies held together in an exopolymeric matrix, and channels and pores for mass transfer.

2.3.4 X-Ray Fluorescence Spectroscopy

An XRF spectrum of the dried Brittle FSB confirmed the presence of sulphur which was detected at peaks K0 at 70.28° and the K**a** at 75.85° (Figure 2.21). Moreover, sulphur was found to be the dominant element in the FSB. However, the result is the sum of all sulphur species in the FSB as XRF can neither differentiate between oxidation states nor distinguish biological from inorganic forms of sulphur.

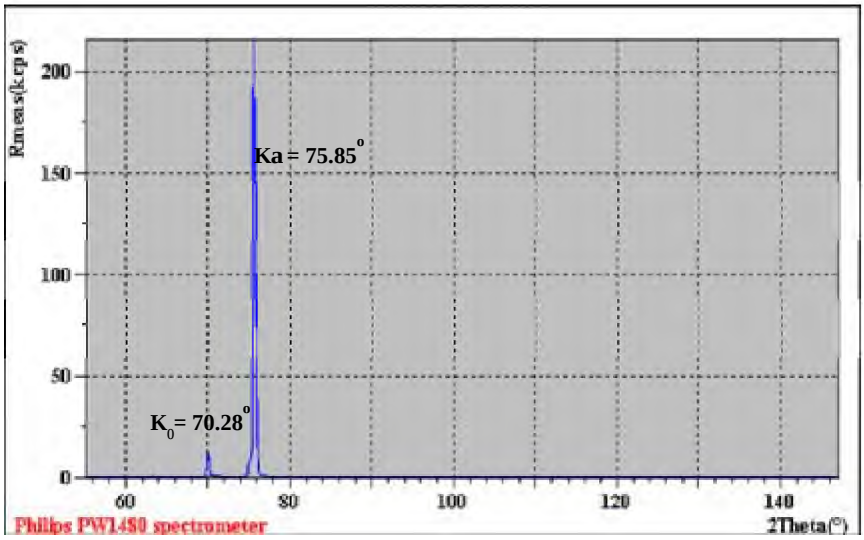

Figure 2.21 An X-Ray fluorescence spectrum of the dried Brittle stage of the floating sulphur biofilm showing the presence of the dominant sulphur peaks K0 at 70.28° and the K**a** at 75.85°.

2.3.5 Biological Sulphur Analysis

The water-hexadecane test showed that the dried Brittle FSB contained both an inorganic S_8 form which partitioned at the meniscus in the hexadecane phase, and a biological (organic) form that settled at the bottom of the test tube in the water phase (Figure 2.22). These results indicated the presence of more than one sulphur formation mechanism active in the FSB. The product in the water phase was confirmed to be sulphur using reverse phase HPLC.

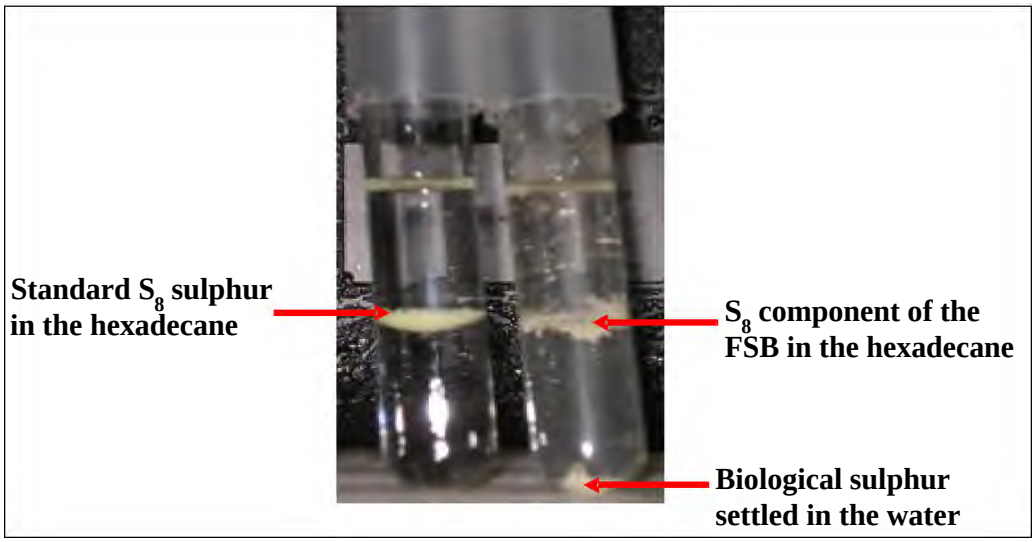

Figure 2.22 A photograph showing a hexadecane sulphur test where the left test tube shows the standard sulphur control and on the right is the dried Brittle floating sulphur biofilm.

2.3.6 X-Ray Absorption Near Edge Spectroscopy

The XANES image (Figure 2.23) as interpreted by Dr Prange showed that the dried Brittle FSB samples consisted of long chain polysulphide with no S_8-rings detected, while the wet Brittle FSB sample consisted of two sulphur atoms in the zero valence, probably as polysulphide chains and not S_8-rings. There was also a component with a valence below zero, associated with H_2S and an additional presence of a higher oxidised sulphur component associated with SO_2.

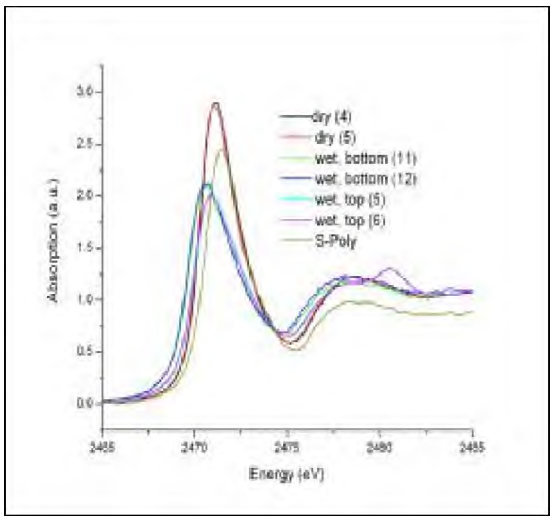

Figure 2.23 An XANES spectrum of dried and wet Brittle floating sulphur biofilm showing tested samples falling at the polysulphide peak (S-poly peak- showing the standard).

2.3.7 Scanning Electron Microscope - Energy Dispersive X-Ray Spectroscopy

The crystalline forms observed in the light microscopy and SEM images (Figures 2.12, 2.17 and 2.18) were provisionally identified as elemental sulphur, on the basis of the water: hexadecane partitioning test, and XRF spectroscopy. However, SEM-EDX analysis of the FSB samples provides an identity of the crystal-like structures analysed *in situ* and was used to confirm the presence of sulphur in the FSB system.

An EDX dot scan on a small part of the outer surface of a large crystal showed the crystal to consist of 100 % sulphur (Figure 2.24). A gold (Au) peak is also detected as a result of the gold coating used for SEM sample preparation.

A comparison of scans of small, medium-sized and large crystals (Figures 2.25 to 2.27) showed increasing amounts of sulphur (39 %, 45 % and 68 %) and decreasing amounts of carbon (59 %, 47 % and 26 %).

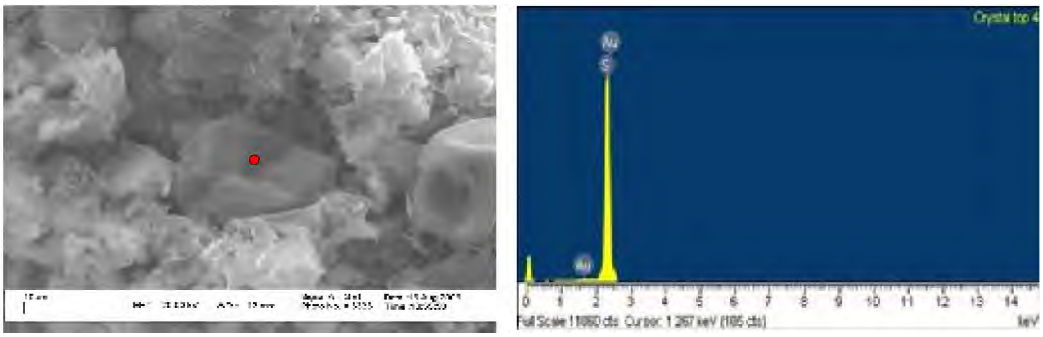

Figure 2.24 Scanning electron microscope micrograph and energy dispersive X-Ray spectrum of a crystal from the Brittle floating sulphur biofilm (spot area indicated in red). (S=100 %).

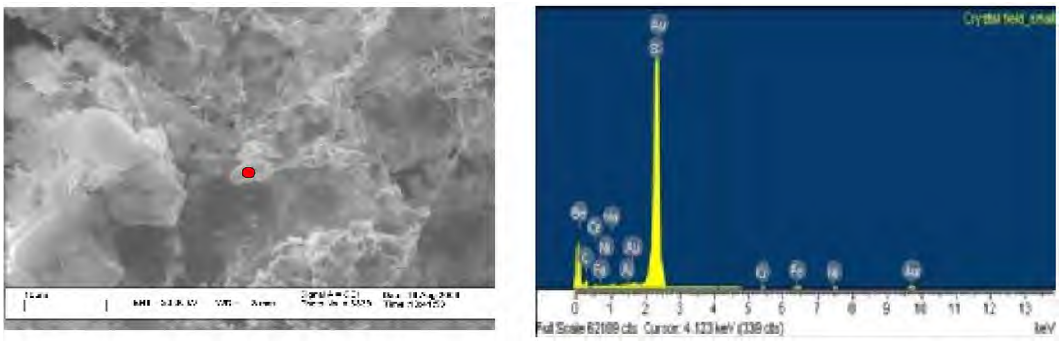

Figure 2.25 A scanning electron microscope micrograph and energy dispersive X-Ray spectrum of the small sulphur crystal (spot area indicated in red). (C=58.6 %, Na=0.342 %, Al=0.106 %, S=38.85 %, Cr=0.124 %, Fe=1.247 %, Ni=0.698 %).

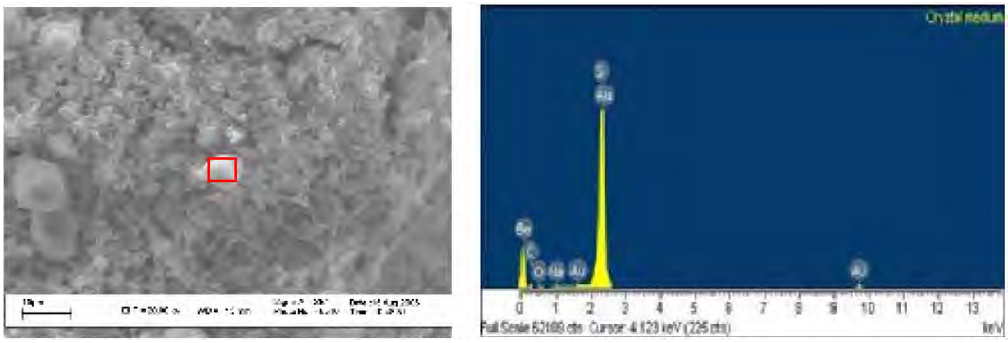

Figure 2.26 A scanning electron microscope micrograph and energy dispersive X-Ray spectrum of the scanned area of the medium crystal. (C=47.4 %, O=7.2 %, Na=0.25 %, S=45.16 %).

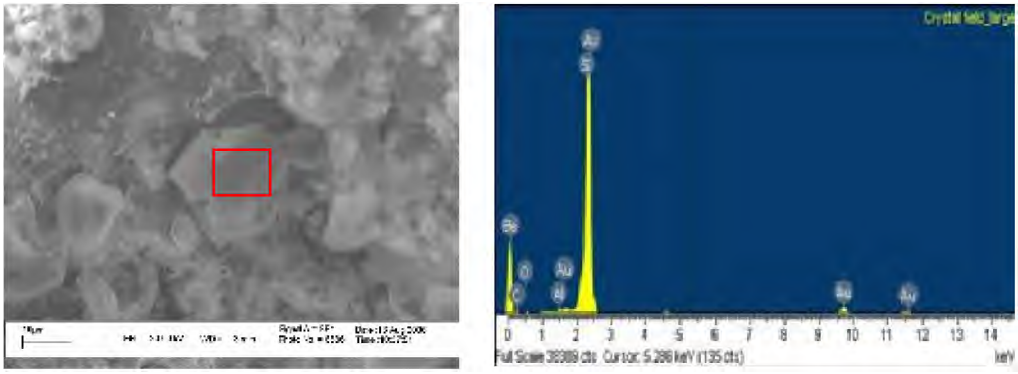

Figure 2.27 A scanning electron microscope micrograph and energy dispersive X-Ray spectrum of a large sulphur crystal (scan area indicated in red). (C=25.8 %, O=5.23 %, Al=0.185 %, S=67.79 %).

The above results raised the question whether organic carbon is incorporated into the crystal structure or whether a sheath or film of variable thickness covers the surface of the crystal. The micrographs and spectra presented in Figures 2.28 to 2.30 show the results obtained for the initial dot scan on a crystal, a square scan on the surface of a crystal which had been scarred by the EDX beam, and a dot scan on the scarred crystal. The initial dot scan (Figure 2.28) showed 34 % sulphur, 59 % carbon and 5.3 % oxygen. When performing a square scan to burn the outer surface off the crystal (Figure 2.29), the sulphur content was found to increase to 44 %, carbon decreased to 49 % and the oxygen decreased to 5.8 %. A subsequent dot scan on the scarred crystal surface showed a sulphur content of 95 % and oxygen further decreased to 3.2 % (Figure 2.30). These results indicate that the crystals are covered with an organic carbon film, decreasing in thickness as the crystal grows.

It is probable that the film of organic carbon which covers the crystal would have rendered the FSB sulphur hydrophilic, so that it partitioned into the water phase with the hexadecane extraction. However, the question whether the refractory globules observed in Figure 2.18c and Figure 2.19 contained sulphur could not be resolved by

SEM-EDX due to a constraint in the smallest particle size range that could be measured. It was thus not possible to confirm whether the globules contained sulphur and whether these were derived from sulphur bacteria as has been suggested in Figure 2.15 and Figure 2.18.

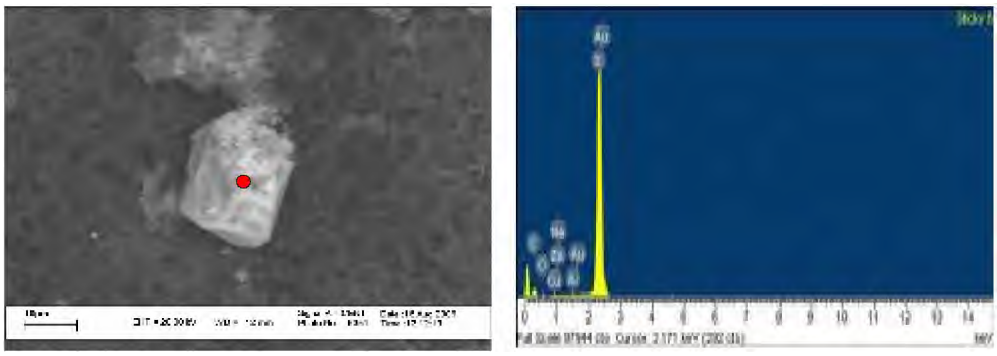

Figure 2.28 A scanning electron microscope micrograph and energy dispersive X-Ray spectrum of a dot scan on a large sulphur crystal from the Sticky floating sulphur biofilm. (C=58.6 %, O=5.311 %, Na=0.076 %, Al=0.042 %, S=34.36 %, Cu=0.378 %, Zn=0.233 %).

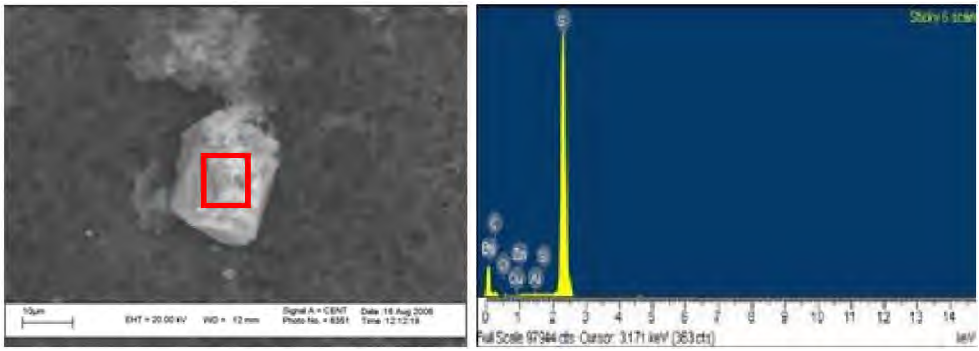

Figure 2.29 A scanning electron microscope micrograph and energy dispersive X-Ray spectrum of a square scan used to burn off the surface of a large sulphur crystal from the Sticky floating sulphur biofilm. (C=48.9 %, O=5.8 %, Na=0.076 %, Al=0.042 %, S=44.3 %, Cu=0.378 %, Zn=0.233 %).

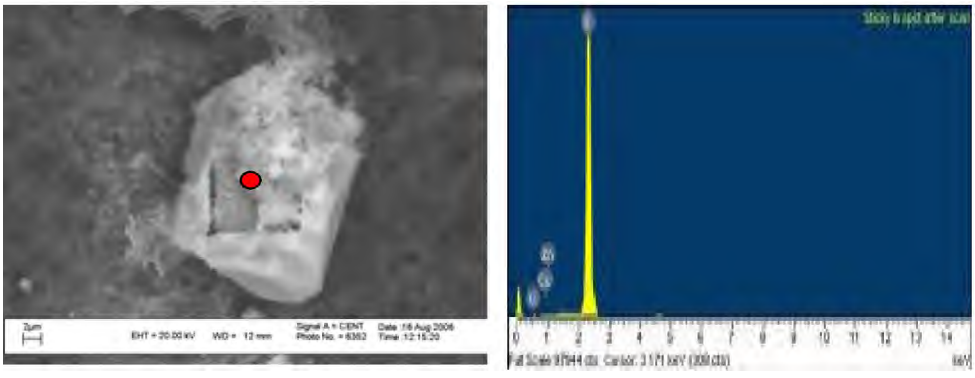

Figure 2.30 A scanning electron microscope micrograph and energy dispersive X-Ray spectrum of a dot scan on the burnt surface of a crystal from the Sticky floating sulphur biofilm. The scan area is visibly damaged from the X-Ray. (O=3.16 %, S=95.2 %, Cu=0.93 %, Zn=0.71 %; C= 0).

However, scanning the FSB matrix a distance away from the crystals showed that sulphur was also present in a dispersed form across the FSB although the concentrations were lower (Figure 2.31 and Figure 2.32). Figure 2.31 is an EDX scan of the EPS matrix at a lower magnification showing 10 % sulphur, 73 % carbon and 16 % oxygen.

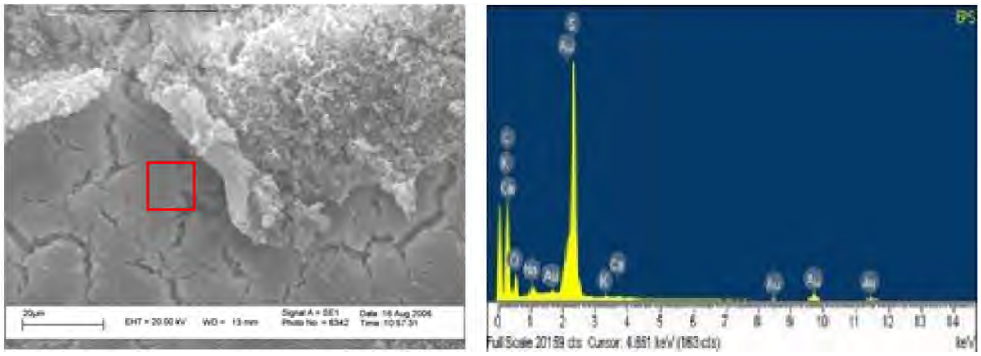

Figure 2.31 A scanning electron microscope micrograph and energy dispersive X-Ray spectrum of the exopolymeric matrix on the Brittle floating sulphur biofilm. (C=72.8 %, O=15.7 %, Na=0.76 %, S=9.45 %, K=0.11 %, Ca=0.13 %).

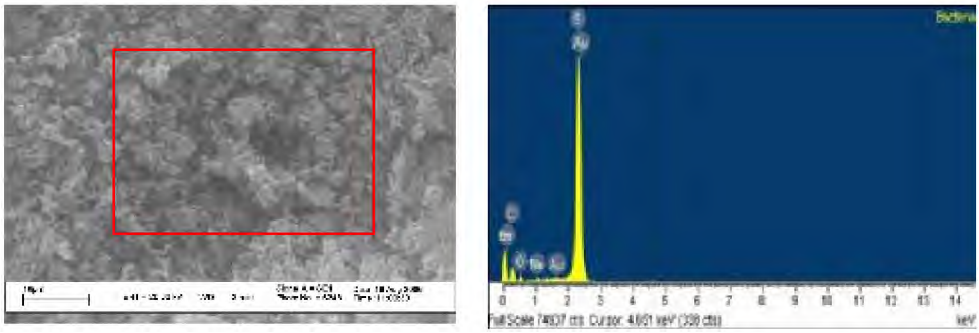

Figure 2.32 Scanning electron microscope micrograph and energy dispersive X-Ray spectrum of an area of the Brittle floating sulphur biofilm containing bacteria only. (C=62.65 %, O=11.2 %, Na=0.3 %, S=25.89 %).

Observation at a higher resolution (Figure 2.32) showed 26 % sulphur, 63 % carbon and 11 % oxygen, indicating the dispersal of sulphur in the FSB. The EDX scan in Figure 2.33 confirms a high carbon composition around the protozoan of 78 %, while sulphur and oxygen was 14 % and 8 % respectively. This further suggested that the protozoa were active in grazing of the FSB and thus ingesting dispersed sulphur, possibly in the form of globules attached to sulphur bacteria.

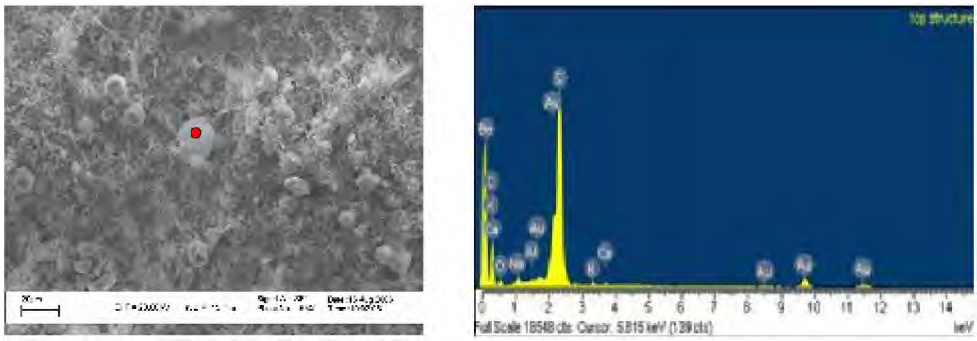

Figure 2.33 A scanning electron microscope micrograph and energy dispersive X-Ray spectrum of a protozoan. (C=77.6 %, O=7.9 %, Na=0.58 %, Al=0.10 %, S=13.5 %, K=0.14 %, Ca=0.15 %).

Figure 2.34 further illustrates the observation of the dispersed sulphur component of the FSB and shows a fairly high resolution SEM of a protozoan (blue arrow and potentially having mainly a carbon and oxygen composition) and nearby sulphur crystals (yellow arrow) against the background of the EPS/bacteria matrix. The SEM was then scanned differentially for sulphur (Figure 2.34b) and carbon (Figure 2.34c) separately. The sulphur scan (Figure 2.34b) shows that sulphur is fairly evenly distributed across the FSB, although richer in content in the region of a crystal in contrast to the low sulphur content in the region occupied by the protozoan (black negative zone).

The carbon scan (Figure 2.34c) showed the inverse of the sulphur scan, that is, the highest carbon content was observed in the region occupied by the protozoan with much less across the remainder of the FSB. This further indicates that sulphur is distributed across the EPS/bacteria matrix, and may be associated with the presence of small sulphur granules which account in part for the biological sulphur present in the system. Crystals of sulphur form and grow within the system.

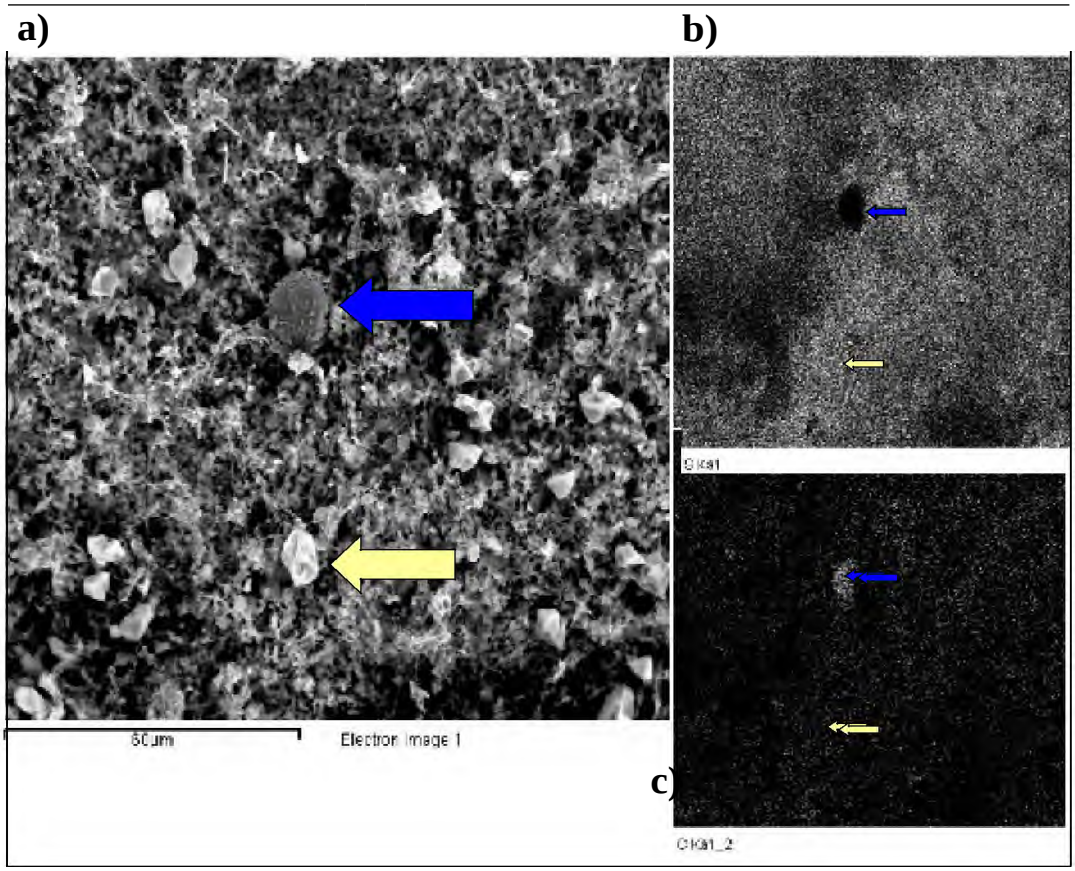

Figure 2.34 An X-Ray spectrum map of the area displayed in the scanning electron microscope micrograph of a Brittle floating sulphur biofilm comprised of crystals, protozoan, bacteria and exopolymeric matrix (a) showing sulphur content (b) and carbon content (c) after specific sulphur and carbon specific energy dispersive X-Ray scans in (b) and (c) respectively.

2.4 CONCLUSIONS

The following conclusions were drawn from this study.

- Light microscopy investigation of the structure of the FSB showed that it was largely composed of both Gram positive and Gram negative bacteria in the Thin FSB stage;
- SEM studies confirmed the presence of orthorhombic and crystalline structures in the FSB. This was associated with the granular nature of the Brittle FSB. The presence of sulphur in the FSB was confirmed by XRF spectroscopy, and the water:hexadecane partition test indicated that biologically produced sulphur is present in the FSB;
- EDX findings confirmed the crystal-like structures observed in the SEM images to be sulphur and were covered by a film of organic matter;
- The growth of the crystals within the FSB is indicated by the size distribution range observed;

- The presence of sulphur bacteria and the association with refractory globules observed could not be confirmed in these studies;
- The observation of protozoa possibly grazing on the bacterial/EPS matrix suggested that this may be associated with the ingestion and break up of sulphur bacteria and their sulphur globules, thereby contributing to the dispersal of sulphur across the FSB;
- Follow-up studies would be required to confirm the presence of sulphur bacteria in the FSB;
- The complexity of the FSB system, the incorporation of bacteria within an EPS matrix with pores and channels, and its occurrence on a surface (albeit usually at the air/water interface), indicated that the FSB were “true” biofilms.

Chapter Three

MICROBIAL ECOLOGY OF FLOATING SULPHUR BIOFILMS

3.1 INTRODUCTION

Identification and quantification of the members of a particular microbial community in a biofilm and a clearer understanding of the functional relationships that exist between its members, is required to fully appreciate, and possibly manipulate, the complex processes that these communities perform (Davey and O'Toole, 2000). Examination of biofilm communities is complicated by methodological problems in identifying its constituent members *in situ*, in quantifying physical, chemical and spatial distributions and in linking processes and functional activity with specific microorganisms (Hermanowicz, 2003).

The application of molecular methods has revolutionized the routine identification of bacteria from environmental and industrial samples (Amann *et al.*, 1990; Head *et al.*, 1998; Santegoeds *et al*, 1998; Davey and O' Toole, 2000; Wuertz, 2003). Techniques based on the analysis of genetic material are currently used to complement conventional microbiological approaches and to determine the presence and distribution of individual bacterial species, including those in complex communities (Santegoeds *et al.*, 1998, Wuertz, 2003).

The study reported in the previous Chapter indicated the complexity of the FSB structure and that these were "true" biofilms. Spatial arrangement showed the presence of channels and pores. This chapter deals with the investigation of the microbial ecology of the FSB and identification of the main population groups that occur within the FSB system.

3.2 MATERIALS AND METHODS

3.2.1 Reactor Development and Sampling

The FSB for this study was cultivated in the LFCR fed by AMD treated in a DPBR (Chapter 2). Floating sulphur biofilm samples were collected at the three distinct phases

of development (Thin, Sticky and Brittle FSB) in sterile 1.5 mL microfuge tubes (Eppendorf) and stored at -20 ^{o}C before total DNA extraction.

3.2.2 Gradient Tube Method Development

A high resolution sampling of the FSB, so that the population distribution across the FSB can be identified, is complicated by the small cross section of the FSB (50 to 60 μm dry Brittle FSB). To address this problem, a method was developed to provide a spatial expansion of the functional physiological compartments occurring within the FSB. This involved establishing an oxygen/sulphide gradient set up in agarose in a test tube (Figure 3.1) the so-called Gradient Tube method (Bowker, 2002).

The FSB sample was thoroughly mixed in agarose and then poured into a 13 cm glass test tube on top of a sulphide plug (Appendix A). The test tubes, although capped were open to atmosphere and an oxygen/sulphide gradient was allowed to establish along the length of the 10 cm agarose overlay (Figure 3.1).

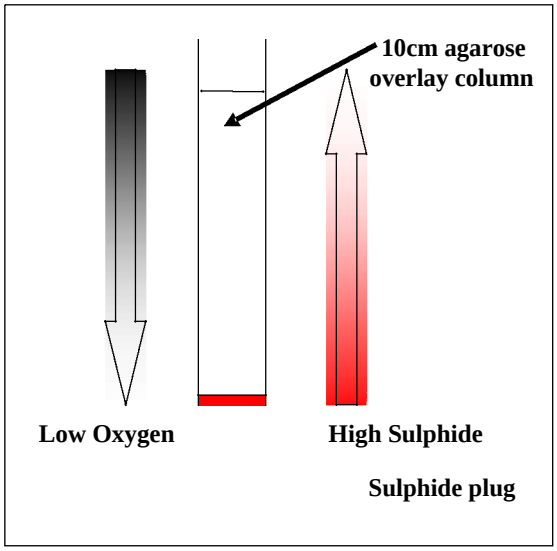

Figure 3.1 Illustration of the Gradient Tube system in which a sample of the floating sulphur biofilm is suspended in a 10 cm agarose overlay column in a test tube. Sulphide diffuses upwards from the sulphide plug in the bottom of the tube and oxygen diffuses downwards from its open top**.**

After incubation at 20 ^{o}C for five to eight days, the test tubes were harvested by extracting the agarose column. The base of the test tube was cracked carefully while

maintaining the integrity of the contents. The agarose overlay column was then extruded and the samples cut into 0.5 cm sections and collected in sterile 1.5 mL microfuge tubes (Eppendorf) and stored at -20 ^{o}C. DNA extraction was undertaken for each section and molecular typing and phylogenetic analysis was used (methods described below). Gradient Tubes were prepared using FSB samples collected at each of the three distinct stages of development (Thin, Sticky and Brittle). The experiment was conducted in triplicate at each stage.

3.2.3 DNA Extraction

The total DNA extraction method according to Sambrook *et al.* (1989) was applied to the sliced Gradient Tube samples. As the samples were in a gel, the first step involved placing the samples in a water bath (Labcon) at 55 ^{o}C to melt the agarose. Glass beads were added to the samples before vigorous shaking on a vortex Genie-2 (Scientific Industries). The samples were then collected in 1.5 mL microfuge tubes (Eppendorf, Merck, South Africa), concentrated by centrifugation at 13 000 rpm for five minutes in an Eppendorf 5415D desktop centrifuge prior to following the DNA extraction method (Sambrook *et al.*, 1989). The extracted DNA was electrophoresed on a 0.8 % agarose gel (Appendix A) containing 100 µl of ethidium bromide for visualization in a UV transilluminator (UVP BioDoc-It^{TM}) fitted with a digital camera. A λ Pst1 molecular weight marker was used to detect the molecular weight of the product.

3.2.4 Polymerase Chain Reaction

The PCR reaction was performed using a universal 16S primer GM5F (Appendix A) and a GC clamped primer 907R from Inqaba Biotec. The enzyme used was Taq DNA polymerase (Promega) at a concentration of 0.5 µl per 25 µl reaction. A 2.5 µl aliquot of buffer containing magnesium chloride ($MgCl_2$) was added per 25 µl reaction (Appendix A). In cases where the $MgCl_2$ concentration was adjusted, 2.5 µl of buffer without $MgCl_2$ was added per 25 µl reaction and the volume of water added was adjusted accordingly to give a final volume of 25 µl. Each of the four deoxynucleoside triphosphates (dNTPs) (Inqaba Biotech) was added to a final concentration of 1 µl per 25 µl reaction. The

reaction was made up to 25 µl with a calculated volume of autoclaved pure water (Sigma).

Amplification was performed on a Hybaid PCR Sprint thermocycler using a touch-down PCR procedure (Appendix C). The PCR product was analyzed on 1 % agarose gel containing ethidium bromide and visualized on a UV transilluminator (UVP BioDoc-It™ system) fitted with a digital camera. Bands were cut out from the gel and purified using QIAprep® spin miniprep Kit (Qiagen).

3.2.5 Denaturing Gradient Gel Electrophoresis

The DGGE method according to Myers *et al.* (1987) was applied for the high probability detection of any differences between two sequences. The technique was based on the reduction in DNA fragment mobility in a dense medium when part of the double helix unravels. Strand separation was induced by using different concentrations of the denaturants, formamide and urea, made up to 50 mL (Appendix A).

For the purpose of this study, the DGGE gels used a 55 to 65 % denaturant gradient prepared from the 100 % denaturant stock. The gradient increased from the top to the bottom of the gel, parallel to the direction of electrophoresis. During electrophoresis the chemical denaturants induced strand separation of the DNA fragments, while the high temperature 65 ^{o}C melted the DNA fragments for easier separation. The fragments were analysed on a 6 % acrylamide gel (Appendix A) from Sigma-Aldrich. The gradient was prepared in a BIO-RAD Model 385 gradient former.

The system used for electrophoresis was a 10 x 10 Protean 5 vertical electrophoresis unit (BioRad). A 1 x TAE buffer was used for electrophoresis at 65ºC and 120 V for two hours. To obtain the different bands that had formed on the gel, a silver staining system from BIO-RAD was used as per manufacturer's instructions. The bands were visualized on a UV transilluminator (UVP BioDoc-It™ system) fitted with a digital camera. After visualization, the bands were excised with sterile scalpel blades, into sterile 1.5 mL

microfuge tubes (Eppendorf) containing 200 µl TE buffer. These were kept at -20 ^{o}C for further use in cloning and sequencing.

3.2.6 Transformation and Cloning

The excised PCR product was extracted using phenol:chloroform:isoamyl alcohol (24:24:1), re-amplified by PCR and confirmed by subsequent DGGE that the product consisted of a single band. The re-amplified PCR product was cloned into the pGEM® -*T* Easy Vector system (Promega, USA) as per manufacturer's instruction, and transformed into high efficiency *E. coli* JM 109 competent cells from which extracted plasmid was prepared for sequencing.

The transformants were screened on Luria Bertani (LB) agar plates containing 100 µg/mL ampicillin (Amp). Before plating, the LB/Amp plates were spread with IPTG and X-Gal after which they were incubated overnight at 37 °C (Appendix A). Transformants with an insert in the **β**–glycosidase gene appeared white on the X-Gal plates as opposed to blue colonies which have a plasmid but no insert in the **β**–glycosidase gene. The white colonies were picked with a sterile toothpick, inoculated into 5 mL LB broth and incubated in a shaker overnight at 37 ^{o}C. The plasmid was extracted using Qiagen® plasmid extraction kit according to the manufacturer's instruction.

To confirm the presence of the insert, EcoR1 digestion of the transformed plasmid was performed. EcoR1 was expected to cut on either side of the 568 bp fragment, resulting in two bands on a gel, one a 3 018 bp plasmid fragment and the other a 586 bp insert. Plasmids with the correct insert were prepared for sequencing.

3.2.7 Sequencing

Plasmids containing inserts were sequenced using Big Dye Terminator 3 sequencing kit (Applied Bio systems) with 100 to 200 ng of template DNA according to the manufacturer's instructions. Sequences were obtained by using a universal sequencing primer T7 or SP6 (Integrated DNA Technology (IDT), USA). Cycle sequencing was

performed on a Perkins Elmer (Applied Biosystems) 9700 thermocycler. The products were purified using DNA Clean & Concentrator TM-5 columns (Zymo Research, USA) as per manufacturer's instructions. The eluted DNA was dried at 37 °C and then stored at 4 °C until sequenced. DNA sequence was determined on an automated ABI 3100 Prism® Genetic Analyzer at Rhodes University, South Africa.

3.2.8 Phylogenetic Analysis

Chromatograms were generated by the ABI PRISM Genetic Analyser Data Collection system 2.0.1 by Applied Biosystems. These chromatograms were converted into text format using Gene Tools and then put into the National Centre for Biotechnology Information Basic Local Alignment Search Tool (NCBI BLAST) database. BLAST is a set of similarity search programs designed to explore all of the available sequence databases (Altschul *et al.*, 1997). The percentage similarity to an identified species was recorded, also the length of the match and the E value, which is important for determining the accuracy of the result. To obtain the phylogenetic relationship between the clones, the data was analyzed using the Neighbor Joining (*N*-J) algorithm.

3.3 RESULTS AND DISCUSSION

The data obtained from the molecular microbial analysis of the Gradient Tube system and for total FSB samples were compared to identify similarities and differences in the interpretation of the phylogenetic results.

3.3.1 Gradient Tubes

After incubation for five to eight days in a sterile hood, a range of clearly identifiable bands were observed in the Gradient Tubes (Figure 3.2).

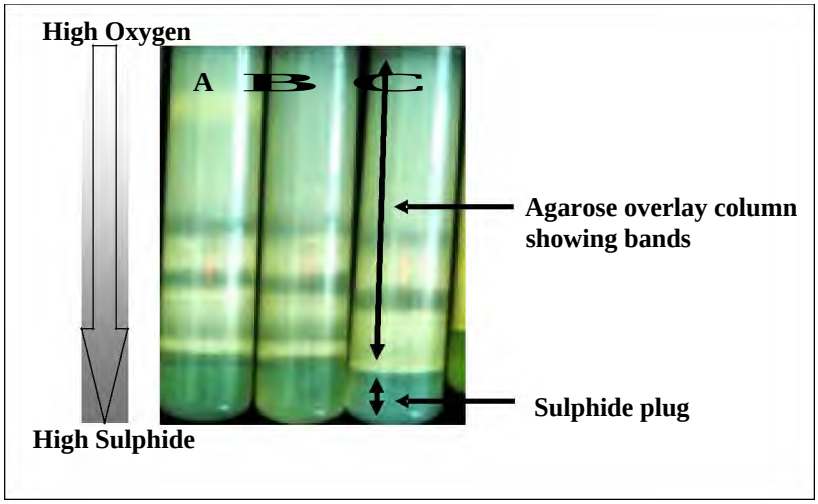

Figure 3.2 Clearly defined bands in the Gradient Tubes showing sulphide plug and agarose overlay column, and A) Brittle, B) Sticky and C) Thin floating sulphur biofilm.

It was assumed that the aerobic to micro-aerophilic forms present in the inoculum would grow in the upper layers of the agarose overlay column and that the anoxic to anaerobic sulphide tolerant forms in the lower layers. In this way, the microorganisms in the agar overlay would be selected according to their sulphide and oxygen preference in the Gradient Tubes, with growth establishing in those zones providing the appropriate physiological requirements. The expansion of the FSB in this way could be compared to the population identified in the total FSB sample.

3.3.2 Molecular Typing

3.3.2.1 Gradient Tubes

Following electrophoresis on 0.8 % agarose gel, successful extraction of the high molecular weight DNA could be observed at the top of the gel (Figure 3.3).

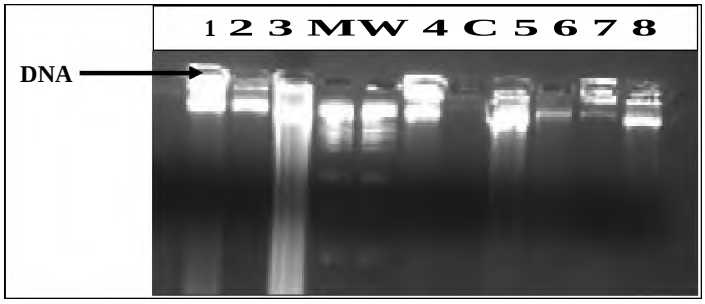

Figure 3.3 A 0.8 % agarose gel showing high molecular weight DNA of the different floating sulphur biofilm samples from the Gradient Tubes and linear flow channel reactor (1 – 8), MW denotes λPst1 molecular weight marker and C the negative control.

The 16S rDNA gene was amplified using the PCR primers GM5F and 907R, and yielded a 586 bp amplification product (Figure 3.4).

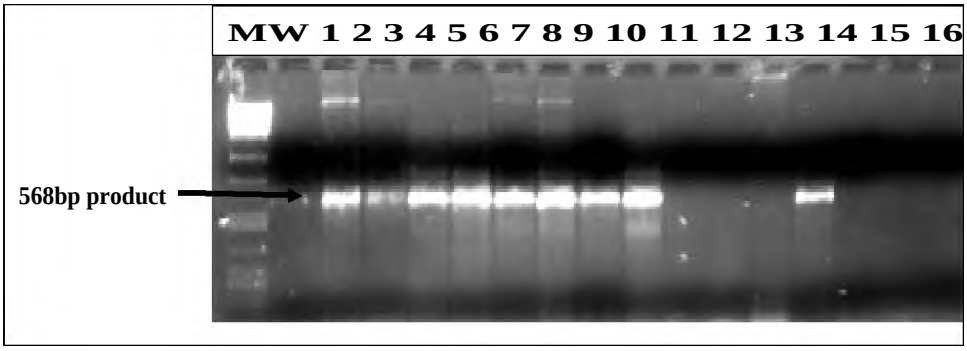

Figure 3.4 A 1 % agarose gel showing 568 bp amplified polymerase chain reaction products of the Gradient Tubes and linear flow channel reactor samples.

The PCR product was separated by DGGE using a 55 to 65 % denaturing gradient and yielded different bands on the acrylamide gel after silver staining and visualization in an ultra violet (UV) transilluminator (Figure 3.5).

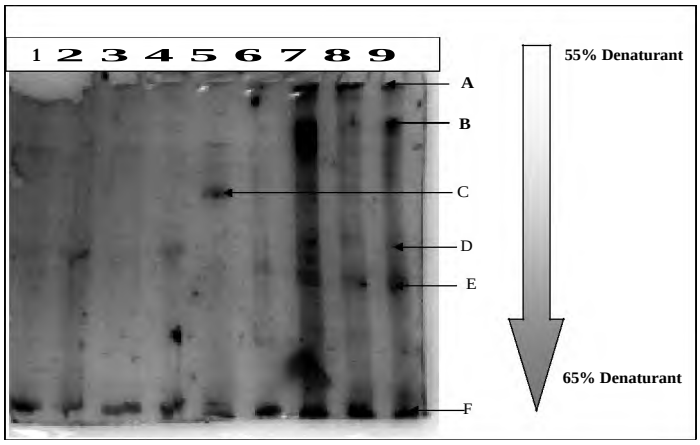

Figure 3.5 A 55 to 65 % gradient denaturing gradient gel electrophoresis acrylamide gel of the Brittle floating sulphur biofilm showing the separation of the various bands.

The PCR products obtained were analysed using DGGE (Figure 3.5). Samples one to nine were collected at different points in the Gradient Tube and amplified by PCR, with 1 denoting the first sample from the bottom of the tube at (13.0 cm) and nine being one of the bands at the top of the Gradient Tube. The bands formed on DGGE acrylamide gel were marked A to F according to their position on the acrylamide gel where A is at the top and F at the bottom.

The excised and amplified DGGE bands were transformed into high fidelity competent *E. coli* JM109 cells using a pGEM^{TM}-*T* Easy Vector and digested with EcoR1 prior to the extraction of the plasmids. Figure 3.6 shows the two bands cut on either side of the 586 bp fragment. The top band on the gel (Figure 3.6) represents the 3 018 bp plasmid fragment and the bottom is the 586 bp insert. The data obtained from the NCBI was used to determine the description of the sequenced sample based on the percentage relationship of the sequenced sample to bacteria in the NCBI database, and also to prepare a phylogenetic tree (Figure 3.7).

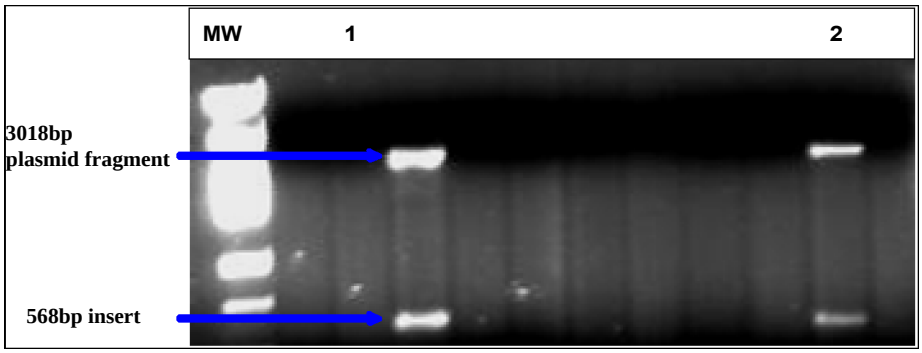

Figure 3.6 A 1 % agarose gel showing the plasmid fragment and insert of the 1F and 2D samples from the Brittle floating sulphur biofilm denaturing gradient gel electrophoresis acrylamide gel after digestion with EcoR1.

3.3.2.2 Total Floating Sulphur Biofilm

The extract from the original FSB samples were also examined using DNA extraction, PCR and DGGE and cloning as outlined above and the results were used for the preparation of a phylogenetic tree (Figure 3.7).

3.3.3 Phylogenetic Analysis

3.3.3.1 Gradient Tubes

Table 3.1 shows a summary of the Gradient Tube samples and matches obtained from the NCBI database and a resultant phylogenetic tree respectively.

Table 3.1 Summary of the Gradient Tube samples identified in the National Centre for Biotechnology Information database showing the number and name, family and location where the microorganism was isolated.

Name/Number	Family	Isolate
Clone 3a		**Gradient Tube (top)**
AF011343 *Azoarcus communis*	Bacteria; Proteobacteria; Betaproteobacteria; Rhodocyclales; Rhodocyclaceae; *Azoarcus*	Identification of N2-fixing plant- and fungus-associated *Azoarcus* species by PCR-based genomic fingerprints
AJ007007*Azoarcus sp.*	Bacteria; Proteobacteria; Betaproteobacteria; Rhodocyclales; Rhodocyclaceae; *Azoarcus*	Analysis of the relative abundance of different types of bacteria capable of toluene degradation in a compost biofilter

AJ430348 *Comamonas kersterii*	Bacteria; Proteobacteria; Betaproteobacteria; Burkholderiales; Comamonadaceae; *Comamonas*	Description of *Comamonas aquatica* comb. nov. and *Comamonas kersterii* sp. nov. for two subgroups of *Comamonas terrigena* and emended description of *Comamonas terrigena*
AY258065 *Acidovorax* sp. 98-63833	Bacteria; Proteobacteria; Betaproteobacteria; Burkholderiales; Comamonadaceae; *Acidovorax*	Undescribed bacterial pathogens isolated from human tissues
AY168755 *Hydrogenophaga* sp. YED6-4	Bacteria; Proteobacteria; Betaproteobacteria; Burkholderiales; Comamonadaceae; *Hydrogenophaga*	Characterization of Arsenite Oxidizing biofilms: Molecular and Cultivation Approaches and Community Rates of Arsenite Oxidation
AY569978 *Hydrogenophaga sp.* Esa.33	Bacteria; Proteobacteria; Betaproteobacteria; Burkholderiales; Comamonadaceae; *Hydrogenophaga*	Characterization of a novel selenium methyltransferase from freshwater bacteria showing strong similarities with the calicheamicin methyltransferase
Clone 10AQP		**Gradient Tube (top)**
X97534 *Acidithiobacillus* sp.	Bacteria; Proteobacteria; Betaproteobacteria; Hydrogenophiliceae; *Acidithiobacillus*	*Acidithiobacillus* sp. W5, the dominant autotroph oxidizing sulfide to sulfur in a reactor for aerobic treatment of sulphidic wastes
AJ536787 Uncultured bacterium 16S rRNA gene, isolate cMM319-39	Bacteria; environmental samples	Molecular analysis of the microbial community in drainage water from a magnesite mine, in the Graz area, Austria
Clone 8e		**Gradient Tube (Middle)**
AY569302 uncultured *Chryseobacterium sp.*	Bacteria; Bacteroidetes; Flavobacteria; Flavobacteriales; Flavobacteriaceae; *Chryseobacterium*; environmental samples.	Microbial diversity of the pink mat from the Spectacles Hot Spring in Rehai, Tengchong, China
Clone 9.5c		**Gradient Tube (Middle)**
CR933234 Uncultured bacterium partial	Bacteria; environmental samples	Novel major bacterial candidate division within a municipal anaerobic sludge digester
AY953234 uncultured anaerobic bacterium	Bacteria; environmental samples	Unique microbial diversity of anaerobic swine lagoons
AY570639 uncultured bacterium	Bacteria; environmental samples	Microbial diversity in a low-temperature, biodegraded Canadian oil reservoir

AF280841 Uncultured bacterium mLe1-2	Bacteria; Bacteroidetes; environmental samples	Phylogenetic analysis of bacterial communities in mesophilic and thermophilic bioreactors treating pharmaceutical wastewater
Clone 9.5b		**Gradient Tube (Middle)**
AF237975 *Planococcus citreus*	Bacteria; Firmicutes; Bacillales; Planococcaceae; *Planococcus*	Horizontal and Vertical Complexity of Attached and Free-Living Bacteria of the Eastern Mediterranean Sea
AF500008 *Planococcus citreus* strain TF-16	Bacteria; Firmicutes; Bacillales; Planococcaceae; *Planococcus*	Isolated from sea water of a tidal flat in Korea
AY428552 *Planococcus maritimus* strain KMM 3738	Bacteria; Firmicutes; Bacillales; Planococcaceae; *Planococcus*	*Planococcus algae* sp. nov. an unusual 'a-shaped' alkaliphilic Gram positive bacteria isolated from degraded thallus of the brown algae
AY741387 Uncultured bacterium clone Lan-37	Bacteria; environmental samples	Community Constitute and Phylogenetic Analysis on Silkworm Uncultured Intestinal Bacteria
AY735408 *Enterococcus faecium*	Bacteria; Firmicutes; Lactobacillales; Enterococcaceae; *Enterococcus*	Screening and isolation of Lactobacillus from traditional Korean fermented foods
AB009228 unidentified rumen bacterium RFN80	Bacteria; environmental samples	Predominant Bacterial Species of the Rumen
Clone 11b		**Gradient Tube (Bottom)**
Clone 13a		**Gradient Tube (Bottom)**
AB025196 *Caulobacter* sp. MBIC3983	Bacteria; Proteobacteria; Alphaproteobacteria; Caulobacterales; Caulobacteraceae; *Caulobacter*.	Phylogenetic Classification of *Mycoplana* species
AJ717390 *Brevundimonas bullata* isolate AC23	Bacteria; Proteobacteria; Alphaproteobacteria; Caulobacterales; Caulobacteraceae; *Brevundimonas.*	Bacterial diversity in a non-saline alkaline environment: heterotrophic anaerobic populations
AY689051 *Mycoplana* sp. 6C_11	Bacteria; Proteobacteria; Alphaproteobacteria; Rhizobiales; Brucellaceae; *Mycoplana*.	Annual variation phylogenetic diversity of antibiotic-resistant bacteria in the lower Lake Geumgang

DQ177489 *Brevundimonas* sp. Tibet-IX23	Bacteria; Proteobacteria; Alphaproteobacteria; Caulobacterales; Caulobacteraceae; *Brevundimonas.*	Climate warming and tundra viable bacteria dynamics on Qinghai-Tibet Plateau
Clone5b		**Gradient Tube (Bottom)**
AY050603 Uncultured bacterium clone GOUTA13	Bacteria; environmental samples	Microbial diversity in an *in situ* reactor system treating monochlorobenzene contaminated groundwater as revealed by 16S ribosomal DNA analysis
AY985323 Uncultured bacterium clone C233	Bacteria; environmental samples	Diversity of the human intestinal microbial flora
AY985477 Uncultured bacterium clone C437	Bacteria; environmental samples	Diversity of the human intestinal microbial flora
AY916338 Uncultured bacterium clone C583	Bacteria; environmental samples	Diversity of the human intestinal microbial flora

3.3.3.2 Total Floating Sulphur Biofilm

Figure 3.8 is a composite phylogenetic tree formulated for the total FSB samples collected at the three stages of development and the summary of microorganisms identified from the NCBI database is summarised in Table 3.2

Table 3.2 Summary of the total floating sulphur biofilm species identified in the phylogenetic tree showing the National Centre for Biotechnology Information database number, family and location of isolation.

Name/Number	Family	Isolate
Clone 9f		**Brittle FSB**
DQ168844 Uncultured *Prevotella* sp. clone J28	Bacteria; Bacteroidetes; Bacteroidetes (class); Bacteroidales; Prevotellaceae; *Prevotella*; environmental samples.	Fermentative biohydrogen production using heated anaerobic sludge
AY212535 Uncultured bacterium clone 5.16	Bacteria; environmental samples	Assessment of equine fecal contamination: the search for alternative bacterial source-tracking targets
AY212542 Uncultured bacterium clone up.21	Bacteria; environmental samples	Assessment of equine fecal contamination: the search for alternative bacterial source-tracking targets
AY212521 Uncultured bacterium clone 20.16	Bacteria; environmental samples	Assessment of equine fecal contamination: the search for alternative bacterial source-tracking targets
AY212530 Uncultured bacterium clone 20.35b	Bacteria; environmental samples	Assessment of equine fecal contamination: the search for alternative

		bacterial source-tracking targets
AY831467 Uncultured bacterium clone 4E	Bacteria; environmental samples	Biotransformation and dissolution of petroleum hydrocarbons in natural flowing seawater at low temperature
Clone 1f		**Early Brittle FSB**
AF414444 *Cytophaga* sp. SA1	Bacteria; Bacteroidetes; Sphingobacteria; Sphingobacteriales; Flexibacteraceae; *Cytophaga*	Isolation and characterization of filamentous bacteria from paper mill slimes
AJ634056 *Cytophaga* sp. 0401 852	Bacteria; Bacteroidetes; Sphingobacteria; Sphingobacteriales; Flexibacteraceae; *Cytophaga*	Identification based on 16S rRNA gene sequencing
AJ440996 *Flavobacterium gelidilacus*	Bacteria; Bacteroidetes; Flavobacteria; Flavobacteriales; Flavobacteriaceae; *Flavobacterium*	Diversity of 746 heterotrophic bacteria isolated from microbial mats from ten Antarctic lakes
AJ507151 *Flavobacterium gelidilacus*	Bacteria; Bacteroidetes; Flavobacteria; Flavobacteriales; Flavobacteriaceae; *Flavobacterium*	*Flavobacterium gelidilacus* sp. nov., isolated from microbial mats in Antarctic lakes
AY468484 *Chryseobacterium* sp. LDVH 3	Bacteria; Bacteroidetes; Flavobacteria; Flavobacteriales; Flavobacteriaceae; *Chryseobacterium*	Polyphasic study of *Chryseobacterium* strains isolated from diseased aquatic animals
AY468465 *Chryseobacterium* sp. FRGDSA 4580/97	Bacteria; Bacteroidetes; Flavobacteria; Flavobacteriales; Flavobacteriaceae; *Chryseobacterium*	Polyphasic study of *Chryseobacterium* strains isolated from diseased aquatic animals
AY468454 *Chryseobacterium* sp. UOF CR2995	Bacteria; Bacteroidetes; Flavobacteria; Flavobacteriales; Flavobacteriaceae; *Chryseobacterium*	Polyphasic study of *Chryseobacterium* strains isolated from diseased aquatic animals
AY468455 *Chryseobacterium* sp. UOF CR4395	Bacteria; Bacteroidetes; Flavobacteria; Flavobacteriales; Flavobacteriaceae; *Chryseobacterium*	Polyphasic study of *Chryseobacterium* strains isolated from diseased aquatic animals

Clone2c		**Thick Sticky FSB**
AY532570 Uncultured bacterium clone 1013-28-CG21	Bacteria; environmental samples	Subsurface microbial communities and geochemistry within a vertical transect of a uranium-contaminated aquifer
AF458288 Uncultured epsilon proteobacterium ML615J-7	Bacteria; Proteobacteria; Epsilonproteobacteria; environmental samples	Composition of bacterial assemblages from alkaline, hypersaline Mono Lake, California
AY532543 Uncultured bacterium clone 1013-1-CG20	Bacteria; environmental samples	Subsurface microbial communities and geochemistry within a vertical transect of a uranium-contaminated aquifer
AB197158 *Sulfurimonas* sp. Go25-1	Bacteria; Proteobacteria; Epsilonproteobacteria; Campylobacterales; Helicobacteraceae; *Sulfurimonas*	Distribution, phylogenetic diversity and physiological characteristics of epsilon-Proteobacteria in a deep-sea hydrothermal field
Clone 11a		**Sticky FSB**
Clone 10a		**Brittle FSB**
AF237975 *Planococcus citreus*	Bacteria; Firmicutes; Bacillales; *Planococcus*	Horizontal and Vertical Complexity of Attached and Free-Living Bacteria of the Eastern Mediterranean Sea
AF500008 *Planococcus citreus* strain TF-16	Bacteria; Firmicutes; Bacillales; *Planococcus*	Isolated from sea water of a tidal flat in Korea
AY428552 *Planococcus maritimus* strain KMM 3738	Bacteria; Firmicutes; Bacillales; *Planococcus*	*Planococcus* algae sp. nov. an unusual 'a-shaped' alkaliphilic Gram positive bacteria isolated from degraded thallus of the brown algae
AY221599 Uncultured soil bacterium clone HN1-35	Bacteria; environmental samples	Microbial Community Analysis of Soils Contaminated with Lead, Chromium and Organic Solvents
AB066266 *Enterococcus mundtii*	Bacteria; Firmicutes; Lactobacillales; Enterococcaceae; *Enterococcus*	Biochemical and genetic characterization of mundticin KS, an antilisterial peptide produced by *Enterococcus mundtii* NFRI 7393
AF061013 *Enterococcus mundtii*	Bacteria; Firmicutes; Lactobacillales; Enterococcaceae; *Enterococcus*	Determination of 16S rRNA sequences of enterococci and application to species identification of nonmotile *Enterococcus gallinarum* isolates
AF539705 *Enterococcus ratti*	Bacteria; Firmicutes; Lactobacillales; Enterococcaceae; *Enterococcus*	*Enterococcus hirae* implicated as a cause of diarrhea in suckling rats

AY675247 *Enterococcus faecium*	Bacteria; Firmicutes; Lactobacillales; Enterococcaceae; *Enterococcus*	Identification of bacteria from fermented Korean traditional foods
AY653231 *Enterococcus faecium*	Bacteria; Firmicutes; Lactobacillales; Enterococcaceae; *Enterococcus*	Comparison of three PCR primer sets for identification of vanB gene carriage in feces and correlation with carriage of vancomycin-resistant enterococci: interference by vanB-containing anaerobic bacilli
AY735408 *Enterococcus faecium*	Bacteria; Firmicutes; Lactobacillales; Enterococcaceae; *Enterococcus*	Screening and isolation of *Lactobacillus* from traditional Korean fermented foods
AB009228 unidentified rumen bacterium RFN80	Bacteria; environmental samples	Predominant Bacterial Species of the Rumen
Clone 13bQP		**Thin FSB**
DQ104970 Bacterium SRMC-52-8	Bacteria	Co-selection for microbial resistance to metals and antibiotics in freshwater microcosms
AY957941 Uncultured bacterium clone B3NR69D26	Bacteria; environmental samples	Population diversity in model drinking water biofilms receiving chlorine or monochloramine residual
AY953163 Uncultured anaerobic bacterium clone B-1AW	Bacteria; environmental samples	Unique Microbial Diversity of Anaerobic Swine Lagoons
AY953184 Uncultured anaerobic bacterium clone B-1R	Bacteria; environmental samples	Unique Microbial Diversity of Anaerobic Swine Lagoons
AJ430348 *Comamonas kersterii*	Bacteria; Proteobacteria; Betaproteobacteria; Burkholderiales; Comamonadaceae; *Comamonas*	Description of *Comamonas aquatica* comb. nov. and *Comamonas kersterii* sp. nov. for two subgroups of *Comamonas terrigena* and emended description of *Comamonas terrigena*
AY258065 *Acidovorax* sp. 98-63833	Bacteria; Proteobacteria; Betaproteobacteria; Burkholderiales; Comamonadaceae; *Acidvorax*	Undescribed bacterial pathogens isolated from human tissues

AY168755 *Hydrogenophaga* sp. YED6-4	Bacteria; Proteobacteria; Betaproteobacteria; Burkholderiales; Comamonadaceae; *Hydrogenophaga*	Characterization of Arsenite Oxidizing biofilms: Molecular and Cultivation Approaches and Community Rates of Arsenite Oxidation
AY569978 *Hydrogenophaga* sp. Esa.33	Bacteria; Proteobacteria; Betaproteobacteria; Burkholderiales; Comamonadaceae; *Hydrogenophaga*	Characterization of a novel selenium methyltransferase from freshwater bacteria showing strong similarities with the calicheamicin methyltransferase
Clone 10aQP		**Thin FSB**
AB021404 *Pseudomonas geniculata*	Bacteria; Proteobacteria; Gammaproteobacteria; Xanthomonadales; Xanthomonadaceae	Phylogenetic affiliation of the pseudomonads based on 16S rRNA sequence
DQ192172 *Stenotrophomonas maltophilia* strain flds	Bacteria; Proteobacteria; Gammaproteobacteria; Xanthomonadales; Xanthomonadaceae; *Stenotrophomonas*	Direct Submission
AY038620 Uncultured eubacterium clone GL182.22	Bacteria; environmental samples	16S rRNA sequence analysis and phylogenetic characterization of microbial communities associated with lacustrine subsurface sediments
AY038621 Uncultured eubacterium clone GL184.24	Bacteria; environmental samples	16S rRNA sequence analysis and phylogenetic characterization of microbial communities associated with lacustrine subsurface sediments
AY038629 Uncultured eubacterium clone GL178.1	Bacteria; environmental samples	16S rRNA sequence analysis and phylogenetic characterization of microbial communities associated with lacustrine subsurface sediments
AY038628 Uncultured eubacterium clone GL178.11	Bacteria; environmental samples	16S rRNA sequence analysis and phylogenetic characterization of microbial communities associated with lacustrine subsurface sediments
AF513452 Xanthomonas group bacterium LA37	Bacteria; Proteobacteria; Gammaproteobacteria; Xanthomonadales; *Xanthomonas*	The Hawaiian Archipelago: a microbial diversity hotspot
Clone 1d		**Early Brittle FSB**
Clone 2d		**Thick Sticky FSB**
AJ536782 Uncultured bacterium 16S rRNA gene, isolate cMM319-25	Bacteria; environmental samples	Molecular analysis of the microbial community in drainage water from a magnesite mine, in the Graz area, Austria
AJ536777 Uncultured bacterium 16S rRNA gene,	Bacteria; environmental samples	Molecular analysis of the microbial community in drainage water from a

isolate cMM319-03.		magnesite mine, in the Graz area, Austria
AJ536781 Uncultured bacterium 16S rRNA gene, isolate cMM319-21	Bacteria; environmental samples	Molecular analysis of the microbial community in drainage water from a magnesite mine, in the Graz area, Austria
AJ536792 Uncultured bacterium partial 16S rRNA gene, isolate cMM319-58	Bacteria; environmental samples	Molecular analysis of the microbial community in drainage water from a magnesite mine, in the Graz area, Austria
AJ536802 Uncultured bacterium partial 16S rRNA gene, isolate cMM319-73	Bacteria; environmental samples	Molecular analysis of the microbial community in drainage water from a magnesite mine, in the Graz area, Austria
Clone 1c		**Early Brittle FSB**
AJ536804 Uncultured bacterium partial 16S rRNA gene, isolate cMM319-75.	Bacteria; environmental samples	Planktonic microbial communities associated with fracture-derived groundwater in a deep gold mine of South Africa
DQ088740 Uncultured bacterium clone BE24FW032601C18W17-4	Bacteria; environmental samples	Molecular analysis of the microbial community in drainage water from a magnesite mine, in the Graz area, Austria
AJ536780 Uncultured bacterium 16S rRNA gene, isolate cMM319-18	Bacteria; environmental samples	Isolation, characterization and *in situ* detection of a novel chemolithoautotrophic sulfur-oxidising bacterium in wastewater biofilms growing under micro-aerophilic conditions.
AB118236 *Thiovirga sulfuroxydans*	Bacteria; Proteobacteria; Gammaproteobacteria; Chromatiales; Halothiobacillaceae; *Thiovirga*	Molecular analysis of the microbial community in drainage water from a magnesite mine, in the Graz area, Austria
AJ536785 Uncultured bacterium 16S rRNA gene, isolate cMM319-33	Bacteria; environmental samples	Molecular analysis of the microbial community in drainage water from a magnesite mine, in the Graz area, Austria
AJ536786 Uncultured bacterium 16S rRNA gene, isolate cMM319-34	Bacteria; environmental samples	The distribution of microbial taxa in the subsurface water of the Kalahari shield, South Africa
DQ125329 Uncultured *Halothiobacillus* sp. clone B225FWB5	Bacteria; Proteobacteria; Gammaproteobacteria; Chromatiales; *Halothiobacillus* environmental samples	Molecular analysis of the microbial community in drainage water from a magnesite mine, in the Graz area, Austria
AJ536787 Uncultured bacterium 16S rRNA gene, isolate cMM319-39.	Bacteria; environmental samples	Molecular analysis of the microbial community in drainage water from a magnesite mine, in the Graz area, Austria
Clone S1A		**Brittle FSB**

Clone S2E		**Sticky FSB**
AY096035 *Halothiobacillus* sp. WJ18	Bacteria; Proteobacteria; Gammaproteobacteria; Chromatiales; Halothiobacillaceae; *Halothiobacillus*	Novel acidophiles isolated from moderately acidic mine drainage waters
X97534 *Acidithiobacillus* sp.	Bacteria; Proteobacteria; Betaproteobacteria; Hydrogenophiliceae; *Acidithiobacillus*	*Acidithiobacillus* sp. W5, the dominant autotroph oxidizing sulfide to sulfur in a reactor for aerobic treatment of sulphidic wastes
AF173169 *Acidithiobacillus neapolitanus* DSM 581	Bacteria; Proteobacteria; Gammaproteobacteria; Chromatiales; Halothiobacillaceae; *Halothiobacillus*	*Halothiobacillus kellyi* sp. Nov., a mesophilic, obligately chemolithoautotrophic, sulfur-oxidising bacterium isolated from a shallow-water hydrothermal vent in the Aegean Sea.
AY686547 *Halothiobacillus neapolitanus* strain OSWA	Bacteria; Proteobacteria; Gammaproteobacteria; Chromatiales; Halothiobacillaceae; *Halothiobacillus*	A *Halothiobacillus* from the old sulfur well at Harrogate.
L79962 *Thiothrix fructosivorans* strain Q	Bacteria; Proteobacteria; Betaproteobacteria; Thiotrichales; Thiotrichaceae; *Thiothrix*	Phylogenetic relationships of filamentous sulfur bacteria isolated from wastewater treatment plants.
AJ548906 Uncultured *Acidithiobacillus* sp.	Bacteria; Proteobacteria; Betaproteobacteria; Hydrogenophiliceae; *Acidithiobacillus* environmental samples	High diversity biofilm for the oxidation of sulfide-containing effluents.
Y09280 *Acidithiobacillus baregensis*	Bacteria; Proteobacteria; Betaproteobacteria; Hydrogenophiliceae; *Acidithiobacillus*	A new sulfoxidizing bacterium from sulfurated thermal waters of bareges.

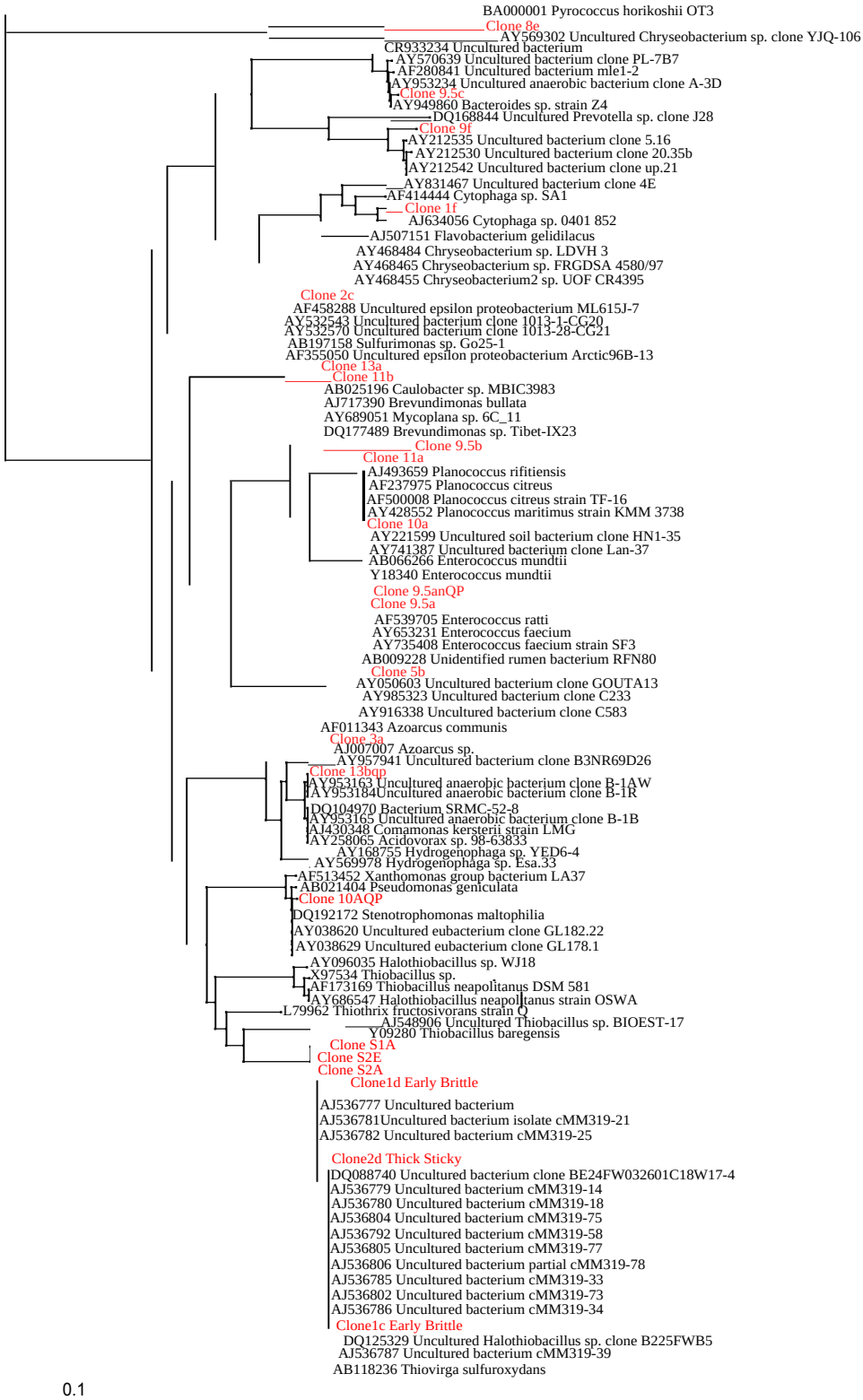

Figure 3.7 Overall Phylogenetic tree relating total floating sulphur biofilm and Gradient Tube section sample sequences to known species from the National Centre for Biotechnology Information database. This tree includes all isolates for the study and represents an aggregate picture of the populations present.

3.3.4 Comparison of Microbial Populations

The data outlined above enabled a comparison of organisms occurring at different levels in the Gradient Tubes with the total population identified in the FSB.

Species found near the top of the Gradient Tube in the aerobic zone (Clone 3a) were found to be related to *Azoarcus* sp. (Altschul *et al.,* 1997) (Figure 3.7). These play a role in the degradation of aromatic hydrocarbons and have denitrifying capabilities (Hurek *et al.*, 1997). *Azoarcus communis* has been associated with plant matter and may have originated from the sulphide generating DPBR reactor which contained grass and other lignocellulosic material (Hurek *et al.,* 1997). Other isolates related to the beta-proteobacter have been associated with sediment samples where *Acidithiobacillus ferro-oxidans* was isolated (Karavaiko *et al.*, 2003).

Clone 8E isolated from the middle (6.5 cm) of the Gradient Tube where the oxygen and sulphide levels were thought to be intermediate was found to be related to an uncultured *Chryseobacterium* sp (Figure 3.7) (Altschul *et al.*, 1997). *Chryseobactrium* belongs to the *Flavobacteria* group, which are commensal organisms and also opportunistic pathogens. *Flavobacteria* are Gram negative facultative aerobic to anaerobic rods with rounded or tapered ends and showing gliding motility (Michel *et al.*, 2005). They are able to decompose several polysaccharides, but not cellulose, and are widely distributed in soil and freshwater habitats. Clone 1f from FSB was also found to be related to *Flavobacteria* (Figure 3.7).

Below the halfway point (4.5 cm) in the Gradient Tube, Clone 9.5c was found to be closely related to *Bacteroides* spp., and other uncultured anaerobic bacteria (Altschul *et al.*, 1997) (Figure 3.7). The *Bacteroides* are obligately anaerobic, Gram negative and saccharolytic, producing acetate and succinate as their major metabolic end-products (Guo *et al.*, 2005). This particular *Bacteroides* type strain was documented to be growing in paper mill wastewater and in our study it bears its origin from the lignocellulose-packed DPBR. Clone 9f from the Thin FSB was found to be closely related to uncultured

bacteria and Clone 9.5c from the Thin FSB gradient Tube (Figure 3.7) (Altschul *et al.*, 1997).

A sample from 4.0 cm in the Gradient Tube, Clone 9.5b was found to be closely related to *Planococcus citreus* (Figure 3.7). *Planococcus* are Gram positive and generally aerobic to micro-aerophilic, with coccoid cells, occurring in pairs, tetrads and aggregates (Ivanova *et al.*, 2002). They are motile by means of a single polar flagellum (Ivanova *et al.*, 2002). *Planococcus* sp. was previously isolated from algal mats collected from a sulphurous spring, and from seawater in a tidal flat, indicating sulphidic environments (Romano *et al.*, 2003). Clones 11a and 10a from the Sticky and Brittle FSB respectively, were found to be related to *Planococcus* sp. (Figure 3.7).

Clones 13a and 11b near the bottom of the Gradient Tubes (2.5 and 3.5 cm respectively) were found to be closely related to *Brevundimonas* sp, *Caulobacter* sp. and *Mycoplana* sp. (Figure 3.7) (Altschul *et al.*, 1997). *Brevundimonads* are Gram negative, heterotrophic anaerobic rod-shaped **α**-proteobacteria, and are documented to produce copious exopolysaccharide capsular material (Boer *et al.*, 2005). As an EPS producer, *Brevundimonas* is likely to play an important role within the FSB structure. Its location at the bottom of the Gradient Tube (2.0 cm) suggests that it may also prefer a high sulphide environment. This also suggests that *Brevundimonas* may require the presence of oxygen consuming aerobes and microaerophiles in the FSB above its location to provide the Redox conditions necessary for its growth and function lower down in the biofilm.

Clone 5b from the bottom of the Gradient Tubes (1.5 cm) was found to be closely related to uncultured bacteria associated with rumen and human intestinal microbial flora, indicating its preference for low oxygen environment (Figure 3.7).

Figure 3.8 summarises the phylogenetic relationships of the organisms isolated from the different levels in the Gradient Tubes.

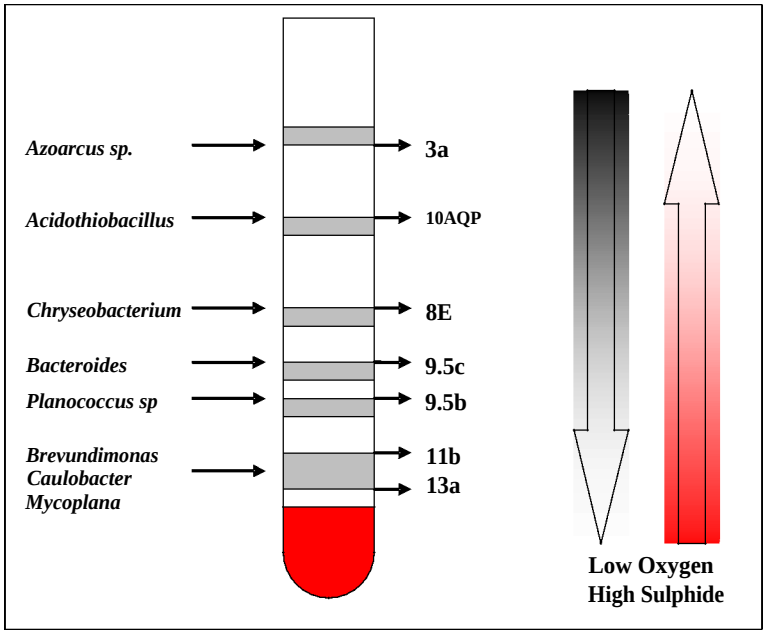

Figure 3.8 A diagrammatic illustration of the results obtained from sequencing of the Gradient Tube samples drawn from different zones along the length of agarose overlay column.

The occurrence of a number of aerobic sulphur bacteria including *Acidithiobacillus* and *Halothiobacillus* correlate with the presence of *Acidithiobacillus* in the upper layer of the Gradient Tube. This suggests that the sulphide oxidation function occurs at or near the top of the FSB. *Bacteroides* and *Planococcus* are found in both total FSB and the middle layers of the Gradient Tube which indicates their presence in an intermediate position in the FSB. Possibly their role in oxygen scavenging is to poise the system for the growth of the anaerobes in the lower layer of the FSB. Given the occurrence of *Brevundimonas* here, it is apparent that the EPS production of the FSB may also originate in part from this layer.

A number of possibly important clones were observed in the different FSB stages which were not found in the Gradient Tubes. This may have been due to the different growth conditions required for the different microorganisms to thrive as an FSB community on the LFCR but were not duplicated under the artificial culture conditions provided in the Gradient Tube system.

Table 3.3 shows a comparison of organisms identified in the total FSB and those separated in the Gradient Tube study.

Table 3.3 A comparison of populations identified at the various zones in the Gradient Tubes and the total floating sulphur biofilm samples.

Distribution	Gradient Tube	FSB
Top (aerobic)	*Azoarcus* *Acidithiobacillus*	*Acidithiobacillus* *Halothiobacillus* *Thiothrix* *Thiovirga* *Sulfurimonas*
Middle	*Chryseobacterium* *Bacteroides* *Planococcus*	*Bacteroides* *Planococcus*
Bottom (anaerobic)	*Brevundimonas*	*Uncultured anaerobe*

Although the method must, by its definition, produce only indicative results, correlations of interest were observed. This includes the presence of chemoautotrophic sulphide oxidisers in the upper layer of the FSB closest to the air/water interface. The mid zones (5 to 7 cm) showed a high level of comparability between the systems and showed species related to oxygen consuming bacteria, with possible Redox poising capabilities.

3.4 CONCLUSIONS

In this study the Gradient Tube method was used to expand the cross section of the FSB and, thus, enabling a high resolution sampling through its vertical profile. Results indicated that the findings can be related to physiological domains within the FSB. This may be a first report of such a methodology.

A number of conclusions may be drawn from these results:

- The complex microbial population structure of the FSB was confirmed;

- The comparison of the gradient Tube and total FSB population analysis indicates both a spatial and functional differentiation of the microbial population occurring as three distinct layers in the FSB system;
- The results suggest a structural relationship to function in the FSB system.

Chapter Four

ASPECTS OF FUNCTION IN THE FLOATING SULPHUR BIOFILM

4.1 INTRODUCTION

Okabe *et al.* (1999a and b) had noted that studies which relate microbial community structure to the function of nutrient removal, oxygen depletion and by-product production, and thereby determine individual contributions to the aggregate population performance, are quite scarce in the literature. (This may be attributed in part to methodological problems presented in effective *in situ* monitoring of microbial activities in thin structures, such as biofilms. Within biofilms a reduced diffusion of compounds limits nutrient transport to the cells and (thereby) substrate conversion rates (Amann, *et al.*, 1992; Santegoeds *et al.*, 1998). Because of the slow mass transfer, biofilms develop various micro-environments, which can differ markedly from the bulk liquid. This complicates the interpretation of community structure/function analysis because extrapolation of individual cell behaviour to the same species within a community is impossible without some knowledge of their micro-environment (Santegoeds *et al.*, 1999).

A direct and robust way to study the microenvironments is by use of microsensors (Schramm *et al.*, 1999). Microsensors are used to measure a range of physico-chemical parameters such as Redox potential, pH, sulphide and dissolved oxygen (de Beer and Schramm, 1999). Micro-gradients can be measured with high fidelity due to the small size of the microsensor tip, causing minimal disturbances in the biofilm system (Santegoeds *et al.*, 1999). These gradients are a function of local transport rates (usually diffusion), and also substrate conversion rates, and thus allow for the spatial distribution of microbial activity to be derived from the substrate profiles.

An advantage of microsensor use is that the spatial gradient information acquired may be used to unravel closed cycles in a biofilm such as sulphate reduction coupled with sulphide oxidation. Santegoeds *et al.* (1999) noted that the measurement of net substrate

conversion usually underestimates the processes taking place within the biofilm as some internal metabolic cycles can be hidden, even though these could play a major role in the biofilm.

Ramsing *et al.* (1993) used microsensors and molecular techniques for the first time while investigating sulphate reduction in a trickling-filter biofilm. Schramm *et al.* (1999) combined microsensors and molecular techniques to study nitrification also using a trickling–filter biofilm. Both studies showed a good correlation between microbial conversion (sulphate reduction and nitrification) and microbial population composition in the biofilm.

While considerable use has been made of microprobes in recent years, and these have been applied to the study of fixed biofilm systems (de Beer *et al.*, 1994), no literature reports were found describing their use to study floating biofilm systems.

The objective of this study was to use microprobes to explore the presence of gradients occurring across the depth of the FSB.

4.2 MATERIALS AND METHODS

The microsensors (Unisense, Denmark) were set up and calibrated according to the manufacturer's instructions and used to measure sulphide, pH and Redox potential gradients present in the FSB at the three stages of development.

4.2.1 Microsensor Set-up

Microsensors were used to measure pH, Redox potential and sulphide gradients within the FSB. All microsensors equipment was sourced from Unisense, Denmark. The *in situ* measurements were taken at the three different stages of sulphur FSB development (Thin, Sticky and Brittle). Prior to microprobe measurements, the inlet and outlet to the channel reactor were closed and the system was allowed to stabilize from a continuous flow operation for one hour.

4.2.2 Microsensor Measurement

A typical set up of the microsensor is illustrated in Figure 4.1.

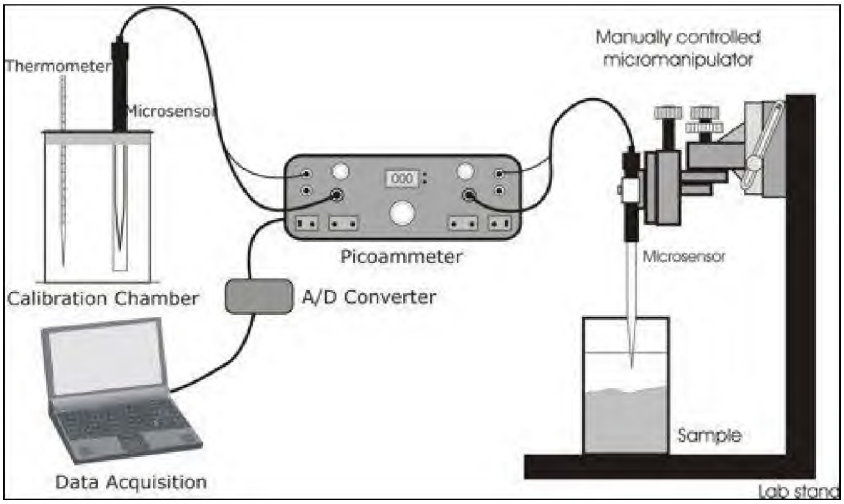

Figure 4.1 Illustration of the microsensor system showing the component instruments used for analyzing floating sulphur biofilm samples. These include the microprobe, a micromanipulator and the interface and computer logger (Unisense, microsensor manual).

The system included a manually controlled micromanipulator MM33. It had a precision range of 10 µm in the x-axis and 100 µm in the y- and z-axes for clamping the microprobes during measurements. The picoammeter (specific for sulphide determination) and pH/ORP millivolt meter (for pH and Redox potential measurements) were used to detect the signal from the microsensor, after which it was converted to an analogue voltage output proportional to the microsensor signal. The output was then sent to the data acquisition device (computer) loaded with the Unisense Profix software that converts the signal reading to pH units and Redox potential millivolts. The sulphide signal measured was converted to concentration (mg/L) using a sulphide standard curve. In order to position the microsensors in the microenvironment, a laboratory stand was designed at EBRU and positioned over the reactor (Figure 4.2).

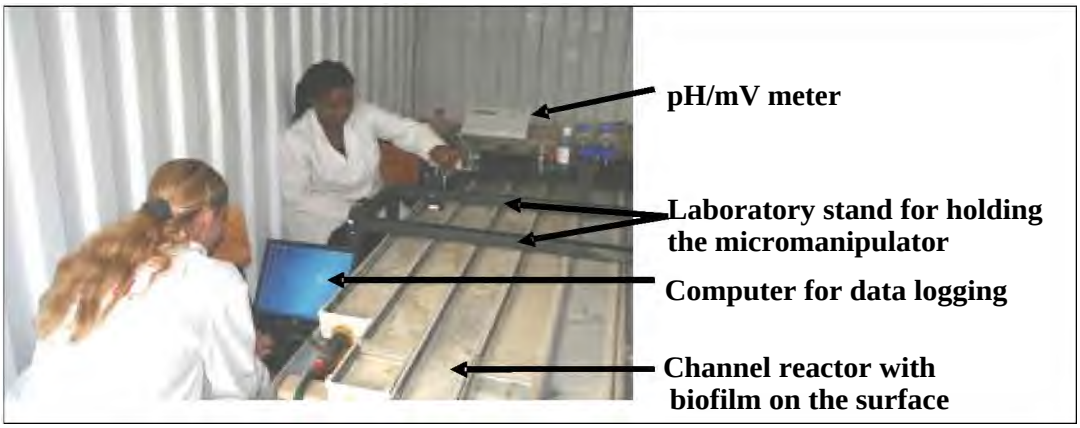

Figure 4.2 The microsensor apparatus as set-up in the floating sulphur biofilm constant environment laboratory which housed the linear flow channel reactor. Measurements of Redox potential, pH and sulphide concentration were recorded.

4.2.3 Microelectrodes

pH and Redox potential electrodes and reference electrode were calibrated (according to the manufacturer's instructions) at 25 ^{o}C in a CE room using standard pH buffers (4, 7 and 10). The pH and Redox potential were measured with glass microelectrodes connected to a high-impedance pH/mV meter (PHM210). The pH and Redox potential electrodes have an outer tip diameter of 2 to 20 µm. The measurements entail use of a reference electrode (REF 5000) used for pH and Redox potential measurements. This was a simple open-ended Ag-AgCl electrode with a gel-stabilized electrolyte and a tip diameter of 5 µm. The reference and microsensor probes were calibrated at the different pH ranges for the *in situ* measurements.

The sulphide microelectrode was calibrated by measuring the signal in a dilution series of a standard solution (hydrogen sulphide dissolved in water from the LFCR flushed with nitrogen to prevent sulphide oxidation). The concentration of the sulphide measured in the FSB was calculated using a calibration curve. The sulphide electrode was found to show a linear response to sulphide concentrations between 0 and 500 mg/L.

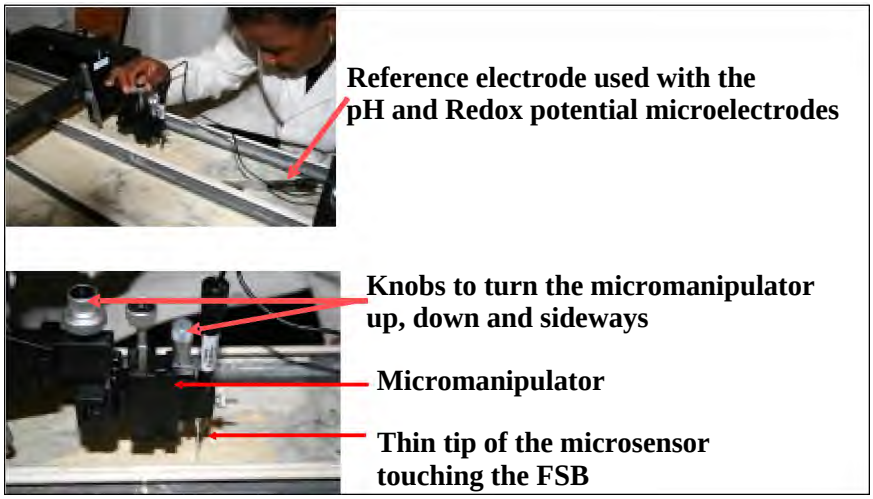

Figure 4.3 A closer view at the micromanipulator and microsensor set up above the linear flow channel reactor while acquiring measurements across the depth of the floating sulphur biofilm.

The measurements were taken across a depth of 50 mm through the FSB and into the underlying bulk liquid. Initial measurements were collected at 5 µm intervals from 0 to 400 µm depth after which the readings were taken at 100 µm intervals until 1mm depth. Readings between 1 and 10 mm depth were taken at 1 mm intervals into the bulk liquid. From 10 mm to 50 mm the readings were taken at 10 mm intervals. Measurements were repeated five times per parameter for each FSB stage (Thin, Sticky and Brittle) and a control (no FSB).

4.2.4 Floating Sulphur Biofilm Thickness Measurement

The thickness of the wet FSB was determined from microprobe penetration during the measurements of sulphide, pH and Redox potential gradients at the three stages of FSB development, where sudden changes in sulphide concentration, pH and Redox potential and tip penetration were monitored. However, the hydrated FSB influences the bulk water system underlying it and clear transitions are less easy to observe, especially for the Thin FSB.

4.3 RESULTS AND DISCUSSION

Results from the microsensor analysis of the Sticky FSB were considered to be unreliable because the FBS tended to adhere to the tip of the microsensor as it was inserted, and these results are not presented here. The sulphide, pH and Redox potential of the Thin and Brittle FSB and the control were found to be reproducible (SD > 2 %; n = 5) and representative profiles were plotted in Figures 4.4 to 4.6. Each determination is comprised of four graphs (A to D) which detail the four different range intervals over which measurements were made (5 µm, 100 µm, 1 mm and 10 mm).

4.3.1 Sulphide

Clearly defined sulphide gradients were observed to occur in the FSB system with pronounced differences between the control and FSB samples as well as between the Thin and Brittle FSB systems (Figure 4.4). From the results presented, the depth of the Thin and Brittle FSB was observed to be 260 and 380 µm respectively (where the sudden decrease in the Thin FSB and increase in the Brittle sulphide concentration was measured), which is a more accurate depth determination compared to the dissecting microscope measurement of 50 to 60 µm in the dry FSB (Figure 2.7).

The control sulphide depth profile showed a fairly constant reading at around 140 mg/L throughout the depth down to 50 mm. The variability in results from the surface to 250 µm may reflect noise due to the increased frequency of measurement taken over this range (Figure 4.4). Both Thin and Brittle FSBs followed similar trends in sulphide concentration in the top 80 µm. Moving below 80 µm, the vertical profiles of sulphide in the respective FSBs differed.

In the Thin FSB, the sulphide level showed a very sharp rise from 50 to 400 mg/L over the narrow depth range of 80 to 110 µm. It then declined gradually to 100 to 150 mg/L over the depth range of 110 to 300 µm. From 300 µm to 50 mm depth, sulphide gradually decreased to range between 25 and 50 mg/L.

The Brittle FSB showed similar trends with a pronounced rise in sulphide starting at 150 µm and then peaking at 250 µm where the sulphide concentration fluctuated between 350 and 450 mg/L. At 260 µm depth, the sulphide concentration decreased rapidly to 140 mg/L and rose once again to 450 mg/L at around the 350 µm depth. This was followed by a gradual declined until the 20 mm depth (Figure 4.4).

The presence of the FSB (from the moment it starts developing Thin FSB), introduced large changes in the sulphide concentration profile of the LFCR, establishing a low-concentration top zone (0 to 100 µm depth) and a high concentration lower-zone (> 260 µm depth). When the FSB matured to the Brittle stage, the depth of the low sulphide concentration zone increased to over 100 µm range. Interestingly, sulphide accumulated again just below the FSB (350 to 2500 µm depth) during the Brittle FSB stage, possibly caused by the low diffusion rate through the Brittle FSB.

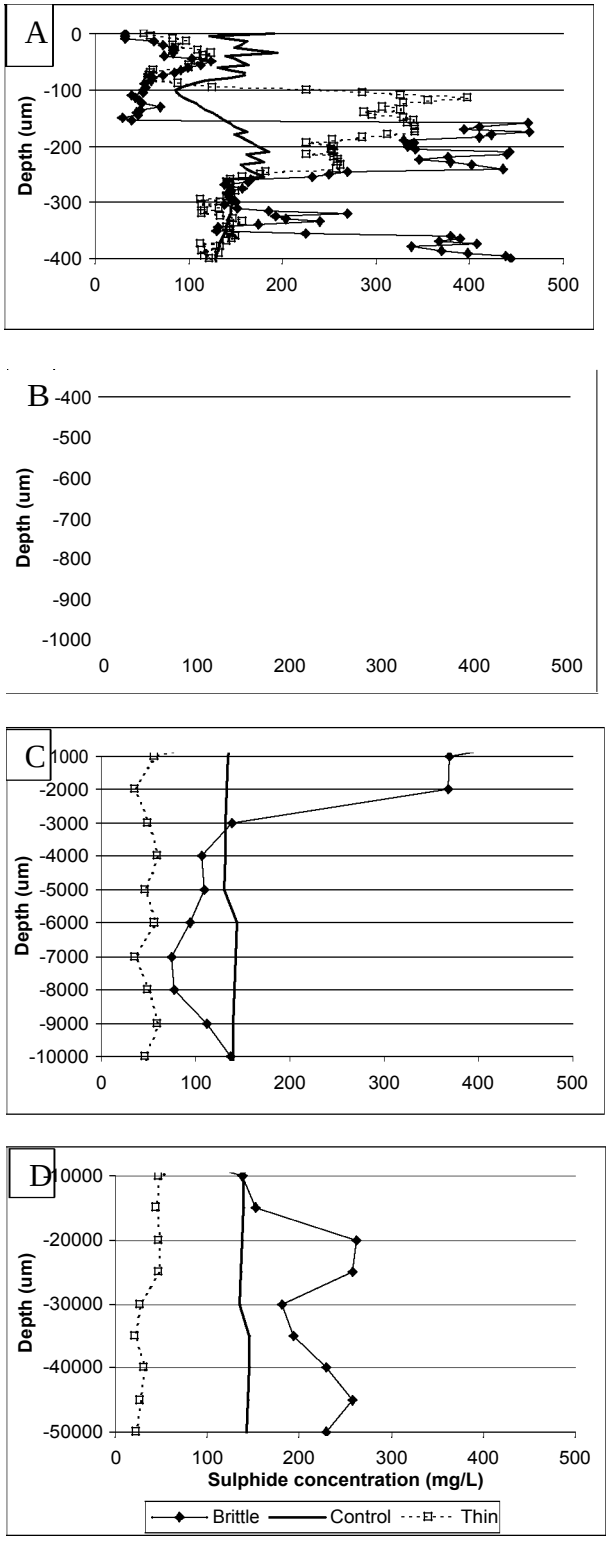

Figure 4.4 Sulphide microsensor measurements of the Thin and Brittle floating sulphur biofilms in the linear flow channel reactor compared to the control (no biofilm) across 0 to 50 mm depth in ranges from 0 to 400 µm at 5 µm intervals (A), 400 µm to 1mm at 100 µm intervals (B), 1 mm to 10 mm at 1 mm intervals (C) and 10 mm to 50 mm at 10 mm intervals (D).

4.3.2 pH

The pH measurements results for the Thin, Brittle FSB and control are shown in Figure 4.5. Both the Thin and Brittle FSBs showed a marked rise in pH in the first 100 µm in contrast to the control, which had an approximately constant pH of 7.3 to 7.8 (Figure 4.5). The pH increase observed in the Brittle FSB was higher than that of the Thin FSB with the maximum pH measured being 8.9 and 10.8 for the Thin and Brittle FSB respectively. This increase in FSB pH could possibly be attributed to the sulphide oxidation reaction in which the production of elemental sulphur is associated with a hydroxyl ion being produced as a product (Steudel, 1996).

This observation correlates with the simultaneous decrease in sulphide (Figure 4.4A) at the same level. The higher pH reading in the Brittle FSB may be correlated with higher sulphur production at this stage. The small rise in sulphide level observed at the depth of maximum pH (Figure 4.4) indicates sulphate reduction may have occurred here during the recycling of sulphur species. This may occur due to some complete oxidation of sulphide taking place in addition to sulphur formation.

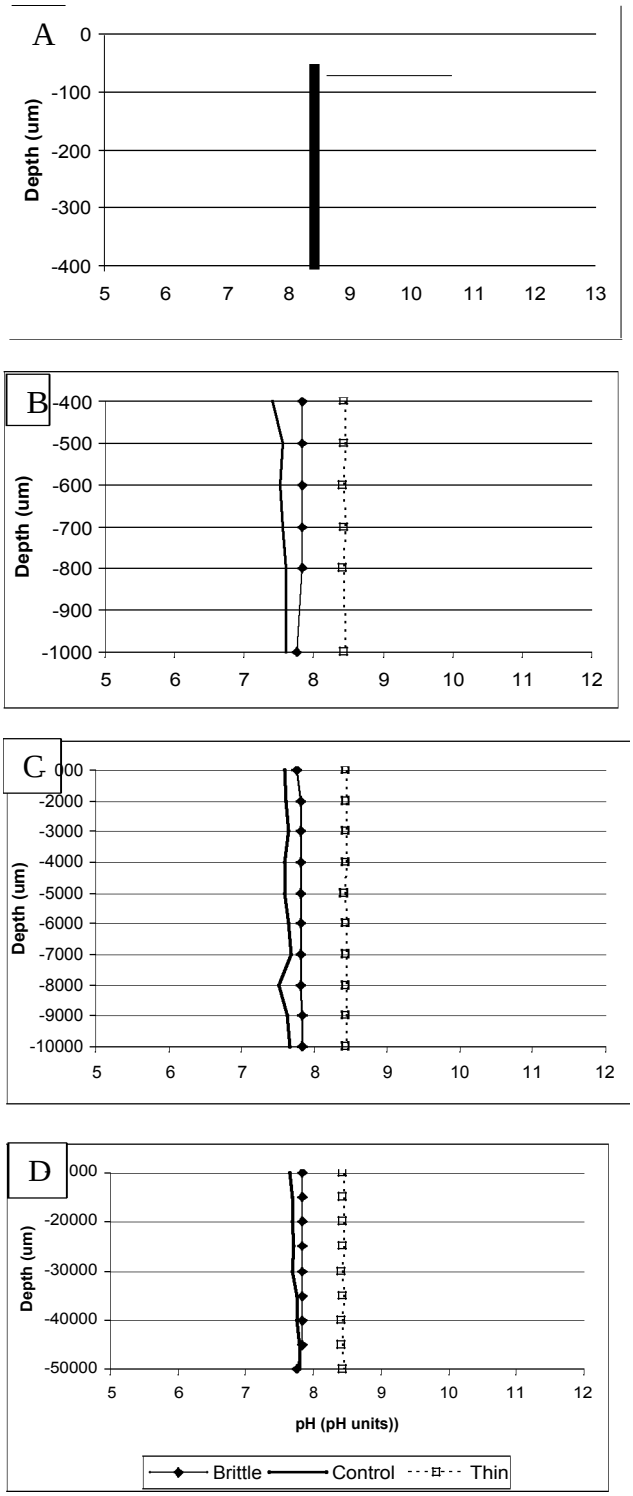

Figure 4.5 pH microsensor measurements of the Thin and Brittle floating sulphur biofilm compared to the control across 0 to 50 mm depth in ranges of 0 to 400 µm at 5 µm intervals (A), 400 µm to 1 mm at 100 µm intervals (B), 1 mm to 10 mm at 1 mm intervals (C) and 10 mm to 50 mm at 10 mm intervals (D)**.**

4.3.3 Redox potential

The Redox potential readings in the three systems studied appear to correlate with the observations of sulphide and pH measurements noted above. The Redox potential in the Thin and Brittle FSBs decreased over the same depth, while the control showed little change (decrease) from +200 to +50 mV near to the surface (~20 µm depth) (Figure 4.6).

A decrease in Redox potential in the 0 to 50 µm depth was recorded for the Thin and Brittle FSBs where the Thin decreased from -25 to -80 mV and the Brittle FSB decreased from -80 to -200mV. This represents an inverse relation between pH and Redox potential over the same depth range. Where the pH decreased in the 50 to 90 µm depth range, the Redox potential increased in both FSBs from -80 to 0 mV in the Thin and from -200 to +50 mV in the Brittle FSB. The increase in Redox potential occurred in the 90 to 190 µm depth range. There was a gradual decrease in the Thin FSB from around 300 µm depth and in the Brittle FSB from around 280 µm depth (Figure 4.6).

Steudel (1996) had noted that a narrow Redox window around -150 mV is required for the chemical oxidation of sulphide to elemental sulphur. This observation could explain why sulphur crystal formation occurs readily in the Brittle FSB compared to the Thin FSB where the Redox potential barely reaches -80 mV and sulphur crystal formation does not occur. This indicates that while biological sulphide oxidation and sulphur globule formation by the various sulphur bacteria present in the system may take place in the upper aerobic layer, oxygen consumption by the aerobes and micro-aerophiles in the middle layer is necessary to poise the redox potential to allow sulphur crystal formation.

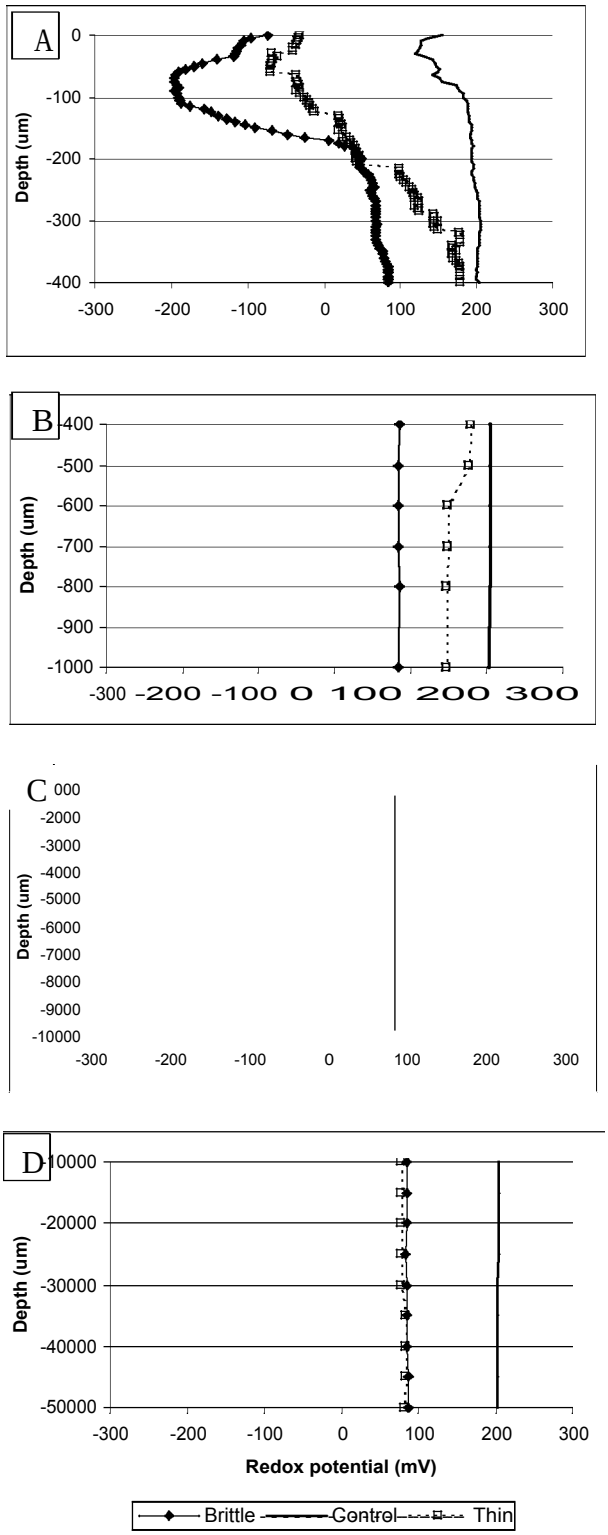

Figure 4.6 Redox potential microsensor measurements of the Thin and Brittle floating sulphur biofilm compared to the control across 0 to 50 mm depth in ranges from 0 to 400 µm at 5 µm intervals (A), 400 to 1 mm at 100 µm intervals (B), 1 mm to 10 mm at 1 mm intervals (C) and 10 mm to 50 mm at 10 mm intervals (D).

4.4 CONCLUSIONS

The conclusions drawn from this study were as follows:

- Microsensors were used for the first time in the measurement of the sulphide, pH and Redox potential gradients in the FSB;
- These findings indicated the presence of steep spatial physico-chemical gradients established across the FSB structures;
- The correlation of distinct physiological compartments within the FSB with microbial population and spatial structural differentiation enables the construction of a structural/functional approach to explain the performance of these systems.
- The demonstration of a functional spatial differentiation in the FSB provides further evidence that these are “true” biofilm systems.

Chapter Five

A STRUCTURAL/FUNCTIONAL DESCRIPTIVE MODEL FOR THE FLOATING SULPHUR BIOFILM SYSTEM

5.1 INTRODUCTION

Floating sulphur biofilms have not been well documented in the literature, despite their role in the natural sulphur cycle and their now apparent potential use in biotechnological process development (Rose, *et al.*, 1996, Jørgensen *et al.*, 1998, Dunn, 1998). Attributes of the structure and function of the FSB have been described in the studies reported here and provide the basis, possibly for the first time, for constructing a descriptive model accounting for the performance of these systems.

The following summarises the main background information that has now been acquired on these structures and provide the basic inputs used to construct a structural/functional descriptive model for the FSB system:

- Floating sulphur biofilms have been noted to occur on the surface of sulphide-rich organic wastewaters including the effluent of sulphate reducing bioreactors, sewage and tannery waste stabilization ponds and sulphidic anaerobic lignocellulose wastes (Dunn, 1998, Jørgensen *et al.*, 1998, Rose *et al.*, 1998);
- In the LFCR system, developed for the study of FSB under laboratory conditions, the FSB was cultivated successfully and was observed to develop in three clearly defined stages termed here as Thin, Sticky and Brittle FSB;
- Light and electron microscopy studies revealed a complex, and differentiated, structure composed of a range of bacterial morphologies, EPS architecture and sulphur crystals. SEM studies also showed that in addition to the crystals, small sulphur granules were dispersed throughout the FSB. The sulphur composition of the crystals and the dispersed sulphur was confirmed in EDX, XRF and XANES studies;
- Molecular microbial ecology studies of the FSB population showed the presence of aerobic sulphide oxidizing bacteria including *Acidithiobacillus*,

Halothiobacillus, *Acidithiobacillus*, *Thiovirga*, *Sulfurimonas* and *Thiothrix* in the upper aerobic layer. Micro-aerophilic and obligate anaerobic bacteria such as *Chryseobacterium*, *Bacteroides*, and *Planococcus* spp. occurred in the middle and the obligate anaerobe and copious EPS producer, *Brevundimonas* sp., was also identified in the bottom layer. This suggested the establishment of both steep physico-chemical and physiological gradients within the system

- The steep sulphide, pH and Redox potential gradients were demonstrated to exist within the FSB;
- These gradients correlated with the differentiation of microbial population established as the different levels;
- It is apparent from the experimental observations summarised above that the FSB appears to be a "true" biofilm structure.

5.2 DEVELOPMENT OF THE DESCRIPTIVE MODEL

A descriptive model accounting for the structure, function and performance of the FSB has been developed and the steps are outlined in Figures 5.1 – 5.4.

Step 1: Aerobic and micro-aerophilic microorganisms establish at the air/Liquid interface, possibly using surfactant production and the liquid surface tension to maintain themselves in this zone initially. Given the anoxic state of the bulk liquid, the growth of these organisms is constrained by oxygen diffusion, and an increasingly reducing environment is established across a steep gradient close to the air/Liquid interface (~ 50 μm). The Eh is reduced from + 180 mV to ~ -50 mV. The aerobic and micro-aerophilic forms that grow in this layer include bacteria such as *Azoarcus* sp., that are able to degrade aromatic compounds and other compounds released in the lignocellulose degradation. These conditions may contribute to the development of the Thin FSB stage (Figure 5.1).

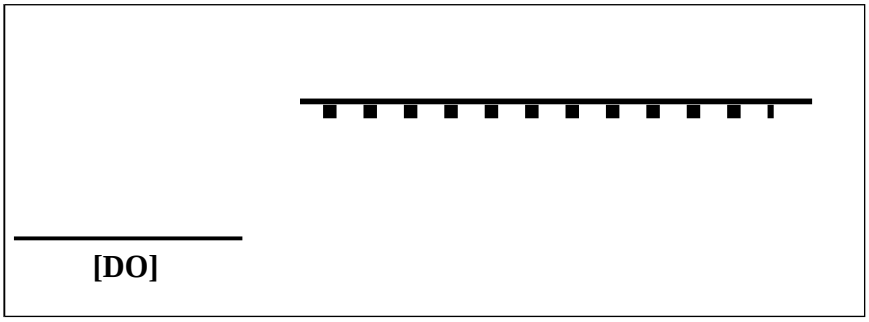

Figure 5.1 Diagrammatic account of proposed events in the Thin FSB formation. Here aerobic bacteria (circle) attach to the liquid surface (black line), the dissolved oxygen (DO) is rapidly reduced (assumed) and results in the establishment of the steep Redox gradients observed.

Step 2: Under anoxic conditions, when the Redox is appropriately poised, anaerobic species such as *Brevundimonas* may start to grow within the lower reaches of the system and copious EPS production commences. The EPS could thus provide an expanding matrix and maintain a correctly poised microenvironment in which the sulphide oxidation reactions may occur (Figure 5.2).

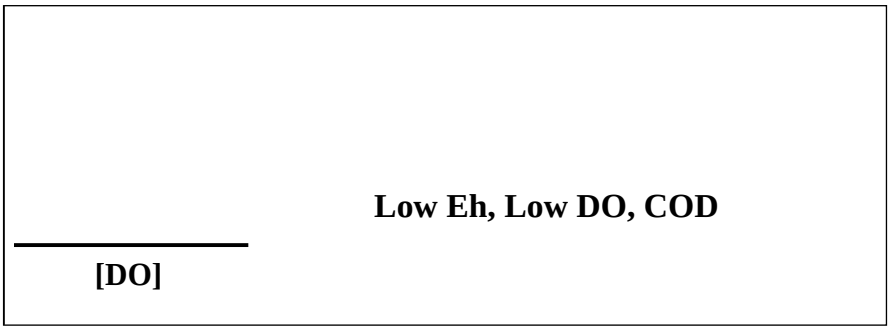

Figure 5.2 Diagrammatic account of proposed events in the Sticky FSB formation. Here micro-aerophilic and anaerobic bacteria establish in the system (circles) and copious EPS production commences (dotted line).

Step 3: Once the above is in place, sulphide oxidising bacteria appear in larger numbers in the upper aerobic part of the FSB with the production of possibly both internal and external sulphur globules. The biological sulphur may be released into the FSB and this may be enhanced, to some degree, by protozoa grazing on the bacterial population in the FSB. Sulphide oxidising bacteria which have been identified in the FSB, and are likely to occur here, include *Acidithiobacillus, Halothiobacillus, Thiothrix, Thiovirga, Sulfurimonas* and *Acidithiobacillus* spp. This may account for the first stage of dispersed sulphur formation observed in the Sticky FSBs (Figure 5.3).

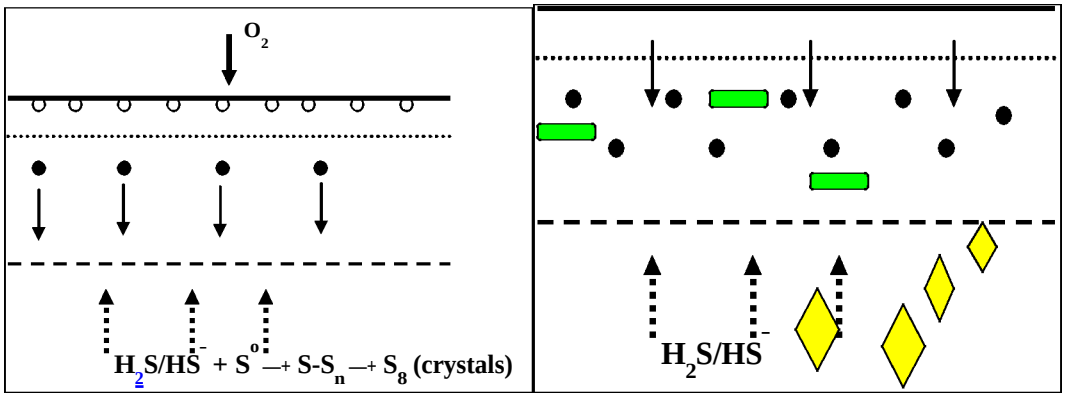

Figure 5.3 Diagrammatic account of proposed events in the Brittle FSB formation. Here sulphide oxidising bacteria (green rectangle) establish in the upper aerobic reaches of the system and firstly small biological sulphur granules (black dot) form and then large sulphur crystals appear (yellow diamond). The arrows indicate the direction gaseous diffusion (dotted – upward diffusion of sulphide and full – downward diffusion of oxygen).

Step 4: Micro-aerophilic forms now remove oxygen in the middle layer and poise the Redox potential for inorganic sulphide oxidation to take place. Where biological sulphur is released and dispersed through the FSB, the formation of inorganic elemental sulphur now occurs, based on the reaction mechanisms proposed to account for elemental sulphur formation in the presence of polysulphide (Steudel, 1996). In the initial steps, sulphide reacts with elemental sulphur and results in chain elongation to form polysulphide molecules of varying length (S_n^{2-}) until n = 9 (above n=9 the polysulphide chain is thought to be unstable (Equation 5.1).

$$HS^- + S_8 \text{ --+ } H\text{-}S\text{-}S_7\text{-}S \text{ --+} H^+ + S_9^{2-} \qquad (5.1)$$

The polysulphide undergoes cleavage to produce a mixture of S_n hybrids where n = 7, 6, 5, 4 and 3. The S_4^{2-} and $S^{5\,2-}$ hybrids are presented in Equations 5.2 and 5.3.

$$S_9^{2-} + HS^- \text{ --+ } H^+ + 2S_5^{2-} \qquad (5.2)$$

$$2S_5^{2-} \text{ --+ } S_4^{2-} + S_6^{2-} \text{..... etc.} \qquad (5.3)$$

Once this chain elongation commences, the presence of biological sulphur may no longer play a major role in the process with the sulphur/sulphide reaction resulting in the formation of elemental sulphur. Subsequently polysulphide chains may concatenate to form S_8^{2-} which in turn will aggregate to give rise to the orthorhombic sulphur crystals observed in the SEM and EDX images.

The increase in pH and decrease in Redox potential at a Redox potential window around -150 mV was recorded associated with the initial development stage (and the Thin FSB stage) where there's consumption of both oxygen and sulphide (sharp decrease from 450 mg/L to 25 mg/L) which react (sulphide oxidation) giving rise to sulphur crystal formation. With the increase in thickness of the biofilm, there is less oxygen diffusion (and consumption), this is associated with the measured increase in Redox potential (less pronounced in the Thin than Brittle FSB).

Figure 5.4 shows a summary overview of the various process steps described above.

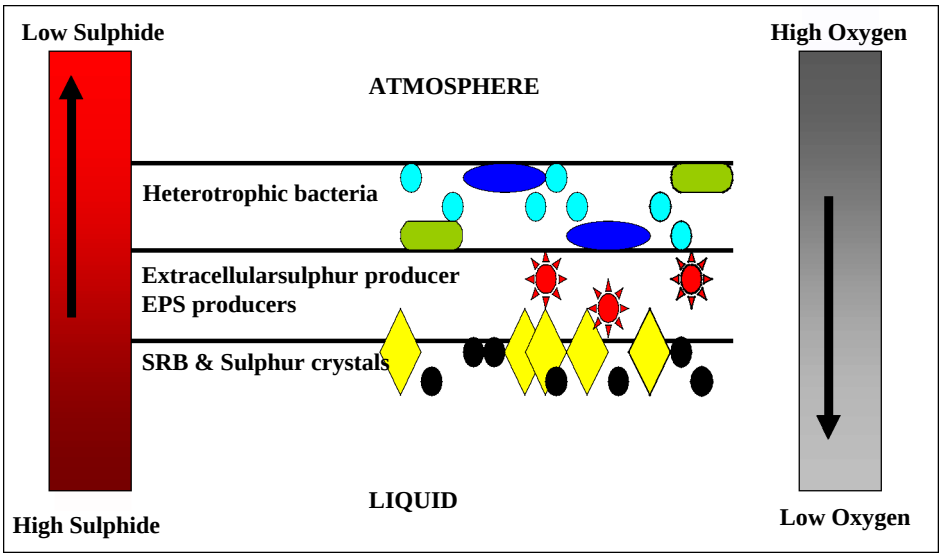

Figure 5.4 Summary illustration of the descriptive model integrating the various processes proposed to occur in the FSB. These occur against falling dissolved oxygen and Redox potential gradients and sulphide migrating upwards into the FSB (indicated by the arrows). Aerobic heterotrophic bacteria (blue dots and green rectangles) establish at the air/Liquid interface and, in consuming oxygen diffusion into the strongly anaerobic system, establish steep DO and Redox gradients at the surface. Below this layer, anaerobic EPS producers generate a copious slime layer which constitutes the matrix of the FSB (red stars). Within the correctly poised Redox window, both biological (black dots) and inorganic sulphur formation occurs and gives rise to large sulphur granules which characterise the Brittle FSB.

5.3 CONCLUSIONS

- The correlation of data and observations accumulated for the FSB enables the formulation of a provisional structural/functional model accounting for the performance of the system;
- This may be a first account for the FSB system;

- The integration of the various findings into a descriptive model further explained the interaction of the different bacterial species and the functions they perform in the development of the FSB;
- The descriptive model of the FSB provides the basis for a rational approach in applying the FSB system in the treatment of sulphidic wastewaters.

Chapter Six

APPLICATION OF THE FLOATING SULPHUR BIOFILM AS A WATER TREATMENT PROCESS UNIT OPERATION

6.1 INTRODUCTION

Sulphide removal in industrial-scale processes has been tackled by a range of physico-chemical systems. These generally have high cost implications that are inappropriate for the treatment of low volumes of AMD which decant over long periods of time. Sulphide removal by the precipitation of metal sulphide has been previously described in low-cost AMD treatment (van Hille and Duncan, 1996; Molipane, 1999; Rose, 2002). However, copious sludges formed in metal precipitation require sustainable disposal. Biological removal has been investigated and the intensively engineered Thiopaq process has been developed (Boonstra *et al.*, 1999) and applied by Paques Bio Systems B.V. at the Buldeco zinc refinery, Netherlands (Janssen *et al.*, 1999). The shortcomings of this process also include cost and the intensive labour and maintenance requirement, and are not applicable where passive treatment technologies are implemented to treat wastewater decanting from closed mines.

The possibility that the FSB system could be developed and applied as a sustainable sulphide removal unit operation in AMD treatment has been suggested (Rein, 2002).

The objective of this study was to investigate how an application of the FSB phenomenon could be used as a post treatment unit operation for the removal of sulphide generated during passive AMD treatment.

6.2 MATERIALS AND METHODS

6.2.1 Reactor Development and Optimisation

The LFCR operated for the cultivation of the FSB in previous laboratory studies (Chapter 2) was scaled up, through various stages from two- to a four- and an eight-channel LFCR. The objective, in addition to process scaling factors was to derive accurate mass balances and rate functions for the operation of the system. Initial

studies using the two-channel LFCR, indicated the presence of residual sulphide detected in the effluent, and the need to account for this fraction in the mass balance calculations required more stringent process operation than applied in the descriptive study (Figure 6.1).

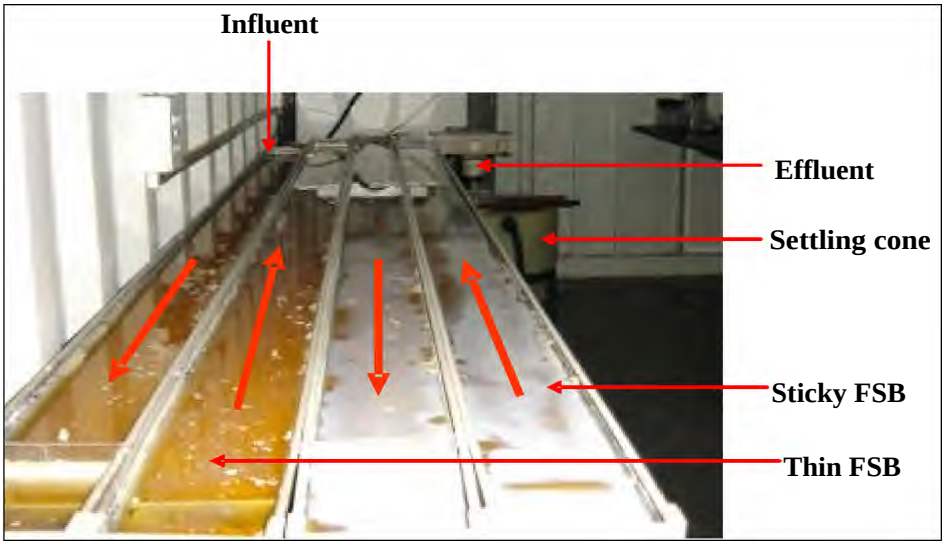

Figure 6.1 Four-channel linear flow channel reactor set up in the constant environment room operating at 25 °C.

The four-channel LFCR had a surface area of 1.1 m^2 (2.5 m x 0.11 m x 4). Four more channels were added to the four-channel LFCR to form the eight-channel LFCR with a total surface area of 2.2 m^2 (Figure 6.2).

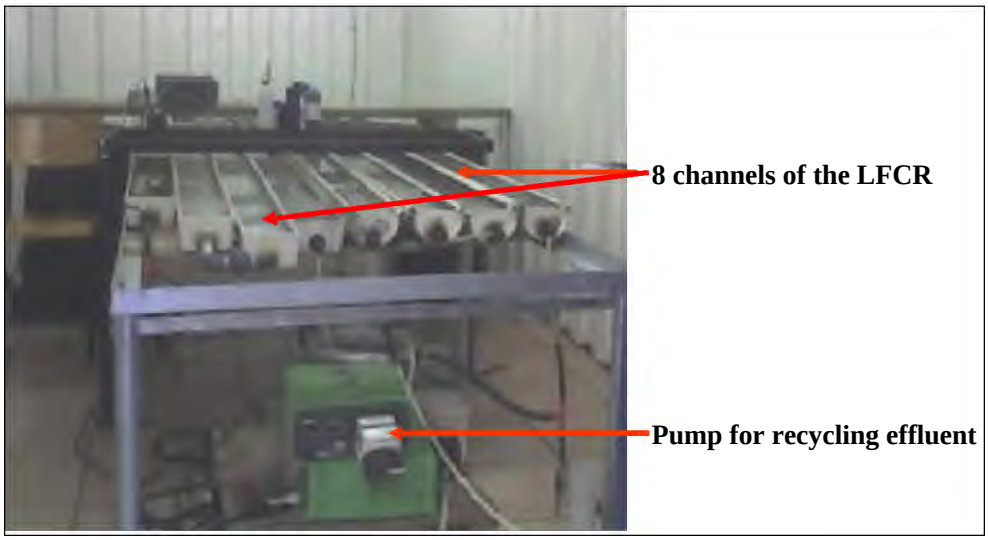

Figure 6.2 Eight-channel linear flow channel reactor operated in the constant environment room at 25 °C.

6.2.2 Process Operation

The start-up of the reactor involved the sourcing of feed from the DPBR (Chapter 2) at a loading rate of 2 618 L/m^2/d (optimum flow) and 1 309 L/m^2/d (half flow) respectively. The flow rates were chosen during the initial FSB cultivation investigation (Chapter 2). The LFCR was allowed to run continuously for 24 to 48 hours until the development of the FSB from Thin through to Brittle was observed (this served as the seeding stage of FSB development, without any harvesting). This was followed by harvesting of the Brittle FSB at 12 to 18 hours for two runs (the harvested sulphur was not collected for mass balance purposes at this stage), after the third harvest, steady state operation of the LFCR was assumed (as the FSB development had stabilized and the harvest and recovery times were constant). The steady state operation of the system was carried out for a period of 7 to 18 days under specific conditions and harvested every 12 to 18 hours during this time as described. Once a run was complete (between 7 and 18 days), the reactor was drained, the settled FSB collected, dried and weighed for mass balance calculations and analysed for total sulphur.

The volume of the drained liquid from the reactor at the end of a run (7 to 18 days), was measured and the volume was used in the mass balance calculations. On a daily basis, influent and effluent samples of the LFCR were collected for analysis.

The temperature of operation was varied over a range representing summer and winter conditions. Operation of the reactor was tested at three temperatures, namely, 25, 20 and 15 ^{o}C. The 20 ^{o}C represents the average operating temperature while 25 ^{o}C and 15 ^{o}C represent the anticipated summer and winter season highs and lows, respectively. Operational phases of the LFCR are summarized in Table 6.1

Table 6.1 Summary of the different operational phases of the linear flow channel reactor at different flow and temperature settings and showing the period of operation in each case.

Phase	Loading rate (L/m^2/d)	Temperature (^{o}C)	Period (Days)
1	2 618	25	24
2	1 309	25	24
3	2 618	20	8
4	1 309	20	9
5	2 618	15	7
6	1 309	15	7

6.2.3 Analysis

Triplicate samples were drawn for each of the data sets reported and analysed for sulphide, sulphate, thiosulphate, sulphur and pH, Redox potential and COD. Results were averaged and reported as the mean of three samples.

6.2.3.1 Sulphide

The Merck spectroquant® system (photometric colour measurement) was used for sulphide determination (Merck, South Africa). Samples were collected in test tubes containing 100 µl of 0.1 M zinc acetate solution. Photometric readings were made using the SQ 118 spectrophotometer (Merck, South Africa).

6.2.3.2 Sulphate and Thiosulphate

Ion chromatography was used for the determination of sulphate with a model 600 Waters HPLC and model 432 Waters conductivity detector (Waters, South Africa) fitted with an IC-Pak™ anion 4.6 x 50 mm column (Waters, South Africa). Samples were prepared using a ten-fold dilution of sample in milliQ water and then filtered through a 0.45 µm nylon filter before passing it through two Waters Sep-Pak® light C_{18} cartridges (Waters, South Africa) to remove contaminating organic compounds. The samples were then injected and run at 1 mL/min and analysed using the EMPOWER software programme (Waters, South Africa). A borate/gluconate buffer concentrate (Appendix B) was used for eluent (Appendix B) preparation. All chemicals and filters were from Merk, South Africa. A standard concentrate (Appendix B) containing Fe^-, Cl^-, NO_3^-, Br^-, HPO_4^{2-} and SO_4^{2-} in milliQ water was prepared. The injected standard was prepared weekly by diluting 100 µl of the concentrate standard in 100 mL of milliQ water.

6.2.3.3 Sulphur

A modified Mockel (1984), reverse HPLC method was used for sulphur determination. Three 1 mL samples were collected, centrifuged for 5 minutes at 13 000 rpm on an Eppendorf, centrifuge 5415D (Merck, South Africa), and air dried. After drying, 1 mL of acetone was added to the pellet, and left to stand for 1 hour with vigorous shaking every ten minutes. The samples were filtered through a 0.45 µm

nylon filter (Merck, South Africa) and analysed using the EMPOWER software on a 600 model Waters HPLC and a 2487 model dual λ absorbance detector fitted with a Nova-Pak® $_{C18}$ 3.9 x 150 mm column (Waters, South Africa). The samples were injected into the HPLC and run at 2 mL/min using a 5:95 ratio of water:methanol (Hypersolv for HPLC, BDH from Merck, South Africa) as the eluent. A 20 ppm standard of elemental sulphur (Appendix B) in acetone was prepared and injected with samples for standardisation.

6.2.3.4 pH

pH was measured using a WTW pH/mV 330 meter (Merck, South Africa).

6.2.3.5 Redox Potential

Redox potential was measured using a WTW pH/mV 330 meter (Meck®, South Africa).

6.2.3.6 Chemical Oxygen Demand

Chemical oxygen demand (COD) was assayed using a digestion and titration method outlined in American Public Health Association (APHA), standard methods (APHA, 1998). A 10 mL sample was oxidised in a boiling solution of acidic potassium dichromate $_{(K2Cr2O7)}$ containing silver sulphate (Ag_2SO_4), glass balls, 1 g mercuric sulphate ($HgSO_4$), 25 mL of water, 40 mL digestion mixture and additional water to make up the solution to 100 mL, in an Elenmeyer flask attached to a condenser. The mixture was refluxed on a hot plate for two hours after which it was cooled. Four drops of ferroin indicator were added before titrating with 0.1 *N* ferrous ammonium sulphate. A red-brown to blue endpoint was used.

The COD concentration in mg/L was calculated as: $\frac{(A-B) \times [M] \times 8\,000}{\text{mL sample}}$

Where:

A = mL ferrous ammonium sulphate solution for blank

B = mL ferrous ammonium sulphate solution for sample

M = Molarity of ferrous ammonium sulphate

8 000 = mL equivalent weight of oxygen x 1 000 mL

6.2.3.7 Floating Sulphur Biofilm Harvesting

After each reactor run at a specific temperature and flow conditions, the system was shut down and drained and the settled FSB collected and dried at 80 ^{o}C for three to five days.

6.2.3.8 Mass Balance

Mass balances were calculated to account for influent, effluent and recovered sulphur species as S. In each case, the data generated over the period between start up and shut down prior to sediment removal from the LFCR and following steady state operation of the system.

The percentage mass balance recovery was calculated as follows:

Total sulphur species IN = Total sulphur species OUT + Total sulphur RECOVERED.

$$(S^{o} + SO_4^{2-} + HS^{-} + S_2O_3^{-})_{IN} = (S^{o} + SO_4^{2-} + HS^{-} + S_2O_3^{-})_{OUT} + (S^{o} + SO_4^{2-} + HS^{-} + S_2O_3^{-})_{RECOVERED}$$

$$\text{Mass balance loss (\%)} = [(S_{IN} - S_{OUT}) + (S_{RECOVERED}) / S_{IN}] * 100$$

Mass balance recovery (%) = 100 – Mass balance loss (%)

$$\text{Sulphide removal (\%)} = [(\text{Sulphide}_{IN} - \text{Sulphide}_{OUT})/\text{Sulphide}_{IN}]*100$$

$$\text{Sulphur recovery (\%)} = [(\text{Sulphur}_{OUT} - \text{Sulphur}_{IN})/\text{Sulphide}_{IN}]*100$$

6.2.3.9 Statistical Validation

Statistical validation of the data was performed using the software package Statistica (data analysis software system) Version 7.1 (StatSoft, Inc. 2005).

6.3 RESULTS AND DISCUSSION

6.3.1 Four-channel Linear Flow Channel Reactor Operation

Following reactor development studies in which the Four-channel LFCR was commissioned, optimization investigations commenced. This involved operation of the LFCR over a range of temperature and loading rate conditions. These are reported below together with the mass balance data. The objective was to determine operational conditions on which a process scale-up programme could be based.

6.3.1.1 Four-channel Linear Flow Channel Reactor Operated at 25 ^{o}C and 2 618 L/m ^{2}/d Loading Rate.

Figure 6.3 shows the results of this study and reports data for analysis of Sulphide (A), Sulphate (B), Sulphur (C) and Thiosulphate (D) over this period. The mean of the distribution of the data is plotted in Figure 6.4 showing sulphide (A), sulphate (B), sulphur (C) and thiosulphate (D).

Fluctuations in the feed concentration of all sulphur species were observed which is consistent with use of the lignocellulose packed bed reactor system and has been reported elsewhere (Molwantwa *et al.*, 2003). The results in Figure 6.3(A) showed maximum influent sulphide concentration of 420 mg/L and a minimum of 175 mg/L with an average influent and effluent sulphide concentration of 264 and 161 mg/L respectively over the 24 days.

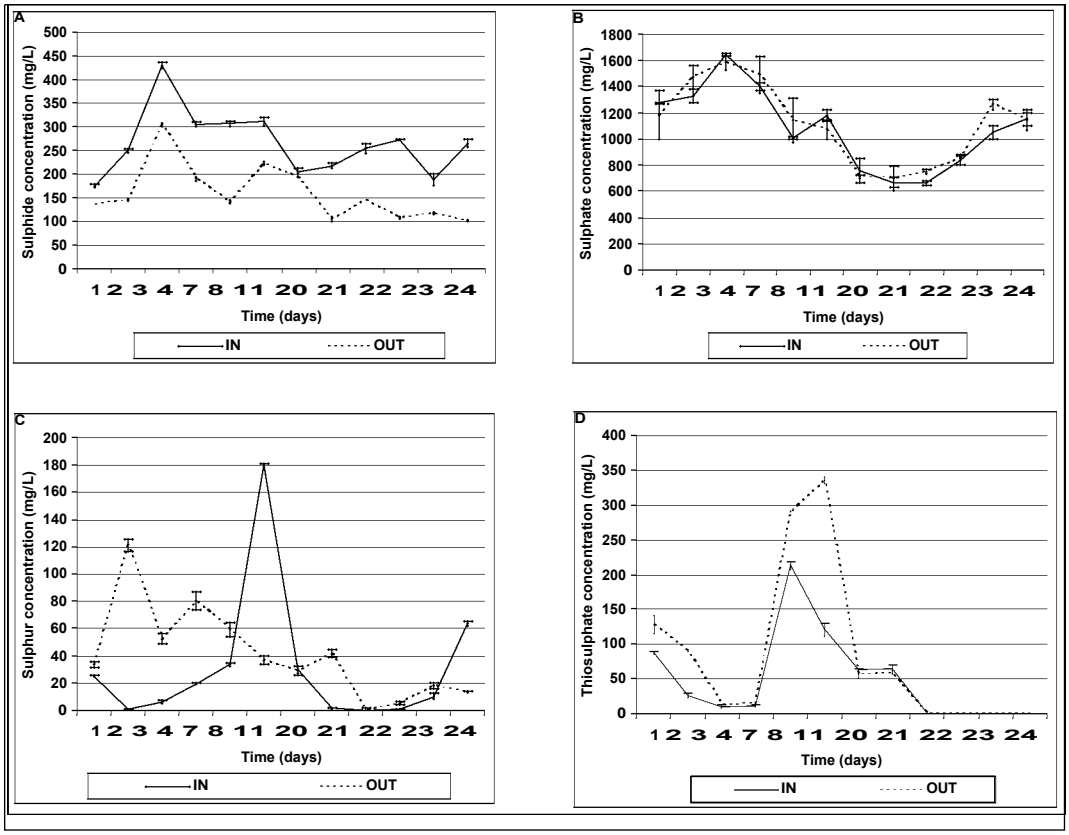

Figure 6.3 Influent and effluent sulphur species measured in the four-channel linear flow channel reactor over 24 days at 25 °C and 2 618 L/m^2/d loading rate. Sulphide (A), Sulphate (B), Sulphur (C) and Thiosulphate (D).

Figure 6.4 indicates a significant average sulphide removal of 39 % (t = 4.024; df = 22; $p<0.05$). Figure 6.4(B) shows an average of 1 079 and 1 108 mg/L influent and effluent respectively which indicates that the average sulphate increase of 2.7 % was not significant (t = -0.28; df = 22; p = 0.78). Thiosulphate increase of 57 % (Figure 6.3D) was also not significant (t = -0.85; df = 22; p = 0.401). These results indicate that sulphide removal was incomplete and that some oxidation of sulphide to sulphate occurred in the LFCR as neither oxygen nor Redox potential is under control in this system. Elemental sulphur in suspension (Figure 6.3C) possibly reflects sulphur that was formed in the feed system and also particles of the FSB which break away and remains in suspension following FSB harvesting. The difference between the average influent concentration of 30.9 and 41.5 mg/L in the effluent sulphur was not significant (t = -0.56; df = 22; p = 0.58). Sulphur recovery at 25 °C and 2 618 L/m^2/d flow rate was 36 %.

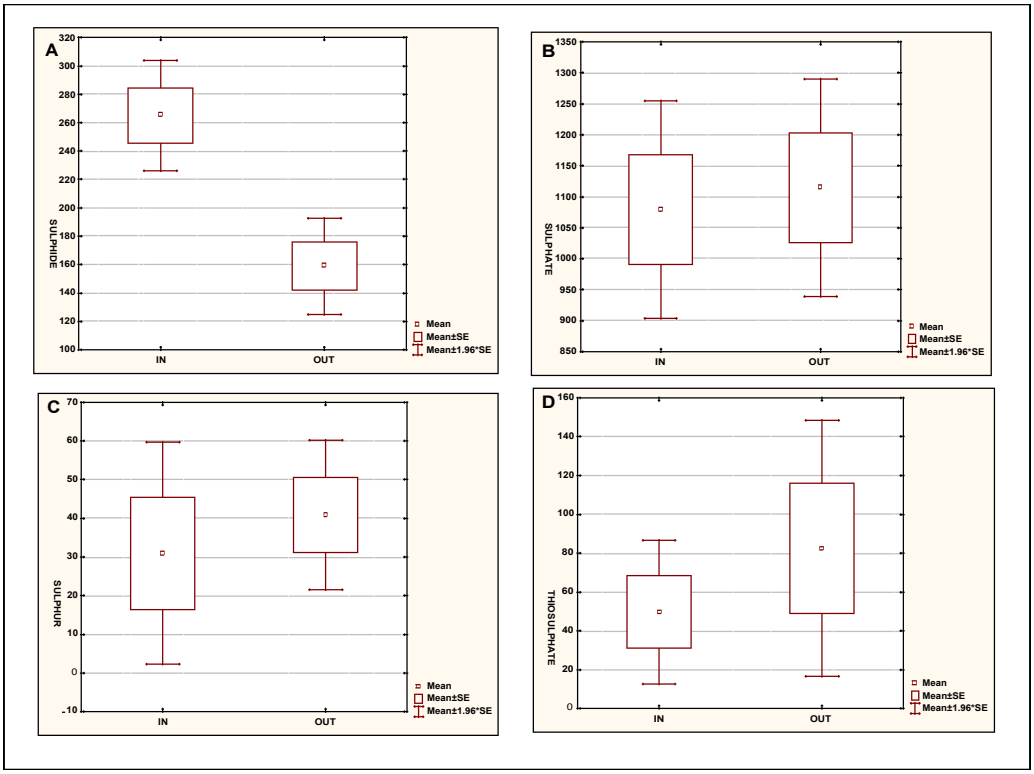

Figure 6.4 Box and whiskers plot showing the mean distribution of influent and effluent sulphide (A), sulphate (B), sulphur (C) and Thiosulphate (D) over a 24 days operation period of the four-channel linear flow channel reactor operated at 25 °C and 2 618 L/m²/d.

6.3.1.2 Four-channel Linear Flow Channel Reactor Operated at 25 °C and 1 309 L/m²/d Loading Rate.

Fluctuations in the feed were also observed when the four-channel LFCR was operated at 25 °C and 1 309 L/m²/d loading rate (Figure 6.5 and 6.6). The results in Figure 6.5(A) showed an average influent and effluent sulphide concentration of 149 and 75 mg/L respectively over the 19 days (Figure 6.5), indicating a significant average sulphide removal of 52 % (t = 7.49; df = 9; $p < 0.05$). Figure 6.5(B) shows an average 7 % increase in sulphate, which was not statistically significant, as was the increase in thiosulphate of 47 % (Figure 6.5D) (t = -1.27; df = 9; p = 0.22). Figure 6.5 and 6.6(C) indicates that the change in sulphur across the system of 5.5 % was not significant (t-test, t = 0.18; df = 9; p = 0.85).

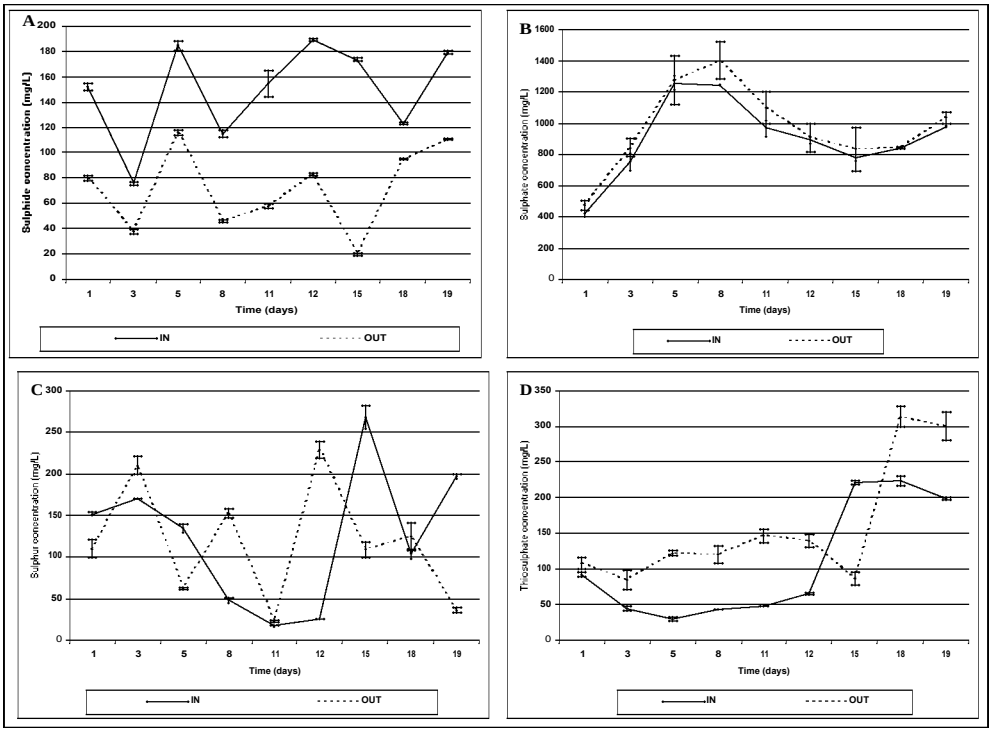

Figure 6.5 Influent and effluent sulphur species measured in the four-channel linear flow channel reactor over 19 days at 25 °C and 1 309 L/m^2/d loading rate. Sulphide (A), Sulphate (B), Sulphur (C) and Thiosulphate (D).

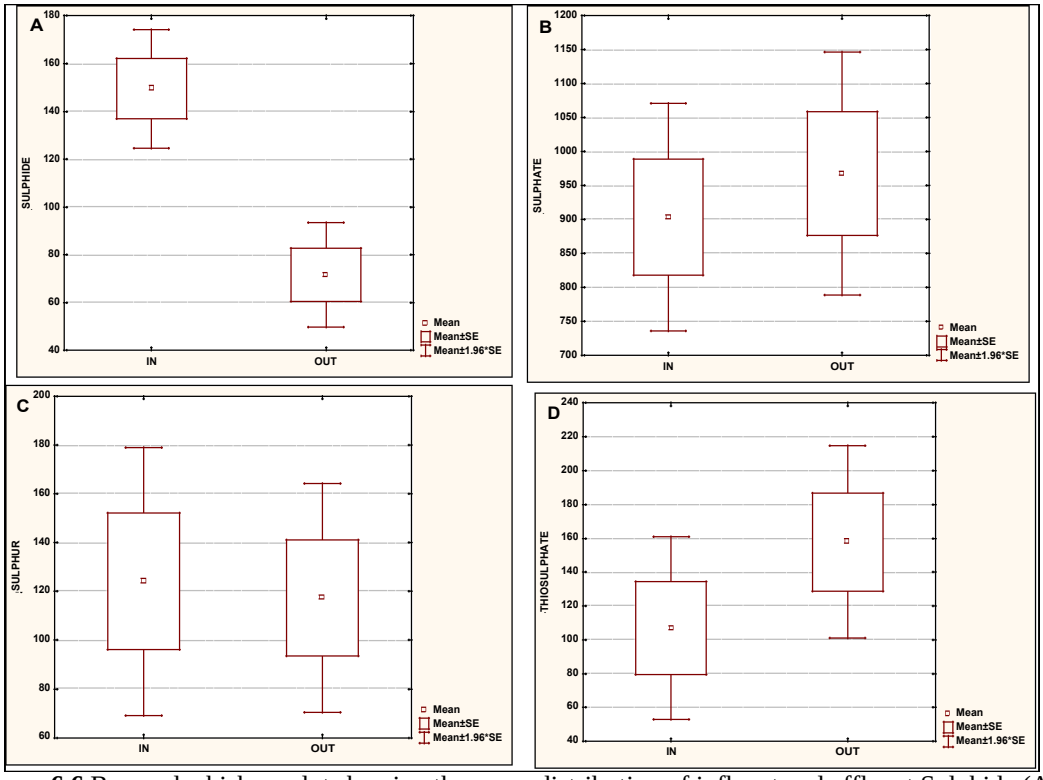

Figure 6.6 Box and whiskers plot showing the mean distribution of influent and effluent Sulphide (A), Sulphate (B), Sulphur (C) and Thiosulphate (D) over the 19 days operation period of the four-channel linear flow channel reactor operated at 25 °C and 1 309 L/m^2/d.

6.3.1.3 Four-channel Linear Flow Channel Reactor Operated at 20 °C and 2 618 L/m²/d Loading Rate.

Sulphide results (Figure 6.7A) showed an average influent and effluent sulphide concentration of 111 and 28.6 mg/L respectively indicating a highly significant average sulphide removal of 74 % (t = 8.07; df = 10; p = 0.001) (Figure 6.8A). Sulphate results (Figure 6.7B) showed that the oxidation of sulphate to sulphide in the system was not significant with an average sulphate increase of 9 % (t = -0.97; df = 10; p = 0.36) (Figure 6.8B). The decrease in thiosulphate of 42 % and increase in sulphur of 43 % was also not significant (t = 0.72; df = 10; p = 0.48) (Figure 6.8C and D).

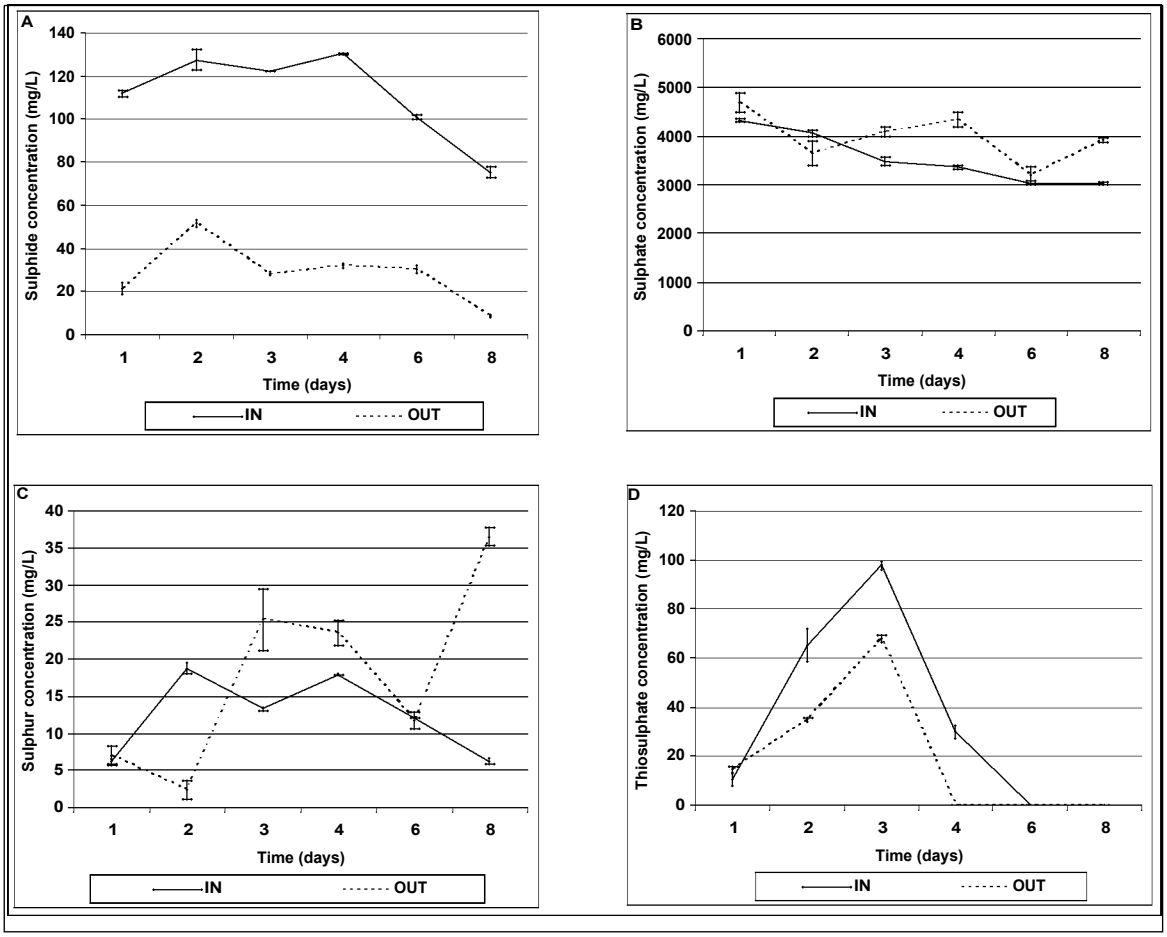

Figure 6.7 Influent and effluent sulphur species measured in the four-channel linear flow channel reactor over 8 days at 20 °C and 2 618 L/m²/d loading rate. Sulphide (A), Sulphate (B), Sulphur (C) and Thiosulphate (D).

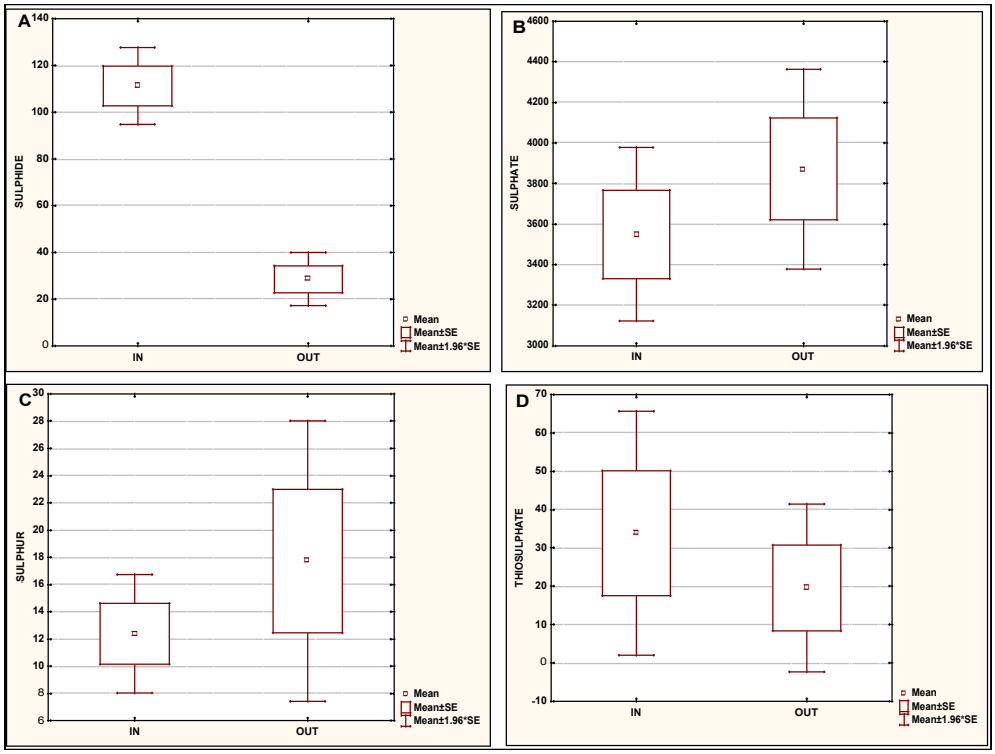

Figure 6.8 Box and whiskers plot showing the mean distribution of the influent and effluent Sulphide (A), Sulphate (B), Sulphur (C) and Thiosulphate (D) over the 8 days operation period of four-channel linear flow channel reactor operated at 20 °C and 2 618 L/m²/d.

6.3.1.4 Four-channel Linear Flow Channel Reactor Operated at 20 °C and 1 309 L/m²/d Loading Rate.

The sulphide results showed an average influent and effluent sulphide concentration of 78 and 30 mg/L respectively (Figure 6.9A) indicating a significant average sulphide removal of 62 % (t = 7.49; df = 10; $p < 0.05$) (Figure 6.10A). The increase in sulphate and thiosulphate were not found to be significant (t = -058; df = 10; $p = 0.57$ and t = 0.96; df = 10; $p = 0.35$ respectively) (Figure 6.10B and D). However, the increase in the sulphur concentration in the effluent of 80 % was found to be significant (t= 2.33; df = 10; $p < 0.05$) (Figure 6.10C).

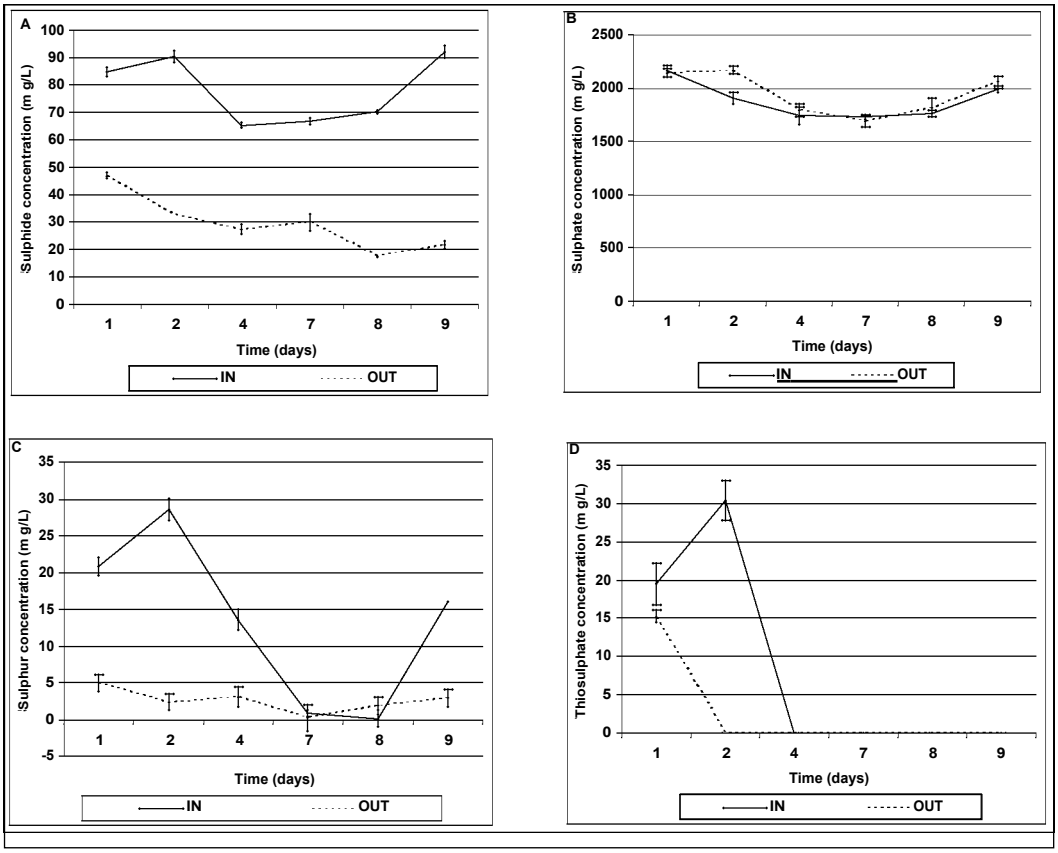

Figure 6.9 Influent and effluent sulphur species measured in the four-channel linear flow channel reactor over 8 days at 20 °C and 1 309 L/m²/d loading rate. Sulphide (A), sulphate (B), sulphur (C) and thiosulphate (D).

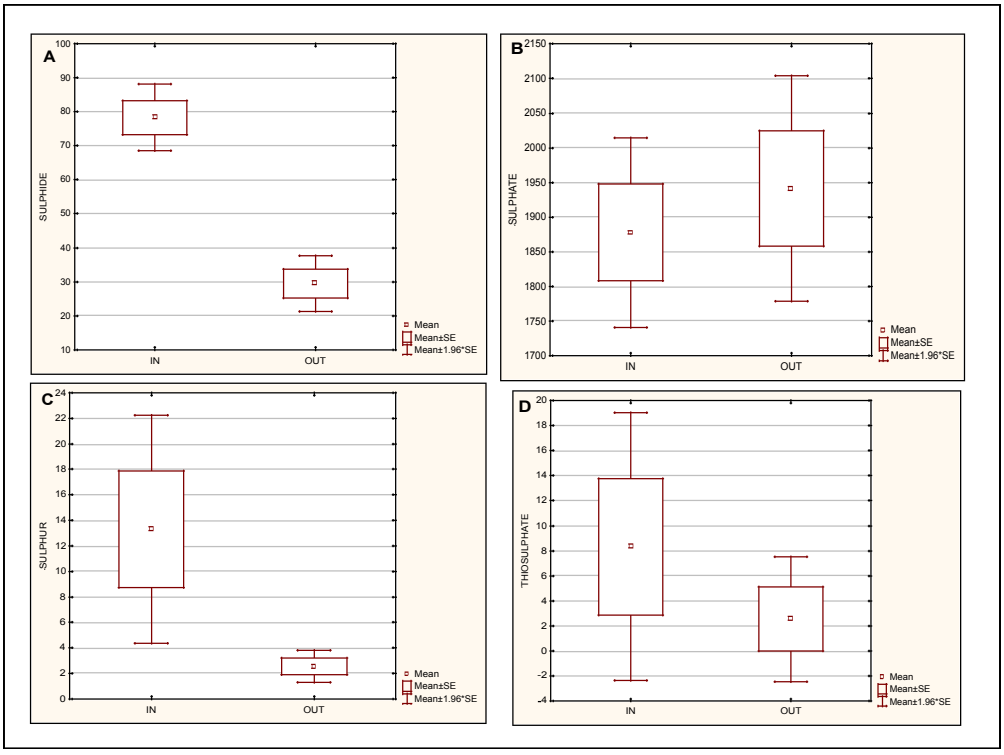

Figure 6.10 Box and whiskers plot showing mean distribution of influent and effluent Sulphide (A), Sulphate (B), Sulphur (C) and Thiosulphate (D) over the 8 days operation period of the four-channel linear flow channel reactor operated at 20 C and 1 309 L/m /d.

6.3.1.5 Four-channel Linear Flow Channel Reactor Operated at 15 C and 2 618 L/m /d Loading Rate.

There was a significant (t = 4.21; df = 8; p <0.05) average sulphide removed (Figure 6.12A) of 53 % from an average influent and effluent concentration of 139 and 65mg/L respectively (Figure 6.11A). The increases in sulphate and thiosulphate (Figure 6.11B and D) were not significant (t-test, t = -0.91; df = 8; p = 0.39) and (t-test, t = 0.64; df = 8; p = 0.53) respectively (Figure 6.12B and D). The decrease in sulphur (Figure 6.11C) in the effluent was not significant (t = 0.56; df = 8; p = 0.56) (Figure 6.12C).

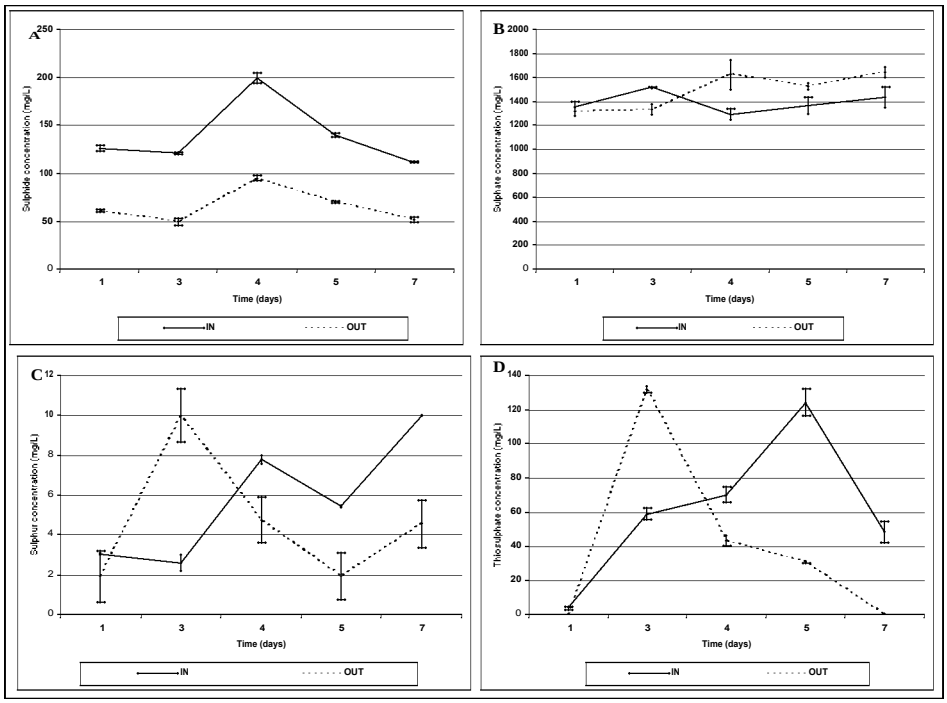

Figure 6.11 Influent and effluent sulphur species measured in the four-channel linear flow channel reactor over 8 days at 15 C and 2 618 L/m /d loading rate. Sulphide (A), sulphate (B), sulphur (C) and thiosulphate (D).

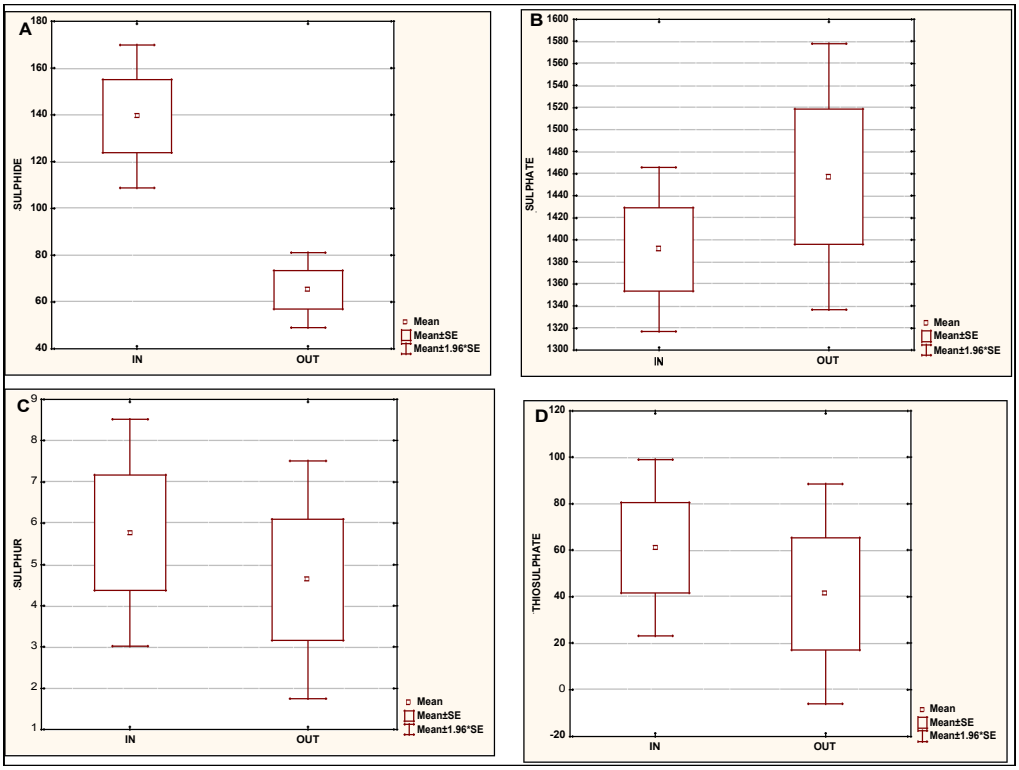

Figure 6.12 Box and whiskers plot showing mean distribution of influent and effluent Sulphide (A), Sulphate (B), Sulphur (C) and Thiosulphate (D) over the 8 days operation period of the four-channel linear flow channel reactor operated at 15 °C and 2 618 L/m /d.

6.3.1.6 Four-channel Linear Flow Channel Reactor Operated at 15 °C and 1309 L/m /d Loading Rate.

A 54 % removal of sulphide (Figure 6.14 A) was found to be highly significant (t = 5.92; df = 12; p = 0.001) resulting from the average influent and effluent sulphide concentration of 161 and 74 mg/L respectively (Figure 6.13A). The average sulphate increase of 8 % and thiosulphate decrease of 37 % (Figure 6.13 B and D) were not significant (t = -0.73; df = 8; p = 0.43 and t = 1.29; df = 12; p = 0.23) respectively (Figure 6.14B and D). The 13 % increase in sulphur (Figure 6.13C) was also not significant (t = 0.87; df = 12; p = 0.40) (Figure 6.14C).

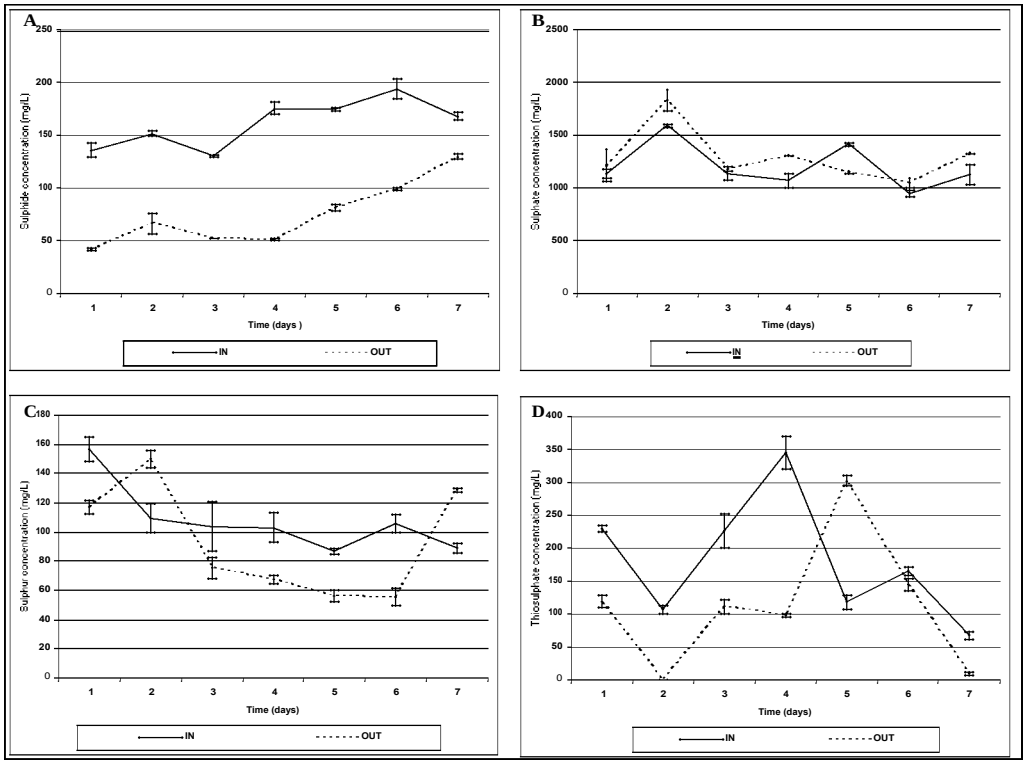

Figure 6.13 Influent and effluent sulphur species measured in the four-channel linear flow channel reactor over 8 days at 15 °C and 1 309 L/m²/d loading rate. Sulphide (A), sulphate (B), sulphur (C) and thiosulphate (D).

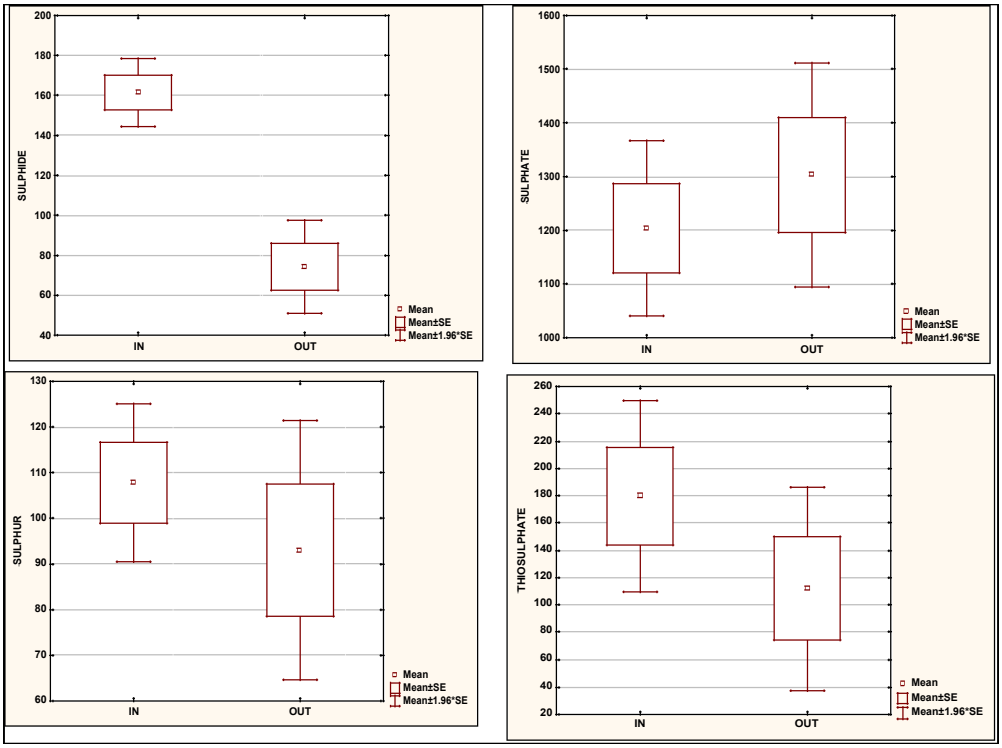

Figure 6.14 Box and whiskers plot showing the mean distribution of the four-channel linear flow channel reactor operated at 15 °C and 1 309 L/m²/d showing the mean of distribution of influent and effluent Sulphide (A), Sulphate (B), Sulphur (C) and Thiosulphate (D) over the 8 days operation period.

The results of the LFCR process optimization studies (Figures 6.2 to 6.14) indicate that both flow rate and temperature have a significant effect on its performance. Although fluctuations of the sulphide concentration in the feed were measured, the narrow standard deviations (t = 8.07; df = 10; p = 0.001) for results in Figures 6.4, 6.6, 6.8, 6.10, 6.12 and 6.14, indicated that temperature effect on sulphide removal (39 to 74 %) was significant. The highest percentage removal of 62 and 74 % was obtained at 20 ^{o}C for 1 309 and 2 618 L/m^{2}/d loading rates respectively. While both 25 ^{o}C and 15 ^{o}C showed poorer performance than the 20 ^{o}C operational temperature, performance was better at 25 ^{o}C compared to 15 ^{o}C.

Although the four-channel LFCR demonstrated effective sulphide removal, residual sulphide remained in the effluent which was assumed to be linked to surface area limitation. Based on this reasoning, four more channels were added to the reactor to form the eight-channel LFCR which is described in the following section.

6.3.1.7 Mass Balance Calculations for the Four-Channel Linear Flow Channel Reactor

The mass balance for the LFCR performance data reported above were calculated as described for the different temperatures and flow rate operations and the results are presented in Table 6.2.

Table 6.2 Summary of the results obtained at different temperature and flow conditions during operation of the four-channel linear flow channel reactor showing system mass balance recovery, sulphide removal and sulphur species (as S) recovery presented as percentages.

Loading Rate (L/m^{2}/d)	**Temperature (^{o}C)**	**Mass Balance %**	**Sulphide Removal %**	**Sulphur Recovery %**
2 618	25	93	39	36
	20	100	74	43
	15	89	53	28
1 309	25	72	52	33
	20	94	62	60
	15	86	54	22

The mass balance recovery accounts for the difference in total sulphur species (as S) entering and exiting the reactor at the different flows and temperatures measured.

Mass balance of total S-species ranged between 70 % and 100 %. Sulphide gas escape into the atmosphere was not measured and this may account for most of the unaccounted loss. The highest sulphide removal, sulphur recovery and mass balance recovery was achieved at 20 ^{o}C for both loading rates.

6.3.2 Eight-Channel Linear Flow Channel Reactor Operation

The investigation of surface area limitation on sulphide removal and sulphur formation rates was carried out in the eight-channel LFCR (Figure 6.2). This study investigated the operation of the eight-channel LFCR at the previously demonstrated optimal operating conditions for sulphide removal at 20 ^{o}C and flow rate set at 2 618 L/m^{2}/d. The reactor was commissioned and operated until steady state conditions were established and then data collected over a period of 18 days.

Figures 6.15A shows a highly significant decrease in effluent sulphide concentration of 88 % with average influent and effluent rates of 133 and 15.4 mg/L measured respectively (t = 9.83; df = 24; p = 0.001) (Figure 6.16A). This percentage sulphide removal was higher than the highest obtained in the four-channel LFCR system. The sulphide concentration in the effluent ranged between 1.45 and 27.4 mg/L throughout the operation time, which was lower than the discharge from passive AMD treatment systems. These have been reported to range between 50 and 120 mg/L (Molwantwa *et al.*, 2003). This result indicates that an increase in surface area can lead to a decrease in the residual sulphide in the effluent.

Figure 6.15B shows the influent and effluent sulphate concentration over the 18 days of operation. Variability in influent and effluent sulphate concentration was observed during the whole operation time. The average sulphate concentration measured was 1 391 and 1 456 mg/L in the influent and effluent, respectively (Figure 6.15B). The increase in sulphate due to complete oxidation in the system was found not to be significant (t = -0.65; df = 24; p = 0.52) (Figure 6.16B), and at an average percentage sulphate increase of 4.7 %, was lower than the 10 % of the four-channel LFCR obtained under comparable operating conditions. The fluctuations in suspended sulphur concentration are shown in Figure 6.15C. The average sulphur in the feed was 1.26 mg/L and that in the effluent was 0.34 mg/L (Figure 6.15C). Although the

average sulphur in the feed was lower compared to the four-channel LFRC, the percentage in the effluent was relatively lower. This was possibly due to the breakage of the sulphur FSB and release of particles into suspension being limited under a larger surface area. There was a decrease in thiosulphate from influent to effluent of 25.7 to 1.45 mg/L respectively (Figure 6.15D), indicating complete oxidation rather than formation of thiosulphate in the system. The reduction in thiosulphate and, sulphide oxidized to sulphate, were recycled back to the reduced form in the LFCR. Thus, not only was sulphide removed from the LFCR by oxidation to elemental sulphur (and trapped as organic sulphur), but some of the oxidized forms of sulphur (thiosulphate) were also removed (by reduction).

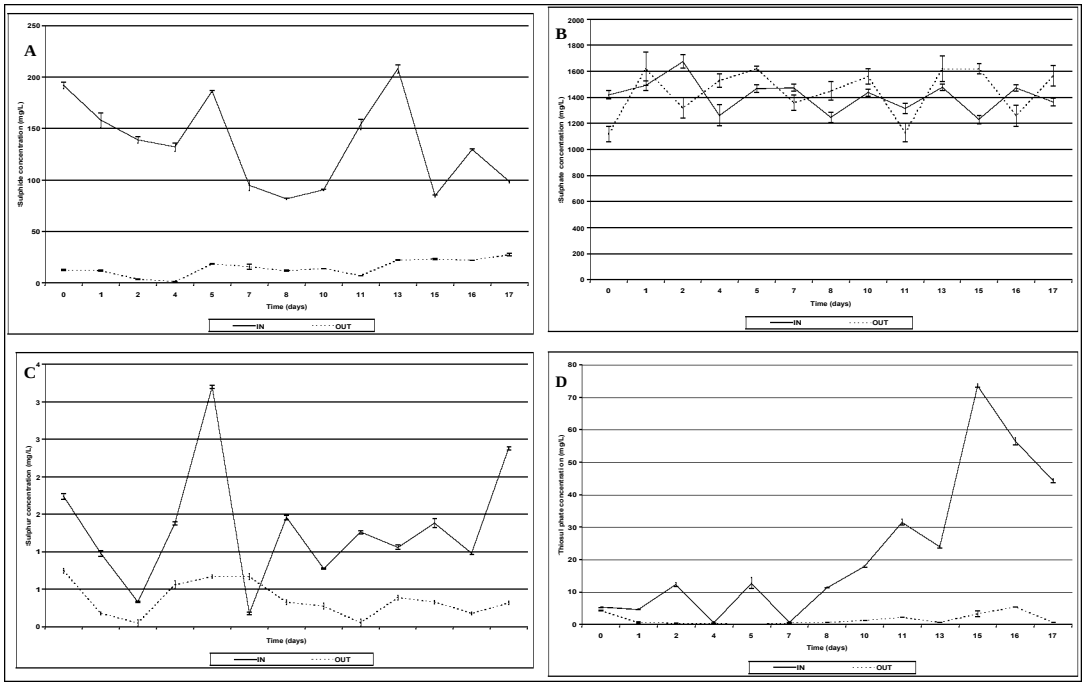

Figure 6.15 Influent and effluent sulphur species measured in the eight-channel linear flow channel reactor over 17 days at 20 °C and 2 618 L/m²/d loading rate. Sulphide A), Sulphate B), Sulphur C) and Thiosulphate D).

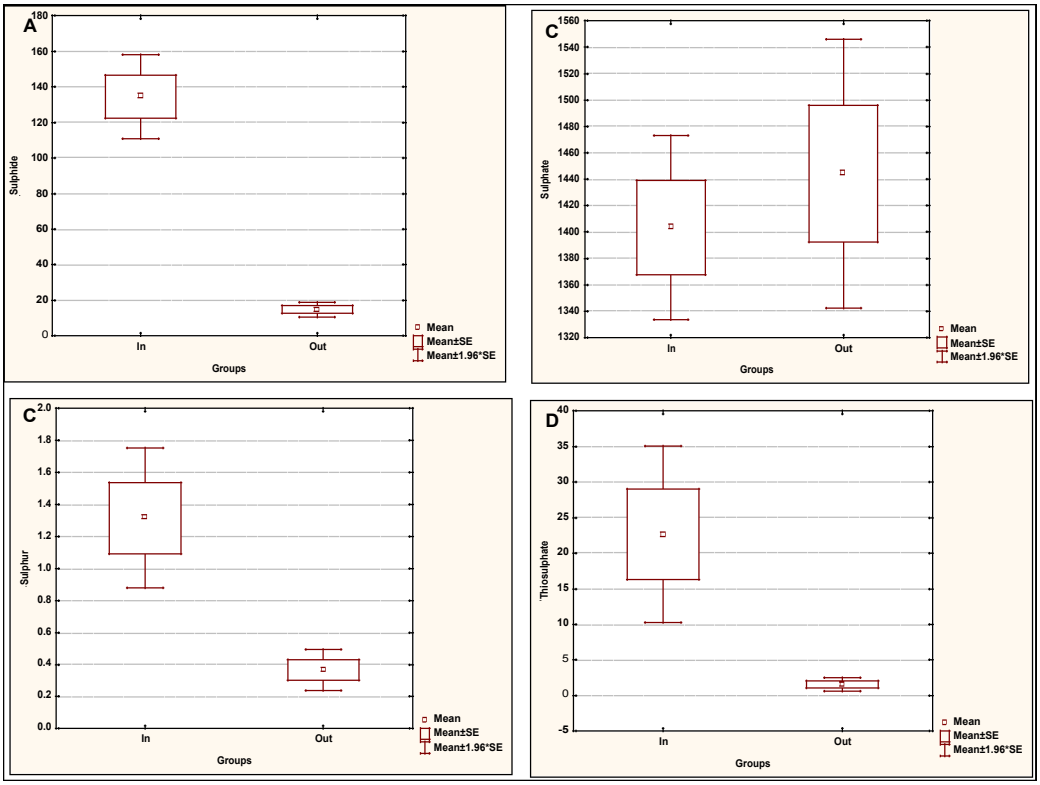

Figure 6.16 Box and whiskers plot showing the mean distribution of the eight-channel linear flow channel reactor operated at 20 °C and 2 618 L/m^2/d showing the mean of distribution of influent and effluent Sulphide (A), Sulphate (B), Sulphur (C) and Thiosulphate (D) over the 18 days operation period.

Other analyses in the eight-channel LFCR included the measurement of pH, Redox potential and COD. These results are shown in Figure 6.17 and the box and whiskers plot summarises the mean of distribution in Figure 6.18.

The increase in pH across the system from influent to effluent from pH 7.5 to pH 8 was found to be highly significant (t = -8.22; df = 24; p = 0.001) and corresponds with active elemental sulphur formation in the reactor (Figure 6.17A and Figure 6.18A).

The Redox potential was found to vary widely between the influent and effluent with ranges between -248 mV and +27 mV in the influent and -208 mV and -88 mV in the effluent (Figure 6.17B and Figure 6.18B). These differences were not found to be significant (t = -1.96; df = 24; p = 0.057). However, it is evident that for some of the time, at least, the Redox potential in the system was poised to operate around the optimal window for oxidation of sulphide to sulphur at ~ -150 mV (Steudel, 1996).

Influent COD concentration ranged between 330 and 885 mg/L while the effluent ranged between 136 and 350 mg/L (Figure 6.17C). The average COD removal of 65 % was found to be significant (*t*-test, $t = 4.38$; df = 24; $p < 0.05$) (Figure 6.18C) probably indicating microbial activity within the reactor. This would be expected within the FSB but may also account for possible sulphate reduction occurring in the anaerobic compartment of the bulk liquid coupled with re-oxidation of sulphide in the LFCR. While difficult to prove, it is possible that the results recorded for the system represent an overall balance for the total oxidation and reduction reactions occurring in the system.

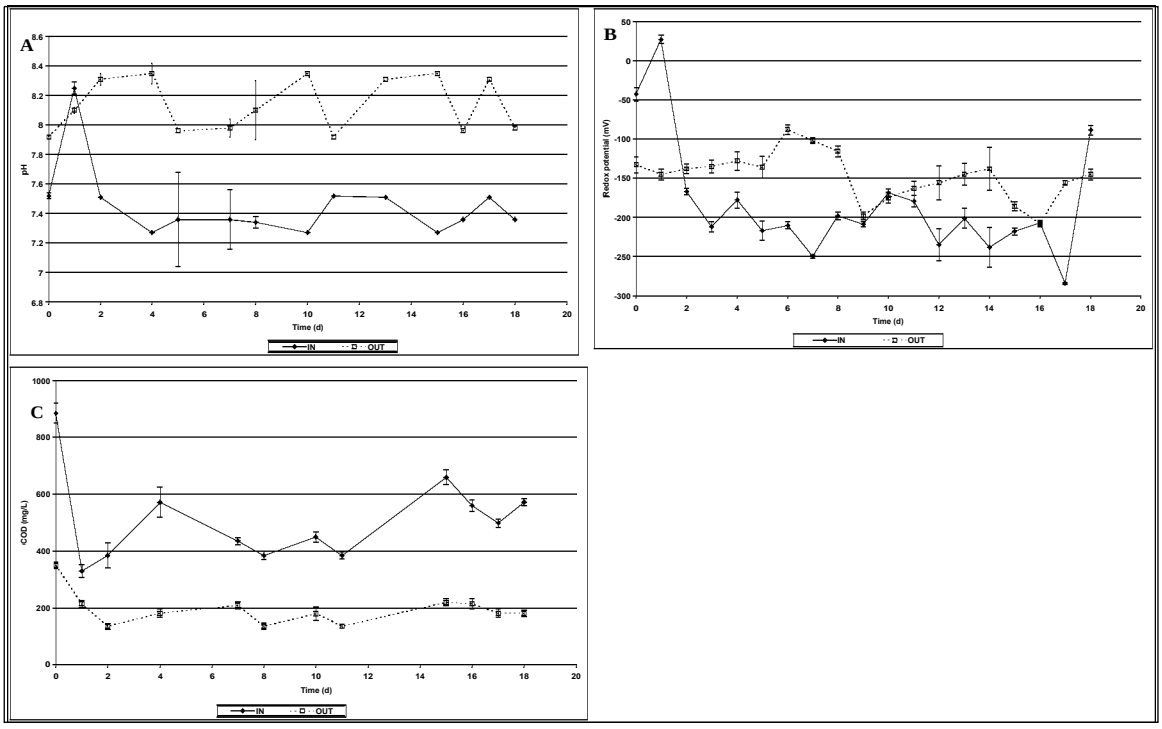

Figure 6.17 Influent and effluent pH, Redox potential and COD data for the eight-channel linear flow channel reactor over 18 days at 20 °C and 2 618 L/m²/d loading rate. pH, A), Redox potential, B) and COD, C).

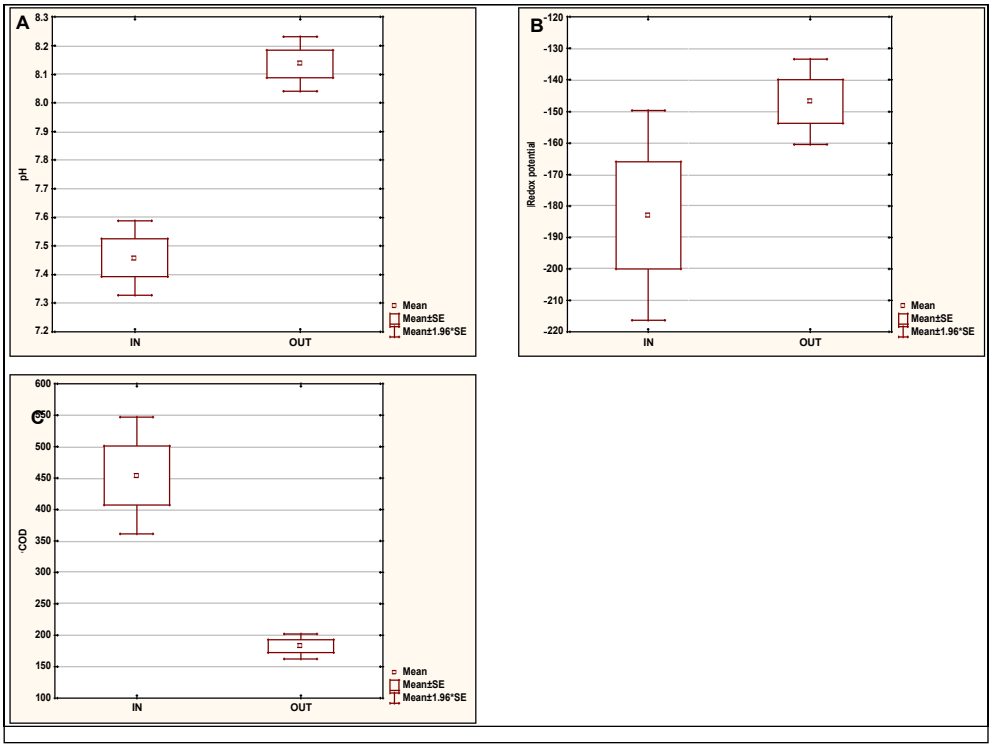

Figure 6.18 Box and whiskers plot showing the mean distribution of influent and effluent pH (A), Redox potential (B), and COD_0 (C) over the 18 days operation period of the eight-channel linear flow channel reactor operated at 20 °C and 2 618 L/m²/d.

6.3.2.1 Mass balance Calculations for the Eight-channel Linear Flow channel Reactor

The mass balance calculations for the eight-channel LFCR are summarised in Table 6.2 showing system mass balance, sulphide removal and sulphur recovery at 20 °C and 2 618 L/m²/d.

Table 6.3 Summary of the results obtained at 20 °C and 2 618 L/m²/d on the eight-channel linear flow channel reactor showing system mass balance, sulphide removal and sulphur species (as S) recovery presented as percentages.

Mass balance (%)	**Sulphide Removal (%)**	**Sulphur Recovery (%)**
82	88	66

Actual sulphide removal of 88 % and sulphur recovery of 66 % were obtained from the mass balance calculations on the eight-channel LFCR and were higher than those calculated on the four-channel LFCR under comparable operation conditions.

6.4 CONCLUSIONS

The following conclusions were drawn from the investigations on the LFCR operation and mass balance calculations.

- The LFCR used in the FSB descriptive studies showed potential to be scaled-up as a basic unit operation for sulphide removal in the treatment of AMD wastewaters;
- The optimum operating temperature was found to be 20 ^{o}C;
- A process trade-off was observed with higher sulphide removal at higher flow rates but the sulphur recovery was reduced;
- Sulphide removal was shown to be surface area and flow rate dependent;
- In the four-channel LFCR sulphide removal of 74 % and sulphur recovery of 43 % was measured at the 2 618 L/m^{2}/d loading rate.
- An average sulphide removal of 88 %, and sulphur recovery of 66 % was obtained for the eight-channel LFCR at the 2 618 L/m^{2}/d.

Chapter Seven

DEVELOPMENT OF THE FLOATING SULPHUR BIOFILM REACTOR AS A WATER TREATMENT PROCESS UNIT OPERATION

7.1 INTRODUCTION

Sulphide removal technologies used in AMD treatment need to be sustainable for long-term operation, especially when coupled with passive mine water treatment systems. According to PHD (2002) “Passive treatment systems rely on the use of naturally available energy sources such as topographical gradient, microbial metabolic energy, photosynthesis and chemical energy which requires regular but infrequent maintenance to operate over its design life”. The limitation in technology options for the passive treatment of AMD and subsequent removal of sulphide requires attention.

The LFCR was shown to be successfully scaled-up as a sulphide removal unit for the treatment of sulphidic wastewaters over the range investigated (0.55 to 2.2 m^2). However, given the rather flimsy nature of the PVC channels used in the LFCR studies, a more robust equipment design was considered necessary for the transfer of the system to field operation conditions. In order to distinguish between the two systems, the field unit was called the floating sulphur biofilm reactor (FSBR).

7.2 MATERIAL AND METHODS

7.2.1 Reactor Development

Reactor development was undertaken in five successive phases.

7.2.1.1 Phase 1: The design, construction and commissioning of the Floating Sulphur Biofilm Reactor treating lignocellulosic sulphide-rich effluent

The FSBR (Figure 7.1) was constructed as a 1 m^3 bioreactor at EBRU, Grahamstown, and commissioned at the PHD research facility in Johannesburg. The reactor was fed with lignocellulosic sulphide-rich water from a passive system DPBR in order to

demonstrate that lignocellulosic effluent would result in the formation of the FSB similar to the LFCR studies reported above.

Figure 7.1 The floating sulphur biofilm reactor as initially set up at Pulles Howard and de Lange laboratories in Johannesburg.

Figure 7.2 is a diagrammatic longitudinal cross-section of the FSBR configuration showing the harvesting system and the reservoir located below the linear flow zone. It was envisaged that harvested sulphur may settle and be collected here. A depth-adjustment plate was later fitted into the FSBR in order to raise and lower the depth of the reactor for maximum FSB formation and sulphide removal.

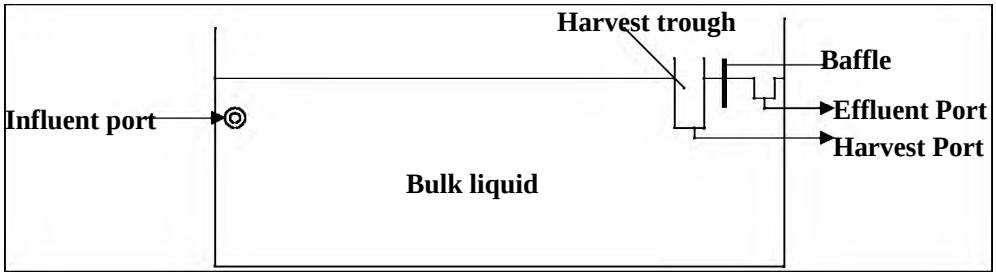

Figure 7.2 Cross-sectional line diagram of the floating sulphur biofilm reactor showing the influent and effluent ports and the harvest port.

A baffle was inserted in the FSBR between the harvest and effluent ports. Here the sulphur harvesting stage was initiated by closing the effluent port valve allowing the water level to rise until the FSB passed into the harvest trough with a small volume of water. The harvest period lasted around five minutes depending on the degree of FSB removal desired in the specific investigation. During harvesting, a portion of the FSB was drawn off the water surface via the harvest port through to the settling cone. During the period when the FSB was allowed to recover on the FSBR surface, the

effluent was passed through the effluent port to waste. Alternatively, during this stage, the entire effluent flow could be directed through the settling cone to pick up any sulphur loss occurring between harvests.

Figures 7.3 to 7.5 show details of the FSBR components. For the collection of the FSB, a funnel was fitted to the inlet of the settling cone to prevent airlocks.

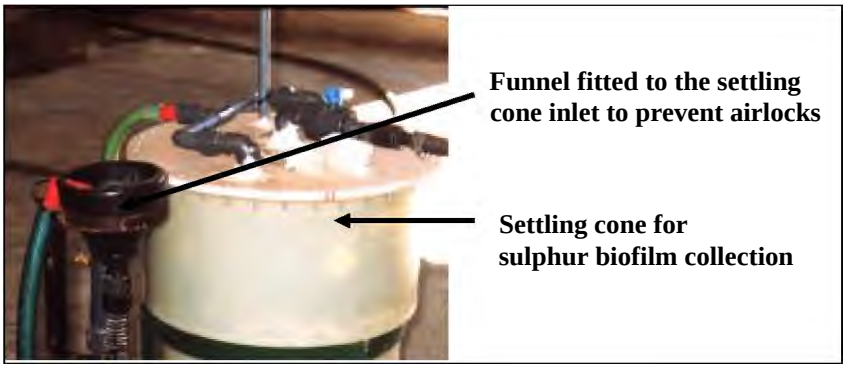

Figure 7.3 Sulphur settling cone showing funnel installed to prevent airlocks.

To measure the flow rate through the FSBR, a tap was installed on the influent line and the valves were installed in case any regulation of flow was necessary (Figure 7.4).

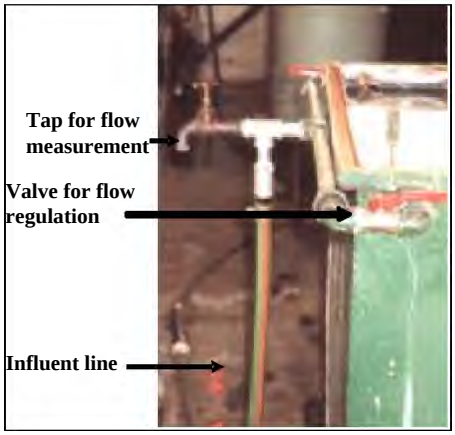

Figure 7.4 Flow rate measurement tap and valve on the influent port.

The FSB from the FSBR was harvested through to the settling cone where it was allowed to settle while the effluent passed to waste (Figure 7.5).

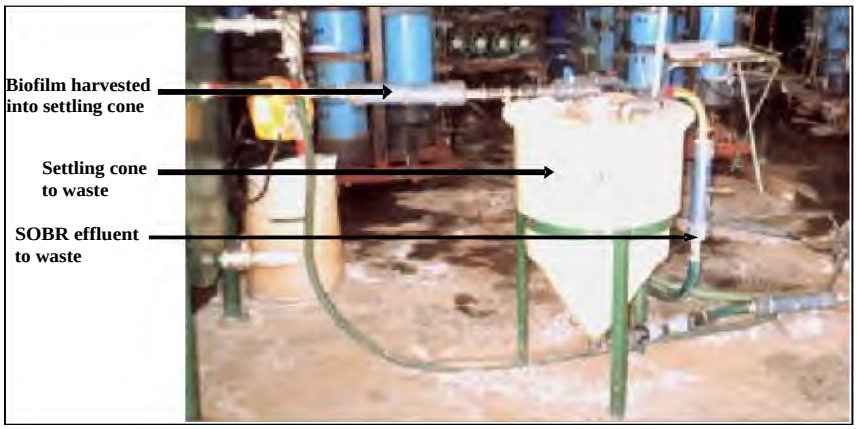

Figure 7.5 Initial configuration showing the floating sulphur biofilm reactor connected to the cone during manual harvesting operations and passing directly to waste during inter-harvest periods.

7.2.1.2 Phase 2: Evaluation of variable sulphide loads

Sulphide-containing wastewater sourced from the DPBR was supplemented with sodium sulphide (Na_2S) to investigate the effects of low and high sulphide concentration in the feed. The maximum influent sulphide concentration reached was 300 mg/L. During winter, the feed temperature was elevated by immersing the influent pipe in a 55 ^{o}C water bath upstream from the bioreactor.

7.2.1.3 Phase 3: Enhancing polysulphide formation by increasing oxygen transfer into the FSBR

Previous studies (Rein, 2002) established that polysulphide formation in the presence of sulphur particles produced by SOB such as *Acidithiobacillus* is a rate-limiting step in the large-scale production of elemental sulphur. Rein *(*2002) also showed that a FSB comprising these organisms could be successfully established on air-fed silicone tubes (Rein, 2002).

A silicone tube frame (Figure 7.6) was constructed and inserted 20 to 30 mm below the water surface (Figure 7.7). Air was diffused through porous silicone tubes into the bulk liquid for enhanced polysulphide production.

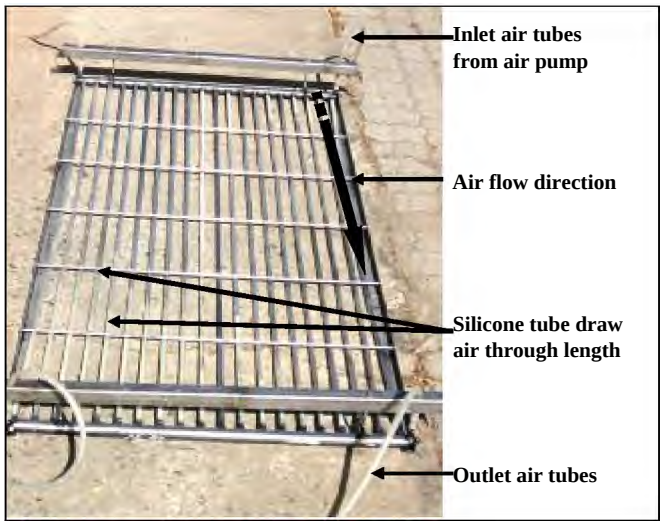

Figure 7.6 Silicone tube frame inserted in the subsurface zone of the reactor. Air was passed through the tubes to enhance polysulphide formation.

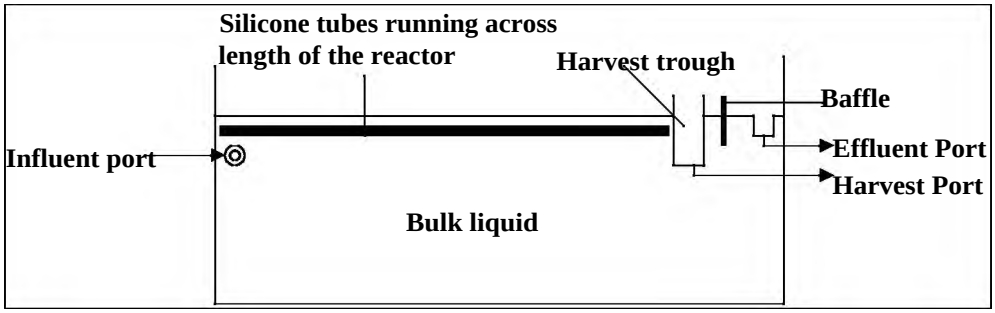

Figure 7.7 Longitudinal cross-sectional line diagram of the floating sulphur biofilm reactor configuration as used in the third stage of operation. The silicone tube rack was inserted in the subsurface zone to enhance polysulphide formation.

The dedicated lignocellulose-DPBR sulphide generator (Figure 7.8) was constructed on site and linked to the FSBR.

Figure 7.8 A lignocellulose packed sulphide generator (blue tank) providing feed to the floating sulphur biofilm reactor.

7.2.1.4 Phase 4: Optimisation of flow and dimensions of the sulphur formation zone

Given the observation of turbulent flow in the sulphur collection reservoir an adjustable plate was fitted inside the FSBR to reduce the depth of the anaerobic compartment from where the sulphide would diffuse up towards the air/water interface. The plate enabled the floor of the FSBR to be lowered and raised as required (Figure 7.9).

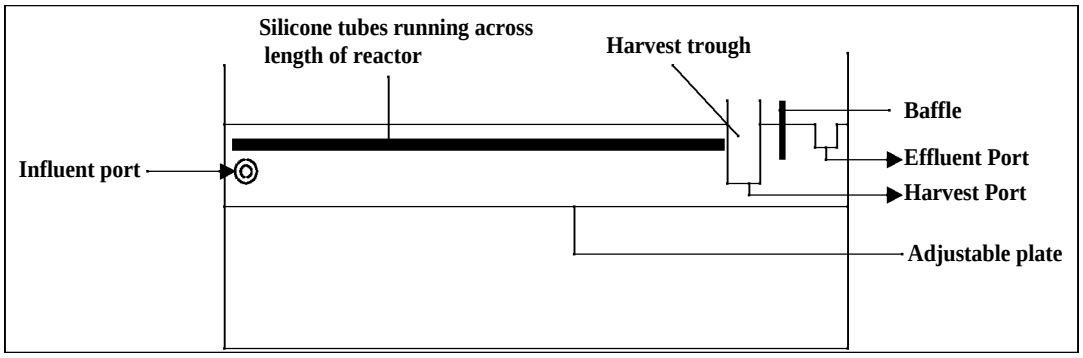

Figure 7.9 Longitudinal cross-sectional line diagram of the floating sulphur biofilm reactor configuration as used in phase 4 showing the fitted adjustable plate used to lower and raise the reactor floor as required.

7.2.1.5 Phase 5: Optimisation of the harvesting procedure, installation of an automated harvesting process.

The automation of the harvesting process was introduced to allow the full optimisation of the sulphide oxidation/sulphur recovery process. Automated valves (EL-O Matic Actuator Valves) were fitted to the effluent and harvest ports and facilitated the determination of optimal harvest and FSB development times. Figure 7.10 shows the automated valves fitted to the FSBR.

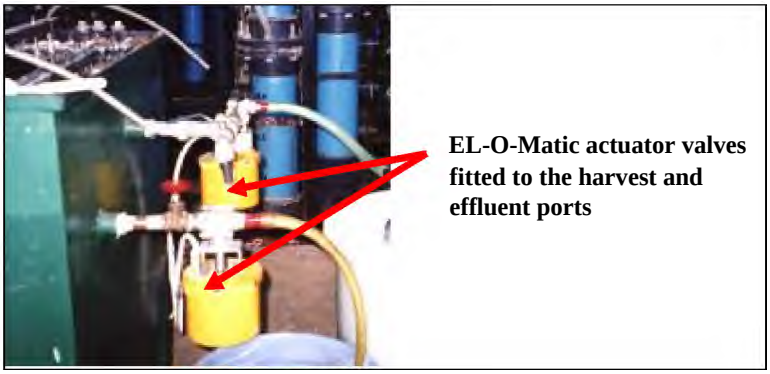

Figure 7.10 The EL-O Matic actuator valves fitted for the automation of the flow and harvesting operations.

A summary of the five Phases of reactor development is presented in Table 7.1.

Table 7.1 Five development phases of the floating sulphur biofilm reactor during the reactor development study.

Phase	Description	Changes in operation
1	Design and construction of FSBR treating lignocellulose-based effluent	Fed FSBR with lignocellulose effluent from PHD carbon columns
2	Evaluation of sulphide loads into the FSBR	Sodium sulphide supplementation into the FSBR feed line
3	Enhancement of polysulphide formation	Installation of silicone tube frame in the subsurface of the FSBR
4	Optimisation of flow and reactor dimensions	Installation of adjustable plate to control the depth of the FSBR
5	Optimisation of the harvesting procedure	Installation of the automated EL-O Matic valves to the effluent and harvest ports

7.2.2 Analysis

7.2.2.1 Sulphide Concentration

An iodometric method (APHA, 1998) was used in this study as it was the standard method for sulphide analysis at PHD laboratories and was validated against the previously used Merck spectroquant® method (Chapter 6) prior to its use. This was analysed on a 200 mL aliquot of sample collected from the reactor into a sample bottle containing eight drops of 0.22 mg/L zinc acetate preservative. A standard iodine solution (0.05 *N*) containing 25g KI, 3.2 g iodine and 100 mL ddH_2O was prepared, made up to 1 l with ddH_2O, and standardized against 0.025 *N* sodium thiosulphate ($Na_2S_2O_3$), using starch solution as an indicator. An excess volume of the iodine solution and 2 mL of 6 *N* HCl was added into a 500 mL beaker. The sample

was pipetted into the flask, until the iodine colour disappeared. More iodine was added to the flask until the colour remained. This solution was back-titrated against the sodium thiosulphate solution, adding a few drops of starch solution as the end-point approached, and continuing until the blue colour disappeared. The sulphide concentration was calculated as follows:

One mL 0.0250 *N* iodine solution reacts with 0.4 mg S^{2-}:

$$\text{mg } S^{-2}/L = \frac{(AxB) - (CxD) \times 16\,000}{\text{mL sample}}$$

Where:
A = mL iodine solution,
B = normality of iodine solution,
C = mL $Na_2S_2O_3$ solution, and
D = normality of $Na_2S_2O_3$ solution.

7.2.2.2 Sulphate and Thiosulphate Concentration

Sulphate and thiosulphate determination was carried out as previously described (Waters, South Africa).

7.2.2.3 Sulphur

Sulphur determination was carried out using the previously described method (Mockel, 1984).

7.2.2.4 Redox Potential and pH

Redox potential and pH was measured using a Zeiss 300 pH meter.

7.2.2.5 Alkalinity

Alkalinity was assayed using two titration method (APHA, 1998). Firstly, the solution was titrated with 0.02bN sulphuric acid (H_2SO_4) to an orange to pink end point with

methyl orange as indicator (pH 4.4) and secondly, to a dark pink to clear end point with phenolphthalein as indicator (pH 8.3).

Where:

1. Control (water) titration with $_{H2SO4}$ (0.02 *N*) = $\frac{\text{mL x 1 000}}{\text{mL sample}}$

2. Sample (influent or effluent) titration with $_{H2SO4}$ (0.01 *N*) = $\frac{\text{mL x 5 000}}{\text{mL sample}}$

7.2.2.6 Chemical Oxygen Demand

COD was analysed as previously described.

7.2.2.7 Mass Balance Calculations

Mass balance calculations were carried out as previously described.

7.2.2.8 Statistical Validation

Statistical validation was carried out as previously described.

7.3 RESULTS AND DISCUSSSION

7.3.1 Bioreactor Development

A progressive increase in the thickness of the FSB and the sulphur content of the harvested sediment of FSB was observed through the various phases of the reactor development investigations.

The FSBR was successfully commissioned and operated for 400 days using a lignocellulose-based sulphide-rich effluent for FSB formation. The resulting FSB (Figure 7.11A) was Thin and speckled and had an inter-harvest period of three to four days. In the second phase, the increased sulphide concentration in the influent resulted in increased FSB thickness (Figure 7.11B) and the inter-harvest period was reduced from three to four days, to one to two days. The inserted silicone air diffusion tube

rack 20 mm below the FSB enhanced the oxygen diffusion underneath the FSB, which in turn, could enhance polysulphide formation. This resulted in the increase in the thickness of the FSB (Figure 7.11 C).

The adjustable plate inserted into the FSBR allowed for variation of reactor depth in relation to sulphur FSB formation. The introduction of an automated harvesting process allowed for more accurate measurement of inter-harvest and FSB recovery periods.

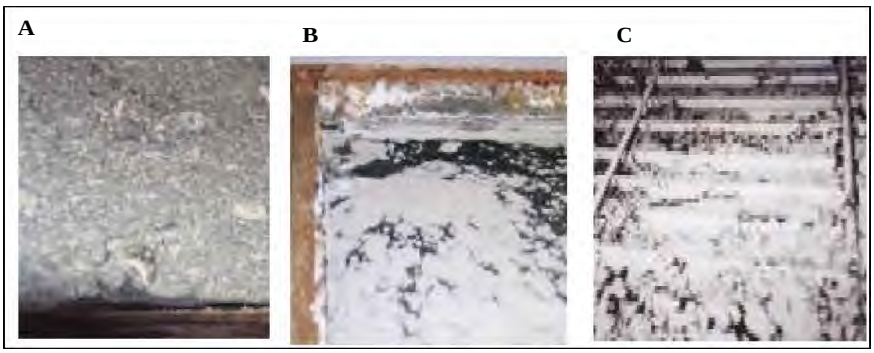

Figure 7.11 Changes in floating sulphur biofilm characteristics through the various phases of reactor development investigation. (A) Phase 1: Standard floating sulphur biofilm reactor design utilising lignocellulose effluent. (B) Phase 2: With sulphide supplementation. (C) Phase 3: with enhanced polysulphide formation. The sub-surface located silicone tube frame has been lifted to indicate the attached biofilm.

7.3.2 Sulphide

Sulphide concentration in the influent feed and the effluent from the FSBR are reported for the various phases of the study as accumulated data sets in Figure 7.12.

The influent sulphide concentration ranged between 150 and 200 mg/L and decreased to between 50 and 80 mg/L during most part of phase 1. This decrease was attributed to the cold weather and the onset of winter. The average decrease in sulphide concentration for phase 1 was 27 mg/L. Supplementation of Na_2S into the influent line during phase 2, led to an increase in sulphide availability within the FSBR with an average feed concentration of 130 mg/L. During phase 3 about 10 mg/L sulphide removal was observed. The average influent sulphide concentration in phase 4 was 102 mg/L and the average effluent was 198 mg/L indicating an average increase in sulphide concentration of 96 mg/L. This increase in sulphide was attributed to active sulphate reduction taking place in the FSBR as a result of the readily available carbon

leaching from the new sulphide generator during start-up. Once the reactor was optimized and automated during phase 5, there was an average sulphide removal of 150 mg/L.

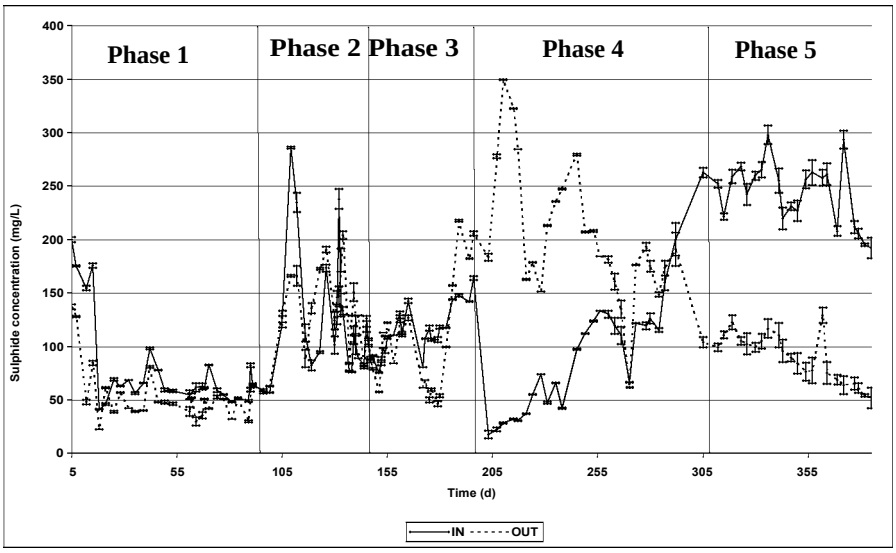

Figure 7.12 Influent and effluent sulphide concentrations over the five phases of the reactor development study. The error bars indicate standard deviations.

Figure 7.13 shows the mean distribution for influent and effluent sulphide concentration for each phase together with standard error and standard deviations for the data sets and shows no significant sulphide removal during phase 2 (n=13; p=0.744, df =30) and phase 3 (n=21, p=0.838, df =56) of the experiment. However, the decrease in sulphide during phase 1 (n=26, $p<0.05$, df =50) and phase 5 (n=21, $p<0.01$, df=40) was found to be significant. As expected the increase in sulphide (n=21, $p<0.01$, df =56) in phase 4 was found to be significant as a result of active sulphate reduction during start-up of the new sulphide generator.

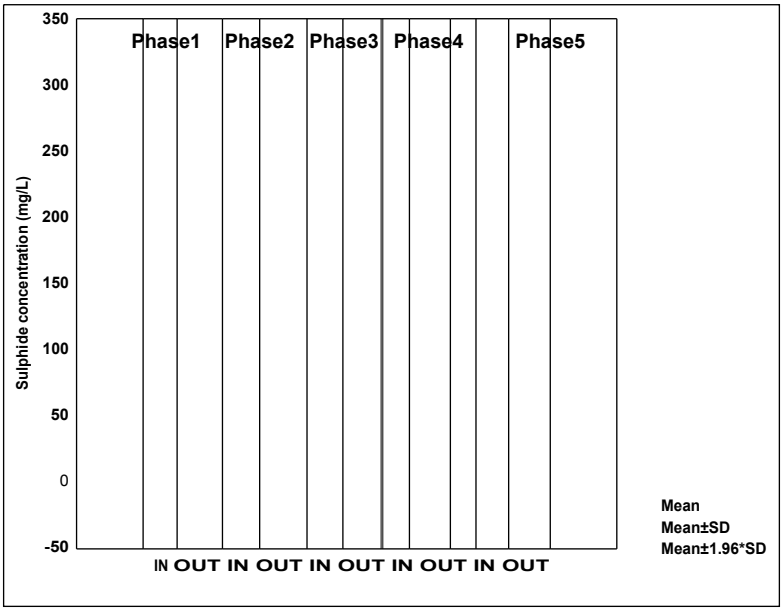

Figure 7.13 Box and whisker plot indicating the means of influent and effluent sulphide concentration for each of the phases of the reactor development study.

7.3.3 Sulphate

Influent and effluent sulphate concentrations over the phases of FSBR operation are presented as accumulated data sets in Figures 7.14 and mean distribution of the data in a box and whiskers plot (Figure 7.15). Sulphate levels in both influent and effluent concentration ranged between 1 500 and 4 000 mg/L over the experimental period (Figure 7.14). An average decrease in sulphate concentration in all phases of the experiment was observed with 282 mg/L in phase 1, 116 mg/L in phase 2, 115 mg/L in phase 3 and 917 mg/L in phase 4. The decrease in sulphate observed was attributed to sulphate reduction. During phase 5, there was a slight increase in sulphate of 31 mg/L possibly due to oxidation of sulphide to sulphate.

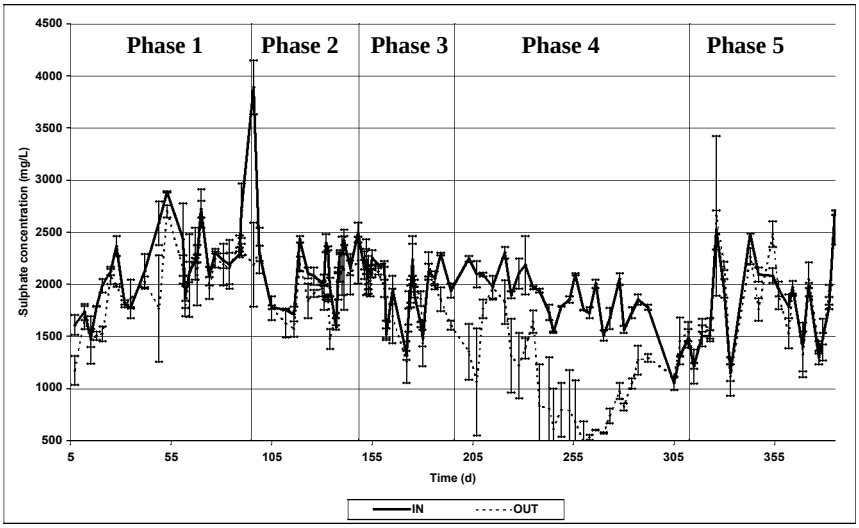

Figure 7.14 Influent and effluent sulphate concentrations over the five phases of the reactor development study. The error bars indicate standard deviations.

Figure 7.15 indicates that a significant decrease in sulphate occurred during phase 1 (n=26, $p<0.05$, df= 50) and phase 4 (n = 21, $p< 0.01$, df = 42) attributed to sulphate reduction taking place in the reactor. The decrease in sulphate in phases 2 and 3 and increase in sulphate in phase 5 were not found to be significant ($p>0.05$).

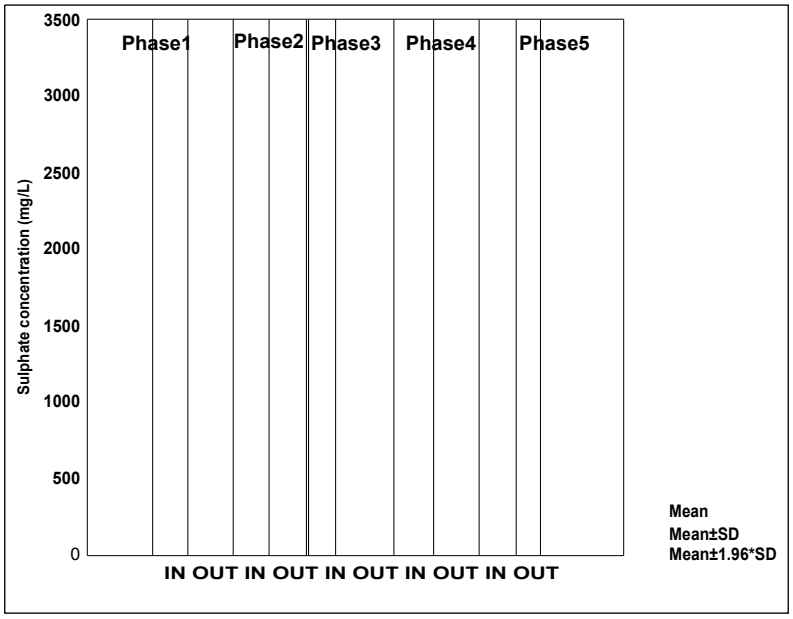

Figure 7.15 Box and whisker plot indicating the means for influent and effluent sulphate for each phase of the reactor development study.

7.3.4 Redox potential

Influent and effluent Redox potential values over the phases of FSBR operation are presented as accumulated data sets in Figure 7.16. Redox potential ranged between 50 and -350 mV over the period of reactor development investigation (Figure 7.16). The negative Redox potential values (mV) measured is generally favourable for sulphate reduction and sulphide oxidation.

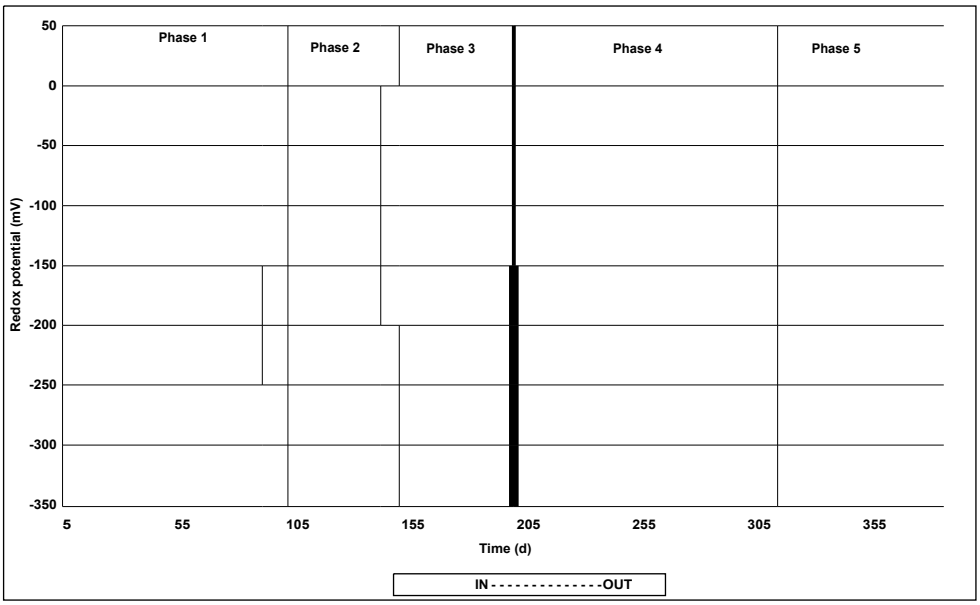

Figure 7.16 Influent and effluent Redox potential data over the five phases of the reactor development study. The error bars indicate standard deviations.

Figure 7.17 reports the mean distribution of the redox potential data. There was no significant increase or decrease in Redox potential in phases 1, 2, 3 and 5 ($p>0.05$), except for phase 4 ($n=21$, $p<0.001$, $df=18$), where the difference was found to be significant. This increasingly negative Redox potential is associated with active sulphate reduction occurring during phase 4 as indicated by the significant increase in sulphide and a significant decrease in sulphate.

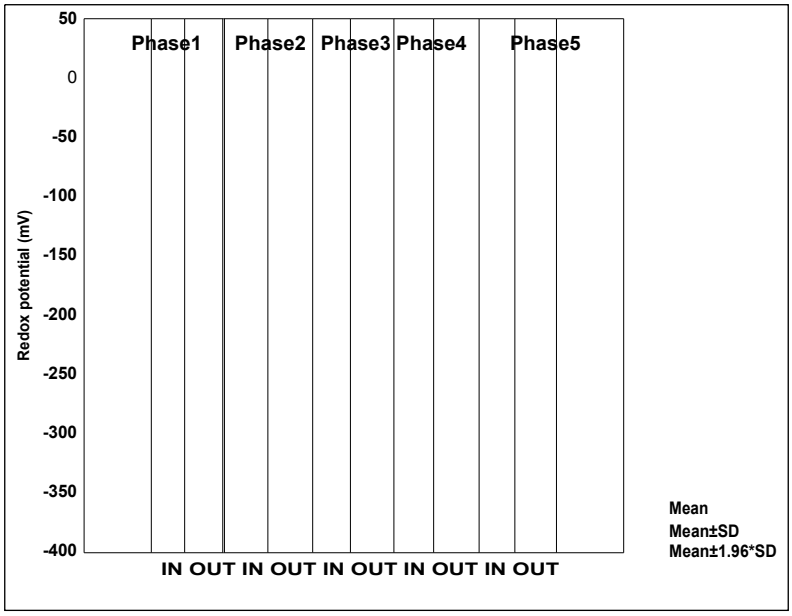

Figure 7.17. Box and whisker plot indicating the means for influent and effluent Redox potential (mV) for the reactor development study.

7.3.5 pH

Influent and effluent pH results are reported in Figure 7.18 as accumulated data sets over the reactor development study. The general trend shows an increase in pH, ranging between 7.6 and 7.2 in the influent, to a range between 7.0 and 7.9 in the effluent. This increase in pH is associated with some sulphate reduction in the system. Although the sulphate levels were reduced in all the phases except phase 5, sulphur cycling is likely to have occurred in the system, including sulphate reduction.

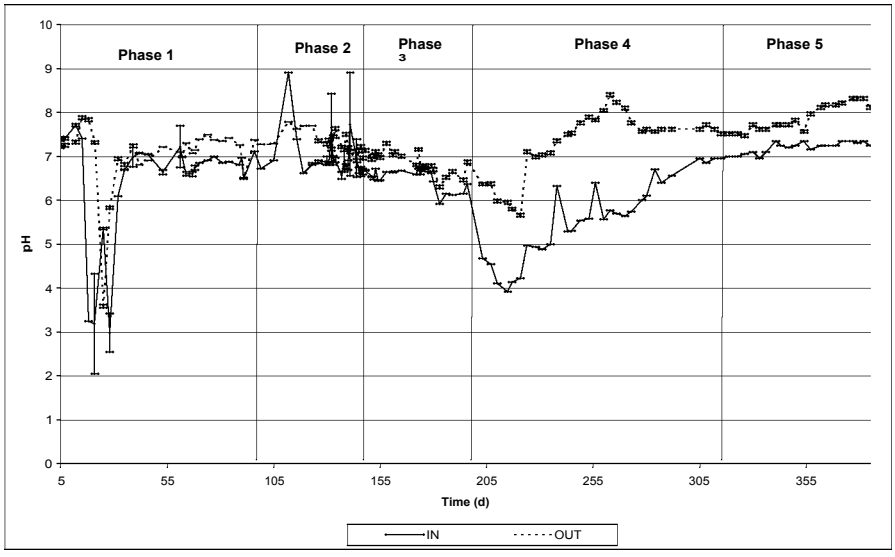

Figure 7.18 Influent and effluent pH data over the five phases of reactor development study. The error bars indicate standard deviations.

Figure 7.19 shows that a significant increase in pH was found for all phases of the reactor development study ($p < 0.05$). The average pH in the effluent after optimization during phase 5 was 7.9.

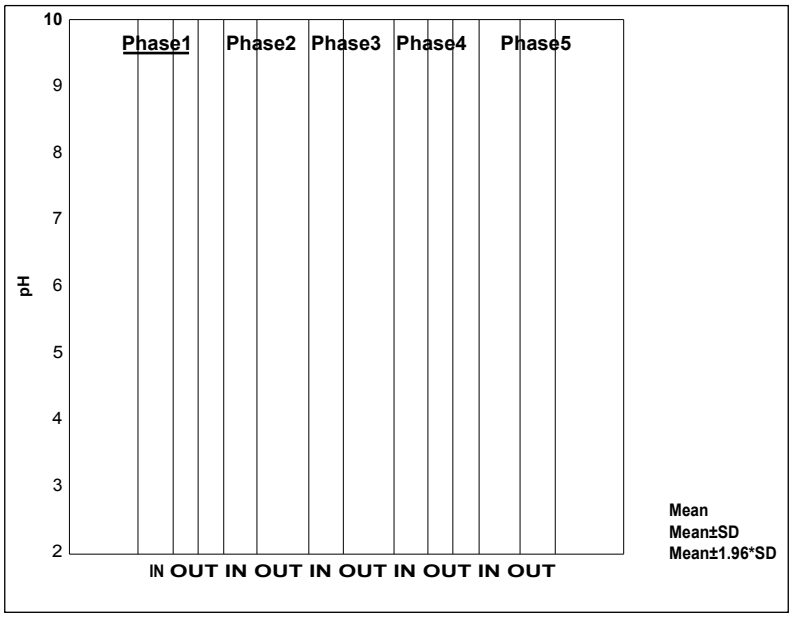

Figure 7.19 Box and whisker plot indicating the means for influent and effluent pH for each phase of the reactor development study.

7.3.6 Alkalinity

Influent and effluent alkalinity (measured as $CaCO_3$ concentration) results are shown in Figures 7.20. There was an increase in alkalinity particularly in phases 2, 3 and 4 (Figure 7.21). This is represented by an increase in alkalinity of 311 mg/L during phase 2, 186 mg/L in phase 3 and 1181 mg/L in phase 4 (Figure 7.20). As noted above, this increase in alkalinity may be correlated with the increase in pH during the same phases of the reactor development study and is associated with the production of bicarbonate ions during active sulphate reduction. This is further indicated by the decrease in sulphate and increase in sulphide concentration over the same period.

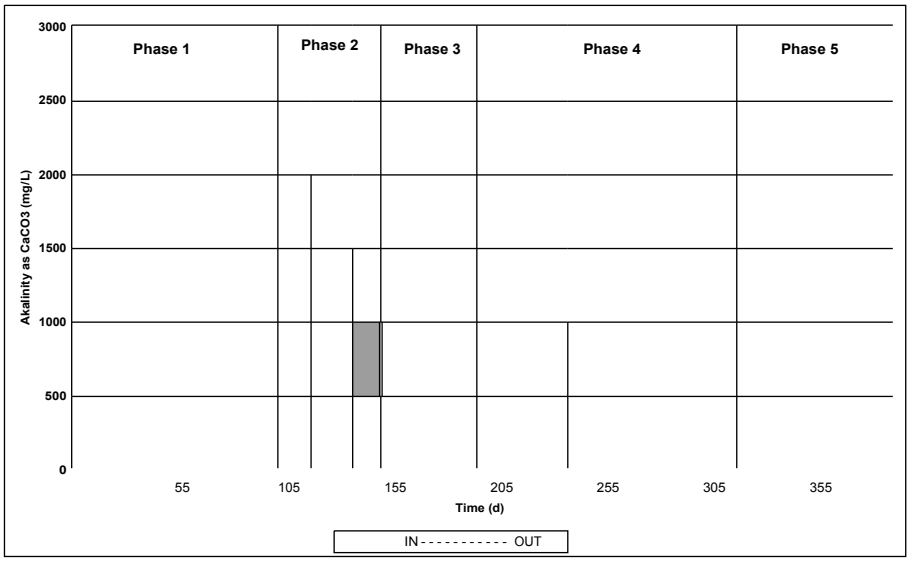

Figure 7.20 Influent and effluent alkalinity (as $CaCO_3$) over the five phases of the reactor development study. The error bars indicate standard deviations.

The means distribution of the influent and effluent alkalinity data is presented in Figure 7.21 and shows a significant increase in alkalinity during phase 2 (n=13, $p<0.05$, df= 26), phase 3 (n=42, $p< 0.01$, df=58) and phase 4 (n=21, $p<0.01$, df=48) while the decrease in alkalinity during phase 1 was not significant (p=0.62). The increase in alkalinity measured in phase 5 was also not significant (p=0.32).

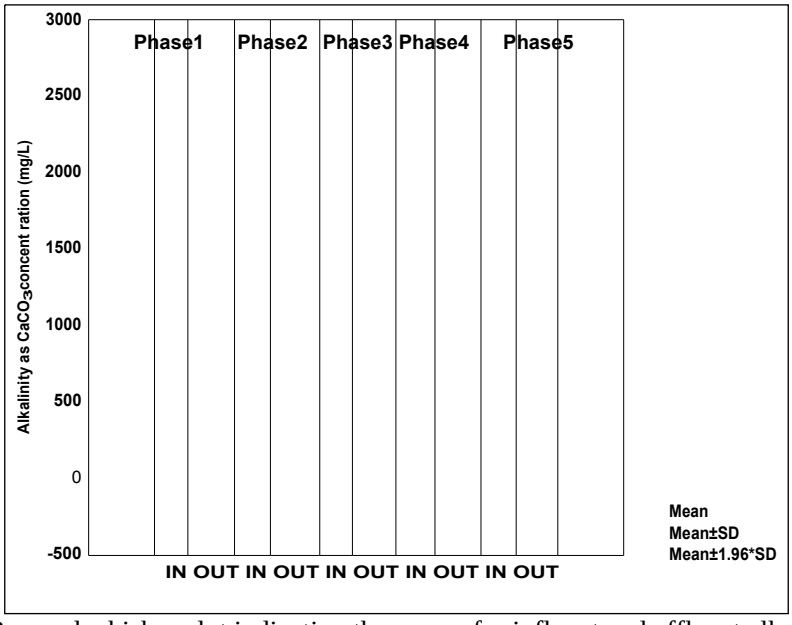

Figure 7.21 Box and whisker plot indicating the means for influent and effluent alkalinity for each phase.

7.3.7 COD

Figure 7.22 reports the influent and effluent COD concentration measured as accumulated data sets over the phases of reactor development study. The general trend showed by the COD data indicates a decrease in COD during all phases of the reactor development investigation. This may be associated with carbon breakdown during active sulphate reduction and during sulphide oxidation.

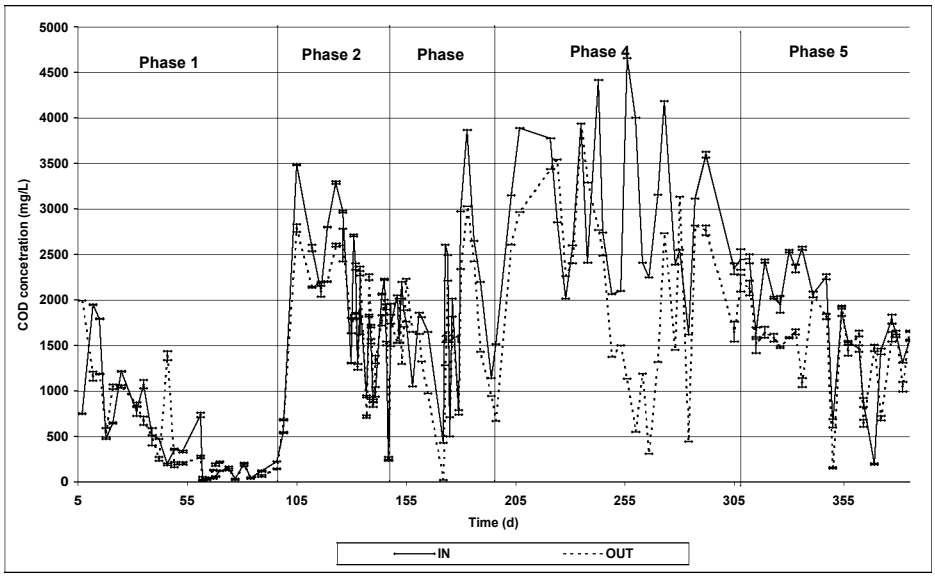

Figure 7.22 Influent and effluent COD concentration data over the five phases of operation. The error bars indicate standard deviations.

The statistical analyses (Figure 7.23) indicate that although there was a general decrease in COD throughout the operational period, the decrease was only significant in phase 4 where sulphate reduction was most active (n=21, $p<0.05$, df =58), while in the other phases the decrease in COD was not significant ($p>0.05$).

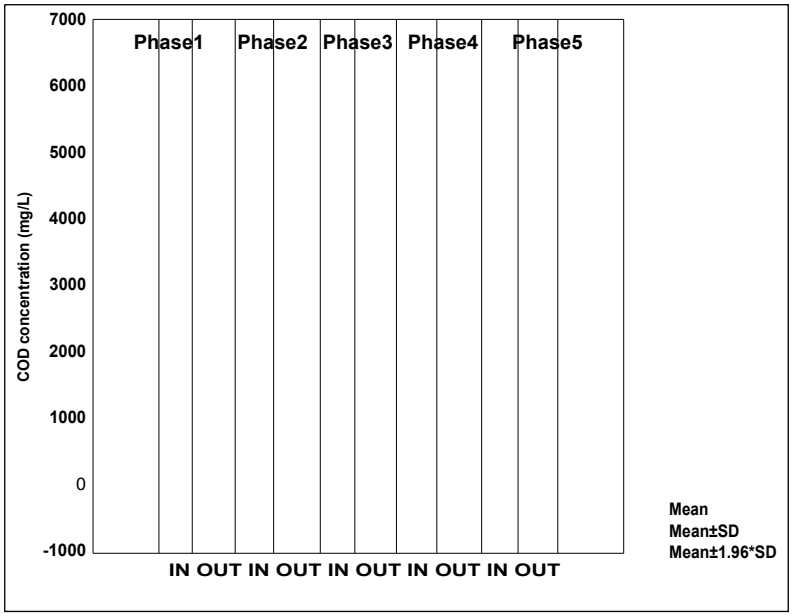

Figure 7.23 Box and whisker plot indicating the means for influent and effluent COD for each phase of the reactor development study.

7.3.8 Mass Balance

Table 7.2 summarises the mass balance data calculated for phase 5 operation as the best optimized system of the investigation, showing percentages of mass balance for sulphide removed and sulphur recovered. An average of 56 % sulphur recovery, 65 % sulphide removed and 15 % sulphur loss was recorded over phase 5 operation (Table 7.2) indicating an almost 1:1 conversion ratio of the sulphide available to elemental sulphur.

Table 7.2 Mass balance summary of the reactor development study showing system mass balance, sulphide removal and sulphur recovery during phase 5 of the investigation.

Phase	Mass Balance recovery (%)	Sulphide removal (%)	Sulphur recovery (%)
5	78	65	56

7.4 CONCLUSIONS

This chapter described preliminary studies undertaken to evaluate the scale-up potential of the LFCR as a sulphide removal operation treating a synthetic mine water simulating low-flow AMD suitable for passive system application.

The following conclusions were drawn from this study:

- While extensively offering more robust reactor design, the FSBR performance was less impressive than the eight-channel LFCR where sulphide removal of 88 % and sulphur recovery of 66 % was recorded.
- The optimum sulphide removal and sulphur recovery during phase 5 of operation of the FSBR was an average of 65 % and 56 %, respectively.
- The recovery rate of the FSB in the FSBR was 6 to 12 hours, which is faster than the 12 to 18 hours recorded for the LFCR.
- While the FSBR again showed potential to be scaled-up as a unit operation for sulphide removal in sulphidic wastewater treatment, it is apparent that further process development is required to optimize performance under reliable operating conditions.

Chapter Eight

GENERAL CONCLUSIONS

8.1 CONCLUSIONS

Floating sulphur biofilms have been noted to occur on the surface of sulphide-enriched wastewater bodies but their structure and function in these environments has not been well documented.

This study undertook an investigation of the system in order to describe the microbial ecology and to develop a structural/functional model for the FSB, as a basis for undertaking the development of the FSB as a biotechnological process for the treatment of sulphidic wastewaters.

A number of conclusions may be drawn from this study:

- An important methodological breakthrough in this study was the development of the LFCR which provided the replication of the FSB and thus enabling its investigation under controlled laboratory conditions;
- The FSB was found to be composed of a large population of microorganisms, with the presence of sulphur crystal-like structures suspended within and on the underside surface of the FSB and being responsible for its colour and grainy texture in the mature form;
- Both organic and inorganic forms of sulphur were found to be present in the FSB indicating both bacterial production and chemical formation processes were probably involved;
- Clearly defined spatial distribution across the FSB of different microbial species was demonstrated using the Gradient Tube method, developed in the study;
- Microsensors were used, possibly for the first time in the measurement of floating biofilms, and indicated the presence of steep sulphide concentration, pH and Redox potential gradients in the FSB system that could be correlated with the spatial distribution of the microbial species;

- A structural/functional descriptive model was developed to account for the performance of the FSB system and indicates that it is a “true” biofilm in terms of Costerton’s criteria, showing complexity of bacteria enclosed within an EPS matrix with channels and pores and the structure occurring at a surface. Although possibly unusual, the ability of the system to suspend itself at the air/water interface may be considered to comply with the requirement for a surface attachment in the strict sense;
- It was also demonstrated that the FSB system could be scaled-up successfully for the removal of sulphide in the treatment of low flow AMD passive wastewater treatment applications. It was shown that the LFCR and the FSBR could be used in this application;
- Average sulphide removal of 88 % and sulphur recovery of 66 % were obtained for the eight-channel LFCR at an operational loading of 2 618 $L/m^2/d$ and temperature of 20 ^oC;
- In process scale-up to the FSBR pilot plant, average sulphide removal of 65 % and sulphur recovery of 56 % was achieved. While conversion was lower than in the LFCR, the regeneration time of 6 to 12 hours were also faster than the 12 to 18 hours recorded for the LFCR;
- The process scale-up demonstrated that a trade-off between flow rate and sulphide oxidation requires optimisation to achieve the best performance for the system.

8.2 FUTURE WORK

Where the study provides a first account of the structure and function of the FSB, it is apparent that substantial further study is required to develop this understanding. Further studies at both the fundamental and applied levels could include investigations of the following:

- X-Ray crystallography, to confirm the crystalline structure of the sulphur forms present in the FSB and which would give more insight into the mechanism by which sulphur is formed in these systems;
- More detailed studies of the chemistry of the FSB system are required to account for the interaction between sulphur bacteria present, and the formation

of biological sulphur by these organisms and the initiation of the chemical processes giving rise to sulphur crystal formation;

- Variability in the stages of formation of the FSB and the factors influencing changes observed should be characterised and possibly related to the structural/functional model accounting for the performance of the system. This could have an important bearing on scale-up engineering of the system;
- While the system is clearly complex and difficult to manipulate by a simple reductive approach, it is evident that further progress in process development will be dependent on deriving accurate kinetic values for the unit operations involved;
- Preliminary development of the LFCR laboratory system, and the FSBR as a bioprocess reactor prototype, has shown potential for the application of the system in the treatment of sulphidic wastewaters. However, substantial room exists for innovation in reactor design and scale-up for application in passive AMD treatment.

References

Altschul, S. F., Madden, T. L., Schäffe, A. A., Zhang, J., Zhang, Z., Miller, W. and Lipman, D. J. (1997). Gapped BLAST and PSI-BLAST: A new generation of protein data programs. *Nucleic Acids Res.* **25:** 3389 – 3402.

Amann, R. I., Binder, B. J., Olson, R. J., Chisholm, S. W., Devereux, R. and Stahl, D. A. (1990). Combination of 16S rRNA-targeted oligonucleotide probes with Flow Cytometry for analyzing mixed microbial populations. *Appl. Environ. Microbiol.* **56:** 1919-1925.

Amann, R. I. and Kühl, M. (1998). *In situ* methods for assessment of microorganisms and their activities. *Cur. Opin. Microbiol.* **1**:352-358.

Amann, R. I., Ludwig, W. and Schleifer, K. H. (1995). Phylogenetic identification and *in situ* detection of individual microbial cells without cultivation. *Microbiol. Rev.* **59**: 143-169.

Amann, R. I., StromL**ey, J., Devereux, R., Key, R. and Stahl, D. A.** (1992). Molecular and microscopic identification of sulfate-reducing bacteria in multispecies biofilms. *Appl. Environ. Microbiol.* **58**: 614-623.

American Public Health Association (APHA). (1989). Standard methods for the examination of water and wastewater, 17th Edition. *American Public Health Association, Washington, D.C.*

Barnes, H. L. and Romberg, S. B. (1986). Chemical aspects of acid mine drainage. *J. Water Pollut. Control Fed.* **40:** 371-384.

Basu, S. K., Mino, T. and Oleszkiewicz, J. A. (1995). Novel application of sulphur metabolism in domestic wastewater treatment. *Can. J. Civ. Eng.* **22**: 1217-1223.

Berbee, M. l. and Taylor, J. W. (1999). Fungal physiology. In: Oliver and Schweizer (Eds.). *Molecular Fungal Biology*. Cambridge, UK: Cambridge University Press, pp: 21-77.

Boer, D. R., Muller, A., Fetzner, S., Lowe, D. J. and Romano, M. D. (2005). On the purification and preliminary crystallographic analysis of isoquinoline 1-oxidoreductase from *Brevundimonas dimuta*. *Acta Crystallogr. Sect. F. Struct. Biol. Cryst. Commun.* **161** (11): 137 – 140.

Boonstra, J., van Lier, R., Janssen, G., Dijkman, H. and Buisman, C. J. N. (1999). Biological treatment of acid mine drainage. In: Amils and Ballster (Eds.). *Biohydrometallurgy and the environment. Toward the mining of the 21st century.* Vol 9B. Elsevier, Amsterdam. pp: 559-567.

Bond, P. L., Hugenholtz, P., Keller, J. and Blackall, L. L. (1995). Bacterial community structures of phosphate-removing and non-phosphate-removing activated sludges from sequencing batch reactors. *Appl. Environ. Microbiol.* **61**(5): 1910-1916.

Boshoff, G., Duncan, J. R. and Rose, P. D. (1996). An algal-bacterial integrated ponding system for the treatment of mine drainage waters. *J. Appl. Phycol.* **8**: 442-449.

Bowker, M. (2002). The microbial ecology of floating sulphur biofilms. MSc Thesis, Rhodes University, South Africa.

Bruser, T., Lens, P. N. L. and Truper, H. G. (2000). The biological sulphur cycle. In Lens and Holsof Pol (Eds.). *Environmental technologies to treat sulfur pollution*: *Principles and Engineering.* IWA Publishing, London, pp: 47 -86.

Buisman, C. J. N., Boonstra, J., Krol, J. P. and Dijkman, H. (1996). Biotechnological removal of sulfate and heavy metals from wastewater. In: *Int. Conference Advanced Waste Water Treatment.* Amsterdam, 1996.

Buisman, C. J. N., Post, R., Ijspeert, P., Geraats, G. and Lettinga, G. (1989). Biotechnological process for sulphide removal with sulphur reclamation. *Acta Biotechnol.* **9**: 255-267.

Carpentier, B. and Cerf, O. (1993). Biofilms and their consequences, with particular reference to hygiene in the food industry. *J. Apppl. Bacteriol.***75** (6): 499 – 511.

Chang, I. S., Shin, P. K. and Kim, B. H. (2000). Biological treatment of acid mine drainage under sulphate reducing conditions with solid waste materials as substrate. *Wat. Res.* **34**: 1269 – 1277.

Chauke, G. (2002). The microbial ecology of sulfate reduction in the Rhodes BioSure Process ®**.** MSc Thesis, Rhodes University. South Africa.

Chung, Y., Huang, C. and Tseng, C. (1996). Biodegradation of hydrogen sulphide by a laboratory scale immobilised *Pseudomonas putida* CH11 Biofilter. *Biotechnol. Prog.* **12**: 773-778.

Christensen, B. B., Sternberg, C., Andersen, J. B., Nielsen, A. T., Giskov, M. and Molin, S. (1999). Molecular tools for study of biofilm physiology. *Methods Enzymol.* **310**: 20-42.

Coetser, S. E. (2004). Microbial sulphate reduction in passive acid mine drainage treatment systems. PhD Thesis, University of Pretoria, South Africa.

Coetser, S. E., Heath, R., Molwantwa, J. B., Rose, P. D. and Pulles, W. (2005). Implementation of the degrading packed bed reactor technology and verification of the long-term performance of passive treatment plants at Vryheid Coronation Colliery. WRC report No.: 1348/ 1/ 05.

Cork, D. J., Jerger, D. E. and Maka, A. (1986). A biocatalytic production of sulfur from process waste streams. *Biotechnol. Bioeng. Symp. Ser.* **16**:149-162.

Costerton, J.W. (1995). Overview of microbial biofilms. *J. Industrial Microbiol.* **15**: 137-140.

Costerton, J. W., Lewandowski, Z., de Beer, D., Caldwell, D., Korber, D. and James, G. (1994). Biofilms, the customised microniche. *J. Bacteriol.* **176**: 2137-2142.

Cross, R. (2000). Microscopy methods. Rhodes University, South Africa.

Cytryn, E., van Rijn, J., Schramm, A., Gieseke, A., de Beer, D. and Minz, D. (2005). Identification of bacteria potentially responsible for oxic and anoxic sulphide oxidation in biofilters of a recirculating mariculture system. *Appl. Environ. Microbiol.***71** (10): 6134 – 6141.

Daims, H., Nielsen, P. H., Schleifer, K-H. and Wagner, M. (2001). *In situ* characterization of *Nitrospora*-like nitrite-oxidising bacteria active in wastewater treatment plants. *Appl. Environ. Microbiol.* **67** (11): 5273-5284.

Danese, P. N., Pratt, L. A. and Kolter, R. (2000). Exopolysaccharide production is required for development of *E. coli* K-12 Biofilm. *Biol. Rev.* **64**: 847 – 867.

Dart, R. K. and Stretton, R. J. (1980). Microbiological aspects of pollution control, Second Edition. Elsevier, Amsterdam. pp: 192-207.

Davey, M. E. and O'Toole, G. A. (2000). Microbial Biofilms: From Ecology to Molecular Genetics. *Microb. Molecular Biol. Rev.* **64**: 847-867**.**

Davidson, W., Reynolds, C. S., Tipping, E. and Needham, R. F. (1989). Reclamation of acid waters using sewage sludge. *Environ. Pollu.*, **57**: 251-274.

de Beer, D. and Muyzer, G. (1995). Multispecies biofilms: report from the discussion session. *Wat. Sci. Tech*. **32**: 269-270.

de Beer, D. and Schramm, A. (1999). Micro-environments and mass transfer phenomena in biofilms studied with microsensors. *Wat. Sci. Tech*. **39**: 173-178.

de Beer, D. and Stoodley, P. (2006). Microbial biofilms. In: *The prokaryotes. Vol 1: Symbiotic Associations.* Dworkin, Falkow, Rosenberg, Schleifer, and Stackebrandt (Eds.). Springer, New York. pp: 904 – 937.

de Beer, D. A., Schramm, C. M., Santegoeds, C. M. and Kühl, M. (1997). A nitrite microsensor for profiling environmental biofilms. *Appl. Environ. Microbiol.* **63**: 973-977.

de Beer, D., Stoodley, P., Roe, F. and Lewandowski, Z. (1994). Effects of biofilm structures on oxygen distribution and mass transport. *Biotechnol. Bioeng.* **43**: 1131-1138.

Dunn, K. M. (1998). The biotechnology of high rate algal ponding systems in the treatment of saline tannery wastewaters. PhD Thesis, Rhodes University, South Africa.

Dunne, W. M. (2002). Bacterial adhesion: Seen any good biofilm lately? *Clinical Microbiology Reviews.* **15**: 155 – 166.

Dvorak, D. H., Hedin, R. S., Edenborn, H. M. and McIntire, P. E. (2004). Treatment of metal-contaminated water using bacterial sulphate reduction: Results from pilot-scale reactors. *Biotech*. *Bioeng.* **40 (**5): 609 -616.

Elder, M. J., Stapleton, F., Evans, E. and Dart, J. K. (1995). Biofilm-related infections in ophthalmology. *Eye.* **9** (1): 102 – 109.

Gadre, R. V. (1989). Removal of hydrogen sulphide from biogas by a chemoautotrophic fixed-film bioreactor. *Biotech. Bioeng.* **34**: 410-414.

Gardner, M. N. (1998). A study of the chemolithoautotrophic bacterial rhodanese, and its potential contribution to cyanide wastage during cyanidation of bio-oxidized concentrates. MSc Thesis, University of Cape Town, South Africa.

Gazea, B., Adam, K. and Kontopoulos, A. (1996). A review of passive systems for the treatment of acid mine drainage. *Miner. Eng.* **9**: 23-42.

Gaudes, A.; Sabater, S.; Vilalta, E. And Munoz, I. (2006). The nematode community in cyanobacterial biofilms in river llobregat, Spain. *Nematology*.**8** (6): 909 – 919.

Gilbert, P., Das, J. and Foley, I. (1997). Biofilm susceptibility to antimicrobials. *Advances in Dental Research*. **11** (1): 160-167.

Gilbert, P., Maira-Litran, T., McBain, A. J., Rickard, A. H. and White, F. (2002). Physiology and collective recalcitrance of microbial biofilm communities. *Annual Reviews in Microbiology*. **46**: 203- 256.

Gilfillan, J. C. (2000). The structure and microbiology of floating sulphide oxidizing biofilms. MSc Thesis, Rhodes University, South Africa.

Goebel, B. M. and Stackebrandt, E. (1994). Cultural and phylogenetic analysis of mixed microbial populations found in natural and commercial bioleaching environments. *Appl. Environ. Microbiol.* **60**: 1614-1621.

Guo, L., Xie, Z., Bian, X., Zhang, W., Lui, X. and Chen, A. G. (2005). Determination of oxytetracycline by flow injection with chemi-luminiscence detection. *Luminiscence.* **20** (3): 129 – 134.

Guoqiang, Z., Jie, P., Yi, Y. and Shimin, Z. (1994). Bacterial desulfurization of the H_2S-containing biogas. *Biotechnol. Lett.* **16**: 1087-1090.

Hammond, C. (1986). The Dow Stredford chemical recovery process. *Environ. Prof.* **5** (1): 1 – 4.

Hansen, L. S. and Blackburn, T. H. (1995). Amino acid degradation by sulphate-reducing bacteria: Evaluation of four methods. *Limnol. Oceanogr.* **40 (3):** 502 – 510.

Harmsen, H. J., Kengen, H. M., Akkermans, A. D., Stams, A. J. and de Vos, W. M. (1996). Detection and localization of syntropic propionate-oxidizing bacteria in granular sludge by *in situ* hybridisation using 16S rRNA-based oligonucleotide probes. *Appl. Environ. Microbiol.* **62** (5): 1656 – 1663.

Hartman, P. (1984). Structural morphology of orthorhombic sulphur. *Physics and Chemistry of Minerals.* **11**(4): 149 – 152.

Head, I. M., Saunders, J. R. and Pickup, R. W. (1998). Microbial evaluation, diversity and ecology: A decade of ribosomal RNA analysis of uncultivated microorganisms. *Microb. Ecol.* **35**: 1-21.

Hermanowicz, S. W. (2003). Biofilm architecture: Interplay of models and experiments. In: Wuertz, Bishop and Wilderer (Eds.). *Biofilms in wastewater treatment: An interdisciplinary approach*. IWA Publishing, London. pp 32 – 45.

Heuer, H., Hartung, K., Weiland, G., Kramer, I. and Smalla, K. (1999a). Polynucleotide probes that target a hypervariable region of 16s rRNA genes to identify bacterial isolates corresponding to bands of community fingerprints. *Appl. Environ. Microbiol.* **65**: 1045-1049.

Heuer, H., Krasek, M., Baker, P., Smalla, K. and Wellington, E. M. H. (1999b). Analysis of *Actinomycete* communities by specific amplification of genes encoding 16S rRNA and gel-electrophoretic separation in denaturing gradients. *Appl. Environ. Microbiol.* **63:** 3233-3241.

Hugenholtz, P., Goebel, B. M. and Pace, N. R. (1998). Impact of culture independent studies on the emerging phylogenetic view of bacterial diversity. *J. Bacteriol.* **180:** 4765-4774.

Hurek, T., Egener, T. and Reinhold-Hurek, B. (1997). Divergence in nitrogenase of *Azoarcus* spp., Preotebacteria of the beta subclass. *J. Bacteriol.* **179** (13): 4172 – 4178.

Ito, T., Okabe, S., Satoh, H. and Watanabe, Y. (2002). Successional development of sulphate reducing bacterial populations and their activities in a wastewater biofilm growing under micro-aerophilic conditions. *Appl. Environ. Microbiol.* **68**: 1392-1402.

Ito, T., Sugita, K. and Okabe, S. (2004). Isolation, Characterisation: An *in situ* detection of novel chemolithoautotrophic sulphur-oxidizing bacterium in wastewater biofilms growing under micro-aerophilic conditions. *Appl. Environ. Microbiol.* **70**: 3122 – 3129.

Ivanova, E. P., Phan, D. K., Wright, J. P. and Nicolau, D. V. (2002). The detection of coccoid forms of *Sulfidobacter* using atomic force microscopy. *FEMS Microbiol Letters.* **214** (2): 177 – 181.

Janssen, A. J. H., Dijkman, H. and Janssen, G. (2000). Novel biological processes for the removal of H_2S and SO_2 from gas streams. In: Lens and Hulsoff-Pol (Eds.). *Environmental technologies to treat sulfur pollution*. IWA Publishing, London. pp: 265 – 280.

Janssen, A. J. H., Lettinga, G. and de Kaizer, A. (1999). Removal of hydrogen sulphide from wastewater and waste gases by biological conversion to elemental sulphur. Colloidal and interfacial aspects of biologically produced sulphur particles. *Physicochemical and Engineering Aspects* **151**: 389-397.

Janssen, A. J. .H., Ma, S. C., Lens, P. and Lettinga, G. (1997). Performance of a sulfide-oxidising expanded-bed reactor supplied with dissolved oxygen. *Biotech. Bioeng.* **53**:32-40.

Janssen, A. J. H., Meijer, S., Bontsema, J. and Lettinga, G. (1998). Application of the redox potential for controlling a sulfide oxidizing bioreactor. *Biotech. Bioeng.* **60**: 147-155.

Johnson, D. B. (2000). Biological removal of sulphurous compounds from inorganic wastewaters. In: Lens and Hulsoff-Pol (Eds.). *Environmental Technologies to Treat Sulfur Pollution: Principles in Engineering.* IWA Publishing, London. pp: 175-193.

Johnson, D. B. (1995). Acidophilic microbial communities: Candidates for bioremediation of acidic mine effluent. *Int. Biodet. Biodeg* .**35**: 41-58.

Johnson, D. B. and Hallberg, K. B. (2005). Acid mine drainage remediation: A mini review. *Science of the Total Environment.* **338**: 3-14.

Johnson, D. B. and Hallberg, K.B. (2003). The Microbiology of Acidic Mine Waters. *Research in Microbiology.* **154:** 466-473.

Johnson, D. B., Dziurla, M-A., Kolmert, A. and Hallberg, K. B. (2002). The microbiology of acid mine drainage: Genesis and biotreatment. *SA J. Sci.* **98:** 249-255.

Jørgensen, B. B., Teske, A. and Cohen, Y. (1998). Sulphate reducing bacteria and their activities in cyanobacterial mats of a solar lake. *Appl. Environ. Microbiol.* **64** (8): 2943 – 2951.

Jørgensen, B. B. and Revsbech, N. P. (1985). Diffusive boundary layers and the oxygen uptake of sediments and detritus. *Limnol. Oceanogr.* **30** (1): 111 - 122.

Kalin, M. M., Cairnes, J. and McCready, R. (1991). Ecological engineering for acid mine drainage treatment of coal waters. *Resour. Conserv. Recycl.* **5**: 265-275.

Karavaiko, G. I., Turova, T. P., Mutyan, L. N. and Pivovarova, T. A. (2003). Phylogenetic heterogeneity of *Acidithiobacillus ferroxidans.* **53** (1): 119 - 119.

Kelly, D. P. (1985). Physiology of the *Thiobacilli*: Elucidating the sulphur oxidation pathway. *Microbiological Sciences.* **2**: 105-109.

Kim, B. W., Kim, I. K. and Chang, H. N. (1990). Bioconversion of hydrogen sulphide by free and immobilised cells of *Chlorobium thiosulfatophilum*. *Biotechnol. Lett.* **12**: 381-386.

Kloeke, F. V. O. (1999). Localization and identification of population of phosphate-active bacterial cells associated with activated sludge flocs. *Microb. Ecol.* **38** (3): 201-214.

Kolmert, A., Henrysson, T., Hallberg, R. and Mattiasson, B. (1997). Optimization of sulphide production in an anaerobic continuous biofilm process with sulphate reducing bacteria. *Biotechnol. Lett.* **19**: 971-975.

Kuenen, J. G. and Robertson, L. A. (1992). The use of natural bacterial populations for the treatment of sulphur-containing wastewater. *Biodegradation*, **3**: 239-254.

Kühl, M. and Jørgensen, B. B. (1992). Microsensor measurements of sulfate reduction and sulfide oxidation in compact microbial communities of aerobic biofilms. *Appl. Environ. Microbiol.* **58**: 1164-1174.

Lagas, J. A. (2000). Survey of H_2S and SO_2 removal processes. In: *Environmental technologies to treat sulfur pollution.* Lens and Hulsoff-Pol (Eds.). IWA Publishing, London. pp: 265 – 280.

Lane, D. J., Harrison, A. P., Stahl, D., Pace, B., Giovannoni, S. J., Olsen, G. J. and Pace, N. R. (1992). Evolutionary relationships among sulfur- and iron-oxidizing eubacteria. *J. Bacteriol.* **174**: 269-278.

Lawrence, J. R., Wolfaardt, G. M. and Korber, D. R. (1994). Determination of diffusion coefficients in biofilms by confocal laser microscopy. *Appl. Environ. Microbiol.* **60**: 1166 – 1173.

Lens, P. N. L., Omil, F., Lema, J. M. and Hulsoff Pol, L. W. (2000). Biological treatment of organic sulfate-rich wastewaters. In: Lens and Hulsoff-Pol (Eds.).

Environmental technologies to treat sulfur pollution. IWA Publishing, London. pp: 153 – 174.

Lewandowski, Z. (1995). Microbial biofilms. *Annual Rev. Microbiol.* **49** 711 – 745.

Lewandowski, Z. and Beyenal, H. (2003). Biofilm monitoring: A perfect solution in search of a problem. *Wat. Sci. Technol.* **47** (5): 9 – 18.

Liesack, W., Weyland, H. and Stackebrandt, E. (1991). Potential risks of gene amplification by PCR as determined by 16S rDNA analysis of a mixed-culture of strict barophilic bacteria. *Micro.l Ecol.* **21**(1): 191-198.

Lin, C. and Stahl, D. A. (1995). Comperative analysis reveals a highly conserved endoglucanase in the cellulolytic genus *Fibrobacter. J. Bacteriol.* **177:** 2543-2549.

Madikane, M. (2002). Biosulphidogenic hydrolysis of lignin and lignin model compounds. MSc. Thesis, Rhodes University, South Africa.

Marikawa, M., Kagihiro, S., Haruki, M., Takano, K., Branda, S., Kolter, R. and Kanaya, S. (2006). Biofilm formation by a *Bacillus subtulis* strain that produces γ-polyglutanate. *Microbiol.* **152**: 2801 -2807.

Maree, J. P. and Hill, E. (1989). An integrated process for biological treatment of sulfate-containing industrial effluent. *J. Water Pollut. Control Fed.* **59**: 1069-1074.

Maree, J. P., Gerber, A., McLaren, A. R. and Hill, E. (1988). Biological treatments of mining effluents. *Env. Tech. Lett.* **8:** 53-64.

Michel, C., Matte-Taillies, O., Kerouault, B. and Bernadet, J. F. (2005). Resistance pattern and assessment of phenicol agents' minimum inhibitory concentration in multiple drug resistant *Chryseobacterium* isolated from fish and aquatic habitat. *J. Appl. Microbiol.* **99** (2): 323 – 332.

Middelburg, J. J. (2000). The geochemical sulphur cycle. In: Lens and Hulsoff-Pol (Eds.). *Environmental technologies to treat sulphur pollution: Principles and Engineering.* IWA Publishing, London. pp 33 – 45.

Mockel, H. J. (1984). Determination of sulphur and sulphur organics in reverse phase liquid chromatography. *J. of Chromatogr.* **317**: 589-614.

Molipane, N. P. (1999). Sulphate reduction utilizing hydrolysis of complex carbon sources. MSc Thesis, Rhodes University, South Africa.

Molwantwa, J. B. (2002). The enhanced hydrolysis of sewage sludge under sulphidogenic conditions. MSc Thesis, Rhodes University, South Africa.

Molwantwa, J. B., Bowker, M., Gilfillan, J., Rein, N., R., Hart, O. O. and Rose, P.D. (2007). Investigation of and development of the biotechnology of the floating sulphur biofilm in the beneficiation and treatment of wastewaster. WRC final report on Project: No.:1454. Water Research Commission, South Africa.

Molwantwa, J. B., Coetser, S. E., Heath, R. and Pulles, W. (2003). The monitoring, evaluation and verification of a long-term performance of passive treatment plants at Vryheid Coronation Colliery pilot plant. Final Report to WRC on Project No.:K5/1348. Water Research Commission, South Africa.

Muyzer, G. and Ramsing, N. B. (1995). Molecular methods to study the organisation of microbial communities. *Wat. Sci. Tech*. **32**: 1-9.

Muyzer, G., de Waal, E. C. and Uitterlindin, A. G. (1993). Profiling of complex microbial populations by denaturing gradient gel electrophoresis: Analysis of polymerase chain reaction amplified genes coding for 16S rRNA. *Appl. Environ. Microbiol.* **59**: 695-700.

Myers, R. M., Miniatis, T. and Lerma, L. S. (1987). Detection and localization of single base changes by degrading gradient gel electrophoresis. *Methods Enzymol.* **155**: 501-527.

Neba, A. (2006). The Rhodes BioSURE Process® and the use of sustainability indicators in the development of biological mine water treatment. PhD Thesis, Rhodes University, Grahamstown, South Africa.

Nielsen, P. H., de Muro, M. A. and Nielsen, J. L. (2000). Studies on the *in situ* physiology of *Thiothrix* spp. present in activated sludge. *Environ. Microbiol.* **2**: 389–398.

Nivens, D. E., Palmer, R. J. and White, D. C. (1995). Continuous nondestructive monitoring of microbial biofilms: A review of analytical techniques. *J. Industrial Microbiol.* **15**: 263-276.

O'Flaherty, V., Colohan, S., Mulkerrins, D. and Colleran, E. (1999). Effect of sulphate addition on volatile fatty acid and ethanol degradation in an anaerobic hybrid reactor II: Microbial interactions and toxic effects. *Biores. Technol.* **68**: 109-120.

O'Toole, G. A., Kaplan, H. B. and Kolter, B. (2000). Biofilm Formation as Microbial Development. *Annu. Rev. Microbiol.* **54:** 49-79.

Okabe, S., Itoh, T., Satoh, H. and Watanabe, Y. (1999a). Analyses of spatial distributions of sulphated reducing bacteria and their activity in aerobic wastewater biofilms. *Appl. Environ. Microbiol.* **65**: 5107-5116.

Okabe, S., Satoh, H., Itoh, T. and Watanabe, Y. (1999b). Microbial ecology of sulphate reducing bacteria in wastewater biofilms analyzed by microelectrodes and FISH (fluorescent *in situ* hybridization) technique. *Wat. Sci. Tech*. **39**: 41-47.

Okabe, S., Hiratia, K., Ozawa, Y. and Watanabe, Y. (1996). Spatial microbial distributions of nitrifiers and heterotrophs in mixed-population biofilms. *Biotechnol. Bioeng.* **50**: 24-35.

Okabe, S., Matsuda, T., Satoh, H., Ito, T. and Watanabe, Y. (1998). Sulfate reduction and sulfide oxidation in aerobic mixed population biofilms. *Wat. Sci. Tech*. **37**: 131-138.

Okubo, K., Sugawa, H., Gojobori, T. and Tateno, Y. (2006). DDBJ in preparation for overview of research activities behind data submissions. *Nucleic Acids Res.* **34**: D6-D9.

Paerl, H. W. and Pinckney, J. L. (1996). A mini-review of microbial consortia: Their role in aquatic production and bio-geochemical cycling. *Microb. Ecol.* **31** (3): 225-247.

Parsek, M. R. and Fuqua, C. (2004). Biofilms 2003: Emerging themes and challenges in studies of surface-associated microbial life. *J. Bacteriol.* **186** (14): 4427-4440.

Poulsen, L. K., Ballard, G. and Stahl, D. A. (1993). Use of rRNA fluorescence *in situ* hybridisation for measuring the activity of single cells in young and established biofilms. *Appl. Environ. Microbiol.* **59**: 1354-1360.

Pulles Howard and de Lange (PHD) (2002). Development of low maintenance self-sustaining biological (passive) systems for the treatment of contaminated mine and industrial effluents. Final report to the DACST Innovation Fund Project No.: 32130. Innovation Fund, South Africa.

Pulles, W., Howie, D., Otto, D. and Easton, J. (1995). A manual on mine water treatment and management practices in South Africa. WRC report no. TT 80/96. Water Research Commission. South Africa.

Ramesh, A., Lee, D. J., Wang, M. L., Hsu, J. P., Juang, R. S., Hwang, K. J., Liu, J. C. and Tseng, S. J. (2006). Biofouling in membrane bioreactors. *Separation Science and Technol.* **41** (97): 1345-1370.

Ramsing, N. (1998). Molecular biological tools to study population dynamics of sulphur cycle bacteria in natural environments and bioreactors (16S rRNA molecular probes, PCR). *TMR Summer School Programme,* Wageningen, Netherlands.

Ramsing, N. B., Kühl, M. and Jørgensen, B. B. (1993). Distribution of sulphate-reducing bacteria, O_2 and H_2S in photosynthetic biofilms determined by oligonucleotide probes and microelectrodes. *Appl. Environ. Microbiol.* **59:** 3840-3849.

Raskin, L., Rittmann, B. E. and Stahl, D. A. (1996). Competition and coexistence of sulphate reducing and methanogenic populations in anaerobic biofilms. *Appl. Environ. Microbiol.* **62**: 3847-3857.

Raskin, L., Poulsen, L. K., Noguera, D. R., Rittmann, B. E. and Stahl, D. A. (1994). Quantification of methanogenic groups in anaerobic biological reactors by oligonucleotide probe hybridization. *Appl. Environ. Microbiol.* **60**: 1241-1248.

Rein, N. B. (2002). Biological sulphide oxidation in heterotrophic environments. MSc. Thesis, Rhodes University, South Africa.

Reinhoudt, H. R. and Moulijn, J. A. (2000). Catalytic removal of sulfur from diesel oil by hydrotreating. In: *Environmental treatment technologies to treat sulfur pollution.* Lens and Hulsoff-Pol (Eds.). IWA Publishing, London. pp: 87 – 103.

Reysenbach, A., Giver, L. J., Wickham, G. S. and Pace, N. R. (1992). Differential amplification of rRNA by polymerase chain reaction. *Appl. Environ. Microbiol.* **58** (10): 3417-3418.

Rigler, R. J. (1966). Microfluorometric characterisation of intracellular nucleic acids and nucleoproteins by acridine orange. *Acta. Physiol. Scand. Suppl.* **267**: 1-122.

Rinaldi, R. P. and Pawley, G. S. (1975). An investigation of the intermolecular modes of orthorhombic sulphur. *J. Phys. C. Solid. State Phys.* **8**: 599 – 616.

Robertson, L. A. and Kuenen, J. G. (1991). The colourless sulfur bacteria. In: *The Prokaryotes, a handbook on the biology of bacteria: Ecophysiology, Isolation, Identification, Applications.* Balows, Trüper, Dworkin, Harder and Schleifer (Eds.). Second edition, Vol. 1. Springer-Verlag. New York. pp: 835-413.

Roman, H. J. (2005). The degradation of lignocellulose in a biologically generated sulphidic environment. PhD Thesis, Rhodes University, South Africa.

Romano, I., Giordano, A., Lama, L., Nicolaus, B. and Gambacorta, A. (2003). *Planacoccus rifierensis* sp. *nov.*, isolated from algal mats collected from a sulfurous spring in Capania (Italy). *Syst. Appl. Microbiol.* **26**: 357 – 366.

Rose, P. D. (2002). Overview Volume 1: In: *Salinity, Sanitation and Sustainability: A study in environmental biotechnology and integrated wastewater beneficiation in South Africa*. WRC Report No.: TT 187/02. Water Research Commission, South Africa.

Rose, P. D., Boshoff, G. A., van Hille, R. P., Wallace, L. C. M., Dunn, K. M. and Duncan, J. R. (1998). An integrated algal sulphate reducing high-rate ponding process for the treatment of acid mine drainage wastewaters. *Biodegradation*. **9**: 247-257.

Rose, P. D., Maart, B. A., Dunn, K. M., Roswell, R. A. and Britz, P. (1996). High rate algal oxidation ponding for the treatment of tannery effluent. *Wat. Sci. Tech*. **33**: 219-227.

Ross, P., Mayer, R. and Benziman, M. (1991). Cellulose biosynthesis and function in bacteria. *Microbiol. Mol. Biol. Rev.* **55** (1): 35-38.

Sambrook, J.; Fritschi, E. F. and Maniatis T. (1989). Molecular cloning: a laboratory manual. 2nd Edition, Cold Spring Harbor Laboratory Press, New York

Santegoeds, C. M., Damgaard, C. M., Hesselink, G., Zopfl, J., Lens, P., Muyzer, G. and de Beer, D. (1999). Distribution of sulphate reducing and methanogenic

bacteria in anaerobic aggregates determined by microsensor and molecular analysis. *Appl. Environ. Microbiol.* **65**: 4618-4629.

Santegoeds, C. M., Ferdelman, T. G., Muyzer, G. and de Beer, D. (1998). Structural and functional dynamics of sulfate reducing populations in bacterial biofilms. *Appl. Environ. Microbiol.* **64**: 3731-3739.

Sauer, K., Camper, A. K., Ehrlich, G. D., Costerton, J. W. and Davies, D. G. (2002). *Pseudomonas euriginosa* displays multiple phenotypes during development of a biofilm. *J. Bacteriol.* **184** (4): 1440-1154.

Scheerem, P. J. H., Kock, R. O. and Buisman, C. J. N. (1993). Geohydrological contaminant system and microbial water treatment plan for metal contaminated groundwater at Budelco. *International Symposium World Zinc.* pp: 373-384.

Schoeman, J. J. and Steyn, A. (2001). Investigation into alternative water treatment technologies for the treatment of underground mine water discharged by the Grootvlei Proprietary Mines Ltd into the Blesbokspruit in South Africa. *Desalination.* **133** : 13-30.

Schramm, A., de Beer, D., Gieseke, A. and Amann, R. (2000). Microenvironment and distribution of nitrifying bacteria in a membrane-bound biofilm. *Environ. Microbiol.* ***2***: 680-686.

Schramm, A., de Beer, D., van den Heuvel, J. C., Ottengraf, S. and Amann, R. (1999). Microscale distribution of populations and activities of *Nitrospira* and *Nitrospira* spp. along a microscale gradient in a nitrifying bioreactor: Quantification by *in situ* hybridization and the use of microsensors. *Appl. Environ. Microbiol.* **65**: 3690-3696.

Schramm, A., Larsen, L. H., Revsbech, N. P. and Amann, R. I. (1997). Structure and function of a nitrifying biofilm as determined by microelectrodes and fluorescent oligonucleotide probes. *Wat. Sci. Tech*. **36**: 263-270.

Scott, R. (1995). Flooding of Central and East Rand Gold Mines: an Investigation into Controls over the Inflow Rate, Water Quality and the Predicted Impacts of Flooded Mines. Water Research Commission Report. No.: 486/1/95. Water Research Commission, South Africa.

Son, H. and Lee, J. (2004). H_2S removal with an immobilized cell hybrid reactor. *Process Biochem*. **40**: 2197–2203.

StatSoft, Inc. (2005). STATISTICA (data analysis software system). Version 7.1. www.statsoft.com.

Steudel, R. (2000). The chemical sulphur cycle. In: Lens and Hulsoff-Pol (Eds.). *Environmental technologies to treat sulfur pollution: Principles and Engineering.* IWA Publishing, London. pp: 1 -28.

Steudel, R. (1996). Mechanism for the formation of elemental sulphur from aqueous sulphide in chemical and microbiological desulphurization processes. *Ind. Eng. Chem. Res.* **35**: 1417-1423.

Stewart, P. S., Murga, R., Srinivasan, R. and de Beer, D. (1995). Biofilm structural heterogeneity visualised by three microscopic methods. *Wat. Res.* **29**: 2006-2009.

Stumm, J. and Morgan, J. J. (1995). Aquatic chemistry–chemical equilibria and rates in natural waters. 3rd Edition. John Wiley and Sons Inc. New York.

Sublette, K. L. (1992.). Microbial stabilisation of active-sulfide sludges. *Appl. Biochem. Biotechnol.* **34/35**: 811-817.

Sublette, K. L. and Sylvester, N. D. (1987) Oxidation of hydrogen sulfide by *Acidithiobacillus denitrificans*: desulfurization of natural gas. *Biotech. Bioeng.* **29**: 249-257.

Takahashi, H., Kimura, B. Yoshikawa, M., Gotou, S., Watanabe, I. and Fujii, T. (2004). Direct detection and identification of lactic acid bacteria in FPP using degrading gradient gel electrophoresis. *J. Food Protection.* **67** (11): 2515-2520.

Thar, R. and Kühl, M. (2002). Conspicuous veils formed by vibrioid bacteria on sulphidic marine sediments. *Appl. Environ. Microbiol.* **68**: 6310-6320.

Van Hille, R. P. and Duncan, J. R. (1996). Bioremediation of heavy metal polluted acidic mine effluents by Spirulina. *J. Appl. Phycol.* **8**: 461-466.

Voordouw, G., Armstrong, S. M., Reiner, M. F., Fouts, B. R., Telang, A. J., Shen, Y. and Gervets, D. (1996). Characterisation of 16S rRNA genes from oil field microbial communities indicates the presence of a sulphate-reducing, fermentative and sulphide-oxidising bacteria. *Appl. Environ. Microbiol.* **62** (5): 1623-1629.

Vroom, J. M., De Graw, K. J., Garretson, H. C., Backsaw, D. J., Marsh, P. D., Watson, G. K., Birmingham, J. J. and Allison, C. (1997). Depth penetration and detection of pH gradients in biofilms by two-photon excitation microscopy. *Appl. Environ. Microbiol.* **65** (8): 3502-3511.

Wagner, M., Erhart, R., Manz, W., Amann, R., Lemmer, H., Wedi, D., Schleifer, K. H. (1994). Development of an rRNA-targeted oligonucleotide probe specific for the genus *Acinetobacter* and its application for *in situ* monitoring in activated sludge. *Appl. Env. Microbiol.* **60**: 792-800.

Wagner, M., Amann, R., Lemmer, H., Schleifer, K. H. (1993). Probing activated sludge with oligonucleotide specific for proteobacteria: Inadequacy of culture-dependent methods for describing microbial community structure. *Appl. Env. Microbiol.* **59**: 1520-1525.

Wantanabe, Y. (1974). The crystal structure of monoclinic γ- sulphur. *ACTA Cryst.* **30** (6): 1396 – 1401.

Ward, D. M., Ferris, M. J., Nold, S. C. and Bateson, M. M. (1998). A natural view of microbial diversity within hot spring cyanobacterial mat communities. *Microbiol. Mol. Biol. Rev.* **62** (4): 1358-1370.

Waterson, K., Bejan, D. and Bunce, N. J. (2006). Electrochemical oxidation of sulphide ion at a boron-doped anode. *J Appl. Electrochem.* **37**(3): 367-373.

Watnick, P. and Kolter, R. (2000). Biofilm, city of microbes. *J. Bacteriol.* **182** (10): 2675-2679.

Weast, R. C. (1981). Handbook of chemistry and physics (62nd edition). CRC Press Inc., Boca Roton, USA.

Weller, R., Weller, J. W. and Ward, D. M. (1991). 16S rRNA sequences of uncultivated hot spring cyanobacterial mat inhabitants retrieved as randomLy primed cDNA. *Appl. Environ. Microbiol.* **57**: 1146-1151.

Whittington-Jones, K. (2000). Sulphidogenic hydrolysis of complex organic carbon substrates. PhD Thesis, Rhodes University, South Africa.

Widdel, F. (1988). Microbiology and ecology of sulfate and sulfur reducing bacteria. In: Zehnder (Ed.). *Biology of anaerobic microorganisms.* Willey and Sons Inc., New York. pp: 469-585.

Williams, T. M. and Unz, R. F. (1985). Filamentous sulfur bacteria of activated sludge: Characterisation of *Thiothrix*, *Beggiatoa* and *Eikelboom* type 021N strains. *Appl. Environ. Microbiol.* **49** (4): 887-898.

Wu, C. J. and Janssen, G. R. (1996). Translation of *vph* mRNA in *Streptomyces lividans* and *Escherichia coli* after removal of the 5' untranslated leader. *Mol. Microbiol.* **22**: 339–355.

Wuertz, S. (2003). Architecture, population structure and function: Introduction. In: Wuertz, Bishop and Wilderer (Eds.). *Biofilms in wastewater treatment*. IWA Publishing London. pp: 125–146.

Yao, W. and Millero, F. J. (1996). Oxidation of hydrogen sulphide by hydrous Fe (III) oxides in seawater. *Marine Chemistry*. **52**: 1-16.

Younger, P. L. (2004). The mine water pollution threat to water resources and its remediation in practice. *IDS-Water Europe* .http://www.idswater.com/.

Younger, P. L. (2001). Mine water pollution in Scotland: Nature, extent and preventative strategies. *Sci. Total Environ.* **265**: 309-326.

Younger, P. L. (1998). Design, construction and initial operation of full-scale compost-based passive systems for treatment of coal mine drainage and spoil leachate in the UK. IMWA Symposium, Johannesburg. pp: 413-424.

Younger, P. L., Banwart, S. A. and Hedin, R. S. (2002). Mine water: Hydrology, pollution, remediation. Kluwer Academic Publishers, Dordrecht.

Younger, P. L., Curtis, T. P., Jarvis, A. and Pennell, R. (1997). Effective passive treatment of aluminum-rich acidic colliery spoil drainage using a compost wetland at Quaking Houses, County Durham. *J. Chartered Inst. Water Environ. Mg.* **11**: 200-208.

Yu, T. and Bishop, P. L. (1998). Stratification of microbial metabolic processes and redox potential change in an anaerobic biofilm studied using microelectrodes. *Wat. Sci. Tech*. **37**: 195-198.

Zhang, T. C. and Bishop, P. L. (1994). Density, porosity, and pore structure of biofilms. *Wat. Res.* **28**: 2267-2277.

Zipper, C. and Jage, C. (2001). Passive treatment of acid-mine drainage with vertical-flow systems. Reclamation guidelines for surface mined land in Southwest Virginia: Powell River Project. Virginia Cooperative Extension, Publication 460-133. pp: 1-16.

APPENDIX A

A-1 MEDIA AND REAGENTS USED IN MOLECULAR MICROBIAL ECOLOGY STUDIES

A-1.1 Gradient Tubes

A-1.1.1 10 cm Agarose Overlay Column

50 mL of the agarose overlay column was prepared using 0.5 g low melt agarose, 25 mL milliQ water and 25 mL double strength media.

A-1.1.2 Double Strength Media

The double strength media was prepared using 1.75 mL 60 % sodium lactate, 1 g $MgSO_4.7H_2O$, 0.5g KNO_3, 0.5 g Na_2SO_4, 0.5 g yeast extract, 0.25 g K_2HPO_4, 0.05 g $CaCl_2.6H_2O$ made up to 250 mL with milliQ water and autoclaved. The medium, water and agarose were heated until the agarose dissolved completely. The solution was then allowed to cool to 45 °C and 1 mL biofilm inoculum was added. Bacteria-free control tubes were set up as above but excluding the biofilm inoculum

A-1.1.3 Sulphide Plug

5 mL of 0.5 g HS^- sulphide plug was prepared per tube. The sulphide plug was made from 0.05 g Agarose, 1.25 mL milliQ water, and 1.25 mL quadruple strength media.

A-1.1.4 Quadruple Strength Media

The quadruple strength media was prepared with 3.5 mL 60 % sodium lactate, 2 g $MgSO_4.7H_2O$, 1 g CH_4Cl, 1 g Na_2SO_4, 1 g yeast Extract, 0.5 g K_2HPO_4, 0.15 g $CaCl_2.6H_2O$ made up to 250 mL with milliQ water and autoclaved. The medium, water and agarose were heated until the agarose dissolved completely. The solution was then allowed to cool to 55 °C and 2.5 mL of 1 g/L HS^- was added in to the sulphide plug, the plug was poured into the bottom of a sterile test tube and allowed to set before the agarose overlay column was poured.

A-2 MEDIA USED FOR MOLECULAR TYPING

A-2.1 DNA Extraction

A-2.1.1 tris /EDTA buffer

The tris /EDTA buffer was made up of 10 mM Tris/HCl, 1mM EDTA and one part 50 % glycerol made up to 1 l in a volumetric flask.

A-2.1.2 0.8 % Agarose gel

The 0.8 % agarose gel was prepared by adding 0.8 g agarose in 100 mL of 1 x TBE buffer.

A-2.1.3 TBE buffer

The TBE buffer comprised 10.78 g Tris base, 55 g boric acid and 7.44 g di-sodium EDTA made up to 800 mL with milliQ water and pH to 8.3 with boric acid. MilliQ water was added to make up to 1 l before autoclaving.

A-2.1.5 Ethidium bromide

Ethidium bromide was prepared by adding 0.5 g of ethidium bromide to 1 mL of milliQ water.

A-2.1.6 Molecular weight marker

The molecular weight marker was made up of 200 **µ**l **a**DNA (0.25 **µ**L/mL) which was digested with 24 **µ**l of 10 x buffer H and 10 **µ**l of *Pst* 1 enzyme for three hours at 37 °C, before adding 550 **µ**l of 10 mM TE buffer (pH 8) and 150 **µ**l of 6 x loading buffer.

A-2.1.7 6 x loading buffer

The 6 x loading buffer was made from 0.25 % bromophenol blue, 0.25 % xylene cyanol and 30 % glycerol.

A-3 REAGENTS AND PRIMES USED FOR PCR

A-3.1 Primers

A universal primer GM5F (5'-cct acg gga gcagc ag-3') and 907R (5'-cgc ccg ccg cgc ccc gcg ccc gtc ccg ccg ccc ccg ccc gcc gtc aat tcc ttt gag ttt-3'), a GC clamped primer from Inqaba Biotech were used for PCR preparation.

A-3.2 PCR reaction mixture

A 25 µl PCR reaction mixture was prepared using 2.5 µl PCR buffer with $MgCl_2$, 1.0 µl dNTPs, 1.0 µl 907R, 1.0 µl GM5F, 1.8 µl milliQ water, 0.2 µl Taq and 1.0 µl DNA (200- 500 ng/µl DNA).

A-4 REAGENTS USED FOR DGGE

A-4.1 100 % denaturant

The 100 % denaturant comprised of 5 mL of 10 x TAE buffer (48.4 g Tris base, 3.72 g EDTA, 11.42 mL Glacial acetic acid made up to 1 l with milliQ water).

A-4.2 TAE buffer

TAE buffer was prepared with 48.4 g Tris base, 3.72 g EDTA, 11.42 mL glacial acetic acid made up to 1 l with milliQ water.

A-4.3 DGGE gel

A 50 mL solution of 100 % denaturant, 7.5 mL of 40 % acrylamide, 21 g urea and 20 mL formamide made up to 50 mL with milliQ water.

A-4.4 40 % acrylamide

The 40 % acrylamide was prepared from 100 g acrylamide and 2.7 g bis-acrylamide in 1 l milliQ.

A-4.5 6 % acrylamide gel

The 6 % acrylamide gel was made up of 3.5 mL denaturant, 4 µl of 20 % ammonium persulphate (APS) and 40 µl of TEMED (Sigma-Aldrich).

A-4.6 Luria Bertani (LB) agar

Luria Bertani (LB) agar was prepared from 30 g LB agar and 1L milliQ.

A-4.7 X-Gal

X-gal was prepared using 20 mg of 5-bromo-4-chloro-3-indolyl-**β**-o-galactoside in 1 mL dimethylformamide.

A-5 PRIMERS USED FOR SEQUENCING REACTIONS

A T7 (5'-taa tac gac tca cta tag gg-3') and a SP6 (5'-tat tta ggt gac act ata g-3') primers was used for sequencing reactions.

APPENDIX B

B-1 MEDIA USED IN HPLC ANALYSIS

B-1.1 Borate/gluconate concentrate for sulphate and thiosulphate analyses

The borate/gluconate concentrate used for eluent preparation was made up in a 1 l volume containing 500 mL milliQ water, 16 g sodium gluconate, 18 g boric acid and 25 g sodium tetraborate decahydrate. Once dissolved 25 mL glygerine was added to the mixture. Further milliQ water was added to make up to 1 l.

B-1.2 Eluent preparation for sulphate and thiosulphate analyses

The eluent was prepared by placing 500 mL of milliQ water was placed in a 1 l volumetric flask to which 20 mL of the borate/ gluconate concentrate, 20 mL *n*-butanol and 120 mL acetonitrile were added. The flask was filled to the mark with milliQ water and mixed thoroughly. Before use, the eluent was filtered through a 0.22 µm Durapore membrane (GVWP).

A concentrate standard containing 1 000 ppm Fe^{-}, 2 000 ppm Cl^{-}, 4 000ppm NO_3^{-}, 4000 ppm Br^{-}, 4 000 ppm NO_3^{-}, 6 000 ppm HPO_4^{2-} and 4 000 ppm SO_4^{2-} in 100 mL milliQ water was prepared. A fresh working standard was prepared weekly by diluting 100 µl of the concentrate standard in 100 mL of milliQ water.

B-1.3 Chemical Oxygen Demand

B-1.3.1 Digestion mixture

A digestion mixture was prepared from 30 g silver sulphate, 12.25 g potassium dichromate made up to 1 l with deionised water to which 3 mL sulphuric acid was added.

B-1.3.2 Ferroin indicator

Ferroin indicator was made up of 1.485 g phenanthroline monohydrate, 0.695 g ferrous sulphate in 100 mL of deionised water.

B-1.3.3 0.1 N ferrous ammonium sulphate

The ferrous ammonium sulphate solution was prepared with 39 g ferrous ammonium sulphate, 980 mL milliQ water and 20 mL concentrated sulphuric acid.

APPENDIX C

Touch-down PCR procedure used for the amplification of DNA fragments.

Table C-1 Touch-down programme used for PCR amplification.

Reaction	Temperature	Duration	No of cycles
Initial Denaturation	95ºC	2 minutes	1 cycle
Denaturation	94ºC	30 seconds	4 cycles
Annealing	68ºC	45 seconds	
Extension	72ºC	2 minutes	
Denaturation	94ºC	30 seconds	4 cycles
Annealing	66ºC	45 seconds	
Extension	72ºC	2 minutes	
Denaturation	94ºC	30 seconds	4 cycles
Annealing	64ºC	45 seconds	
Extension	72ºC	2 minutes	
Denaturation	94ºC	30 seconds	4 cycles
Annealing	62ºC	45 seconds	
Extension	72ºC	2 minutes	
Denaturation	94ºC	30 seconds	12 cycles
Annealing	60ºC	45 seconds	
Extension	72ºC	2 minutes	
Final extension	72ºC	5 minutes	1 cycle